Annex 52

A Report from the Advanced Motor Fuels Technology Collaboration Programme

Fuels for Efficiency

Somnuek Jaroonjitsathian
Padol Sukajit
Atsawin Salee
PTT Innovation Institute, Thailand

Lenoid Tatarkovsky
Arnon Polan
Technion, Israel Institute of Technology

Norbert Grope
Olaf Schröder
Jürgen Krahl
Technologietransfer Automotive
Hochschule Coburg, TAC

Rasmus Pettinen
Timo Murtonen
Petri Söderena
VTT Research & Technology, Finland

Franziska Müller-Langer
Jörg Schröder
Eric Mattheß
Deutsches
Biomasseforschungszentrum, DBFZ

Kim Winther
Teknologisk Institut, Denmark

Annex 52

A Report from the Advanced Motor Fuels Technology Collaboration Programme

Fuels for Efficiency

Somnuek Jaroonjitsathian
Padol Sukajit
Atsawin Salee
PTT Innovation Institute, Thailand

Lenoid Tatarkovsky
Arnon Polan
Technion, Israel Institute of Technology

Norbert Grope
Olaf Schröder
Jürgen Krahl
Technologietransfer Automotive
Hochschule Coburg, TAC

Rasmus Pettinen
Timo Murtonen
Petri Söderena
VTT Research & Technology, Finland

Franziska Müller-Langer
Jörg Schröder
Eric Mattheß
Deutsches
Biomasseforschungszentrum, DBFZ

Kim Winther
Teknologisk Institut, Denmark

October 2017

Executive Summary

This scientific report consists of five research contributions elaborating on the subject "Fuels for Efficiency". The conclusions in the different contributions are summarized as follows:

WP I: The ***survey on advanced fuels for advanced engines*** *finds that the diversity of fuels will increase further. Next to user friendly drop-in fuels that can be implemented using the existing infrastructure, other advanced fuels will be developed or introduced in the market. These fuels can be produced on the basis of biomass (so called biomass-to-x-fuels), but also on renewable electricity together with a carbon source (so called power-to-x-fuels). Furthermore, to achieve the mutual benefit of engine - fuel interaction,* ***new engines should be flexible for a wide range of fuels fulfilling the requirements with regard to minimum $CO_{2\text{-}eq.}$ emissions as well as local emissions like NO_x, particles etc****.*

WP II: Experiments were undertaken to evaluate the ***performance of chemical friction modifier additives*** *for gasoline and diesel fuels to prove the effect of fuel economy. The results show that the effect of* ***chemical friction modifier in gasoline was in the range of 1-2% improvement and the cetane improver in diesel fuel was not a promising solution for fuel efficiency improvement,*** *at least for current engine technology.*

WP III: Experiments showed that the ***methanol steam reformer improved fuel efficiency by 18 to 39%*** *when running under the low-to-medium load condition. The major improvement comes from the wide flammability limit of hydrogen-rich fuel, which allows the engine to operate unthrottled, especially at low-load conditions, and leads to*

reduction of heat transfer losses and maximal cycle temperatures. The extremely high burning velocity of hydrogen-rich reformate enables the engine to get closer to the theoretically most efficient Otto cycle. In addition, the waste heat recovery from exhaust gas helps to maintain the endothermic reactions of methanol steam reforming (MSR). Thus, ***MSR is one of the more promising technologies for fuel efficiency improvement on methanol engines****.*

WP IV: The aim of this project was to ***optimize non-road diesel engines for a paraffinic diesel fuel*** *and compare the results with typical European grade diesel fuel measured with OEM engine parameters. The experiment was undertaken with a fully adaptable engine control. The key message is that paraffinic diesel fuels allow engines to be calibrated for better thermal efficiency with the same engine out emission levels as with fossil diesel fuel, mainly due to the lower engine out soot levels.* ***With optimized injection parameters it was possible to improve the average thermal efficiency by 2%, and with optimal load conditions by 4%****.*

WP V: ***Ethanol blended fuel has significantly improved fuel octane number*** *which results in the possibility of higher engine output, if operated with the advanced ignition timing feature. Since advanced ignition timing is a strategy used in modern Gasoline Direct Injection (GDI) engines, it can be concluded that ethanol blended fuels have high potential for thermal efficiency improvement compared to pure gasoline. Therefore,* ***fuel efficiency improvement in modern gasoline GDI engines can be achieved by using ethanol blended fuel****.*

Authors

Thailand *represented by PTT Public Company Limited, acting as an operating agent, organizing the final report and performing a task sharing contribution on engine experiments for optimizing the ethanol blended gasoline in GDI engine.*

Denmark *represented by Danish Technological Institute and partner "OK AMBA", performing a task sharing contribution on two engines for fuel borne friction modifier and a cetane improver additive assessment. Work was sponsored by Energiteknologisk Udviklings- og Demonstrations Program (EUDP).*

Israel *represented by Technion - Israel Institute of Technology, performing a task sharing contribution on the potential of using Methanol reforming fuel in ICE engines to improve thermal efficiency, with support from the Ministry of National Infrastructures, Energy and Water Resources.*

Finland *represented by VTT Technical Research Centre of Finland, performing a task sharing contribution on collating existing Finnish data on renewable paraffinic diesel and running engine experiments with various fuels in a fully controllable diesel engine for making the new unpublished data available. This study is a part of the IEA-AMF ANNEX 52. All research was performed during fall 2016 in VTT facilities in Espoo, Otaniemi. The research work was financed by VTT and was part of the VTT's TransSmart research program. Fuel suppliers are acknowledged for providing fuels for the measurements.*

Germany *represented by IEA Bioenergy Task 39, performing a comprehensive survey on advanced biofuels for advanced engines and*

agreeing to share information to IEA-AMF Annex 52 because of the common technology alignment between the 2 groups.

Content

Introduction

The trend of vehicle electrification might dominate the global vehicle industry within a foreseeable future; however a seamless transition needs to be addressed. Internal Combustion Engine technology has been developed for almost 100 years, with the ultimate goal of reaching the highest break thermal efficiency such as 60% in Compression Ignition (C.I.) engine and 50% in (Spark Ignited) S.I. engine. Most automotive engineers are aware of the need to achieve maximum thermal efficiency while keeping emissions low, but more focus is needed on the key fuel properties that can enable the highest engine efficiency.

Fuels for efficiency, by the author's definition, means the wayto optimize the fuel blend for gaining higher thermal efficiency or how to chemically modify the fuel to get better overall fuel economy

Objectives

Annex 52, Fuels for Efficiency, has been initiated in compliance with the global requirement of improving fuel efficiency for road transport fuel application. In general, automotive original equipment manufacturers (OEMs) try to improve their engines' efficiency while controlling the exhaust emission with regard to the country's requirement. The implication for advanced motor fuels, or the method for optimizing the fuels in order to maximize engine efficiency, has rarely been discussed worldwide. All members expect that the results will enable a new approach to automotive fuel optimization.

Annex 52 intends to demonstrate how to optimize fuel with specific engines in terms of thermal efficiency gain without any limitation on the format of fuel utilization, engine technology, or chemical additives. All task-sharing members will conduct the experiment based upon their experience and interests. Thus, the format of experiments is fully flexible but needs to be focused on scientific and statistical methods. The scope of interests vary from each distinguished member as below

***Work Program I: Survey on Advanced Fuels for Advanced Engines**: The most complete literature survey program on technical assessment of advanced biofuels and advanced engine technologies via a huge number of publications funded and conducted by IEA Bioenergy Task 39 mainly composes of survey on the relevant advanced biofuels including fuel properties, chemical reaction among advanced biofuels and additives including with the health effect. This WP intend to provide the overall aspects of using advanced biofuels in advanced engines for future policy mandate in any countries.*

***Work Program II: Performance Evaluation of Chemical Friction Modifiers for Diesel and Gasoline Fuels**: Major oil companies have recently released on to the market a new generation of fuel borne friction modifiers that potentially save up to 3 % on consumption. However, there is no solid evidence of the real-life effect because independent organizations still have not tested these additives thoroughly. Friction Modifier additives are widely used in lubricant additive packages. They are generally straight hydrocarbon chains with a polar head group. Typical polar head groups comprise amines, amides and their derivatives or carboxylic acids and their derivatives. The polar head groups are attached to metal surface such as cylinder walls and ring wiping faces, where they form relatively strong bonds, while the long hydrocarbon tail remain solubilized in the film of lubricating oil.*

Work Program III: Waste Heat Recovery/ Thermo-Chemical

Recuperation (TCR): *Results of recent studies suggest that there is a big potential for improvement of internal combustion engine (ICE) technology. It is well known that about 30% of fuel energy introduced to ICE is wasted with engine exhaust gases. Its utilization can lead to a significant improvement of ICE energy efficiency. One of the ways to recover an engine's waste heat is by using the energy of exhaust gases to promote endothermic reaction of fuel reforming. This method is frequently called thermo-chemical recuperation (TCR). In this case an ICE is fed by the gaseous products of fuel reforming, mainly mixture of hydrogen and carbon monoxide, frequently called syngas. The latter has, as a rule, greater heating value than the primary liquid fuel, and may be burned in the engine using extremely lean air/fuel mixtures with the excess air factor λ values up to 1.5. This should ensure more complete combustion under lower temperatures and, as a result, increase of the engine brake efficiency and decrease of noxious species formation. High hydrogen content of this gaseous fuel provides a possibility of faster combustion compared with the primary liquid fuel, thus resulting in higher engine thermal efficiency. The TCR approach is considered nowadays as one of the possible methods of increasing powertrain efficiency and reducing emissions.*

Work Program IV: Performance Assessment of Various Paraffinic Diesel Fuels: *The paraffinic diesels can be produced from various source of vegetable oil such as palm oil, coconut oil or rapeseed oil. The extremely high ignition improver fuel quality is expected by OEM to resolve the tailpipe emission i.e. PM and CO. In addition, there is a number of literatures support that the paraffinic diesels will become the major key success factor for OEM to further achieve on the more stringent emission regulation, while improving fuel efficiency. This WP needs to compare the effect of using paraffinic diesels from various sources*

Work Program V: Opportunity for Enhancing Fuel Efficiency by Ethanol Blended Gasoline Fuels: *Previously, the research team has found that*

using Ethanol blended fuel in GDI engine can potentially advance the engine ignition timing which also return the higher torque output. By the way, the actual engine response onto the higher knock resistance of Ethanol blended fuel need to be evaluated, at least, for proving that the EtOH blended fuel tends to increase engine thermal efficiency or not.

Description of Activities

The report is structured according to the individual work packages and consequently experimental methods, objectives, results and conclusions are described within these work package chapters. The order of work packages is as follows:

- ***WP I:*** ***Information Exchange with IEA Bioenergy Task 39 (Survey on Advanced Fuels for Advanced Engines)***
- ***WP II:*** ***Performance Evaluation of Chemical Friction Modifiers for Diesel and Gasoline Fuels (Denmark)***
- ***WP III:*** ***Fuel reforming by Thermo-chemical Recuperation (Israel)***
- ***WP IV:*** ***Performance Assessment of Various Paraffinic Diesel Fuels (Finland)***
- ***WP V:*** ***Opportunity for Enhancing Fuel Efficiency by Ethanol Blended Gasoline Fuels (Thailand)***

Work Program I:

Survey on Advanced Fuels for Advanced Engines

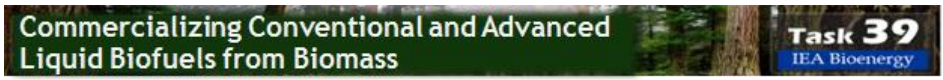

Executive Summary

Survey on Advanced Fuels for Advanced Engines

Funding by IEA Bioenergy Task 39 | 12/2015 – 11/2016

tac
technologietransfer automotive
hochschule coburg

Norbert Grope

Olaf Schröder

Jürgen Krahl

DBFZ

Franziska Müller-Langer

Jörg Schröder
Eric Mattheß

Date: 31.07.2017

The literature study "Survey on Advanced Fuels for Advanced Engines" has been set up as a review-like compilation and consolidation of relevant information concerning recent and upcoming advanced engine fuels for road vehicles with special focus on biomass-based liquid fuels. It is provided as a self-contained report, but at the same time serves as update and complementary resource to IEA-AMF´s online fuel information portal (http://www.iea-amf.org). An attempt is made to describe status quo and perspectives of advanced fuels and to give a broad overview on parameters, tools and experimental approaches necessary for fuel characterization and evaluation. Focus of literature coverage, especially concerning fuel properties and exhaust emission research results, is from recent to approximately five or ten years back, but if appropriate, older resources will be considered too in general discussion of relevant effects and mechanisms.

Introductory Chapter 2 summarizes framework conditions for advanced fuel applications in terms of regulatory measures and incentives for sustainable and fair-trade action, climate change prevention and energy-efficient vehicle operation. Following these non-technical topics, Chapter 3 and 4 gives Information about fuel standards and fuel properties, which should considered when introducing new fuels. Chapter 5 provides tabulated information on feedstocks, production schemes, costs and market issues of main types of advanced biofuels determined for this study, i.e. hydrotreated vegetable oils (HVO/HEFA), biomass-to-liquid (BTL) fuels (i.e. paraffinic Fischer-Tropsch (FT)), methanol, dimethyl ether (DME), oxymethylene dimethyl ether (OME), lignocellulosic ethanol and liquefied biomethane. Also fuel properties and emission trends are shown in this chapter. Accordingly, biodiesel is explicitly included in subsequent discussions and complemented by an excursus on metathesis biodiesel.

Chapter 6 refers to reactivity and stability of fuels with regard to interactions among different fuel components and between fuel and engine oil. Deterioration of fuel and engine oil quality will affect

long-term fuel storage and vehicle functionality by formation of deposits and sludge and are also manifested by laboratory parameters not necessarily detectable macroscopically. Influencing factors like molecular structure, temperature, oxidizing agents, additives, impurities and metal catalysis are discussed according to published research results.

Chapter 7 deals with health effects of engine exhaust and to this end describes important gaseous and particulate constituents, their characterization and measurement. As specific exhaust species, regulated parameters CO, HC, NOx and unregulated components PAC and carbonylics are considered, particular aspects of particle size, number and composition are discussed. Reference is made to formation of ozone and ambient aerosol as secondary impacts of engine exhaust. Short keynotes on research and review articles on issues of toxicology, mutagenicity and other adverse effects of engine exhaust are provided. A thorough introduction to dedicated engine emission testing and a literature survey on published emission measurement results using various engine types and fuels are given.

As a conclusion of the study, the diversity of fuels will increase in the future. New advanced fuels will be introduced in the market (e.g. HVO) or will become the focus of research activities (e.g. OME). One criterion for successful introduction of a new fuel in the market is that the new fuel can be used as drop-in fuel. These fuels have the advantage, that small amount of the fuel can be tested using existing infrastructure and engine techniques. In this phase of market introduction, reactions among fuel components and material interactions can also be detected. At the moment, most research activity deals with the behavior of aging products of biodiesel in non-polar fuel like HVO/HEFA or X-to-liquid (XtL, FT fuels).

Introducing new fuels needing an adaption of the engine technique or a new engine concept in the market requires much more effort. Next to the new fuel, also a new infrastructure and new engines have to be developed and launched. This is only possible if fuel and automotive industries,

politics and broad public support the new development.

Another key factor for advanced fuel is the raw material base. The production of advanced fuels should be independent of fossil resources. Therefore, biomass or regenerative electrical power (e.g. wind power or solar energy) must be the source of advanced fuels. Biomass is intensively used by first generation biofuels, but there is a potential to raise the share of regenerative fuel with the introduction with advanced fuels having a broader base of biomass assortments. Electric power as energy source for advanced fuel will be become interesting, if the share of renewable electricity in the grid will increase. Nevertheless, already today research is necessary to have the technique ready in time.

Last but not least, for further development of engine technique, advanced fuels can be use as construction element. If it is possible to optimize the burning process and to minimize emissions by the use of advanced fuels, new vehicles can have a better performance at the same price.

In summary, advantages and disadvantages of the considered advanced fuels are listed in table 1 (see next page). From today´s point of view, no advanced fuel has the potential to fully replace fossil fuel use in the near or middle future, but all advanced fuel options have the potential to reduce fossil fuels usage significantly.

Table 1: Advantages and disadvantages for the market introduction of advanced fuels (++ clear positive impact, + slight positive impace, 0 no impact, - slight negative impact, -- clear negative impact)

Fuel	Production Technique	Raw material base	Drop-In Fuel	Engine technique	Exhaut gas emissions
HVO	++	+	++	++	+
BtL	0	+/++	++	++	+
DME	++	methanol	--	0	++
OME	--	methanol	0	0	++
Methanol	0/++	+/++	-	0	0
Lignocellulosic Ethanol	+	+/++	+	+	+
Bio-LNG/LBM	++	+	++	++	0 (++)*

** compared to fossil methane (to gasoline)*

Please refer to the link below for full report download,

http://task39.ieabioenergy.com/

http://task39.sites.olt.ubc.ca/files/2018/10/Survey-on-Advanced-Fuels-for-Advanced-Engines-IEA_Bioenergy_T39_AFAE_DBFZ.pdf

Work Program II:

Performance Evaluation of Chemical Friction Modifiers for Diesel and Gasoline Fuels

TEKNOLOGISK
INSTITUT

Kim Winther

Final Report for AMF
Annex 52

DENMARK

2.1) Objectives:

The experiment aims to prove the effect of friction modifier type additive in gasoline fuel whether it can help improving fuel efficiency. While the author also designed the experiment to evaluate whether the cetane improver additive in diesel fuel can gain better fuel economy.

2.2) Experiment Set-up

The test regarding gasoline fuel was done with a one cylinder 125 cm^3 fuel injected engine found in motorcycles such as Yamaha WR125. Diesel fuel was tested on a 4-cylinder 9HX passenger car engine produced by PSA.

Tests were conducted on two dynamometers, suitable for the engine types. Fuel inputs were measured by an electronic balance and a coriolis fuel flow meter, both of which are very accurate.

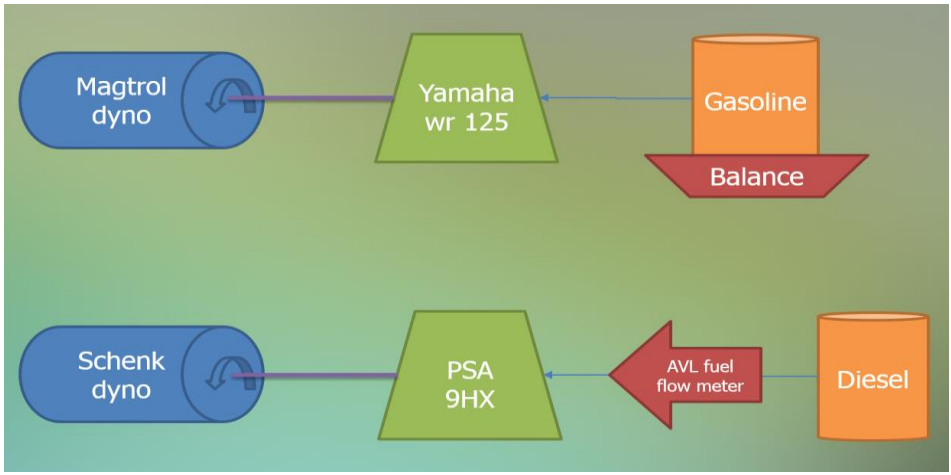

Figure 2.1 Test system configuration

All tests were conducted as steady state tests. The test point for each engine along with some specs are shown in illustrations below.

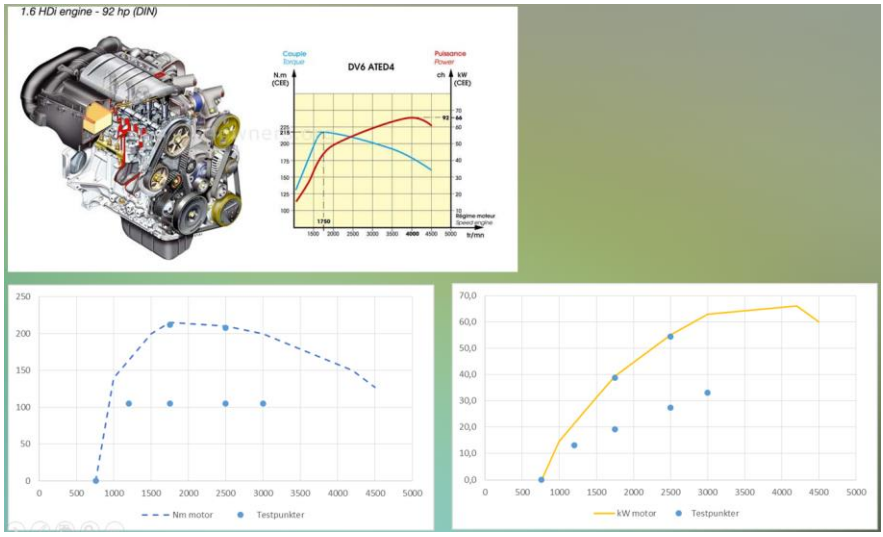

Figure 2.2 Diesel engine steady-state test conditions

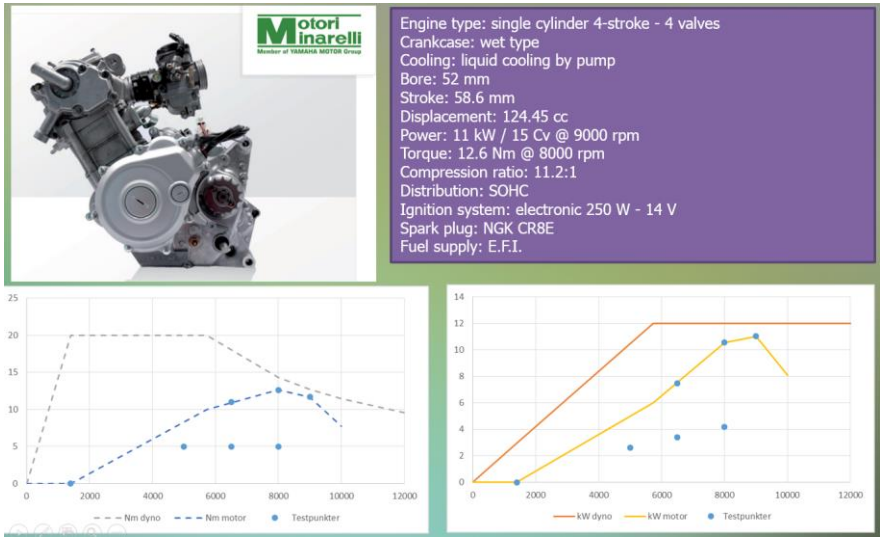

Figure 2.3 Gasoline engine steady-state test conditions

2.3) Test Results

To obtain reliable results each load point test was repeated 9 – 15 times depending on the observed variance. The final uncertainty shown on the graphs was calculated from the observed variance and number of tests according to the ISO JCGM 100 series.

Results showed that 330 ppm friction modifier no. 9525A lowered the specific gasoline consumption by 2,7 % in the best case. However, the benefit was not clear in all test points. One of the seven tests points showed a negative effect. The average improvement was only 0.9 %.

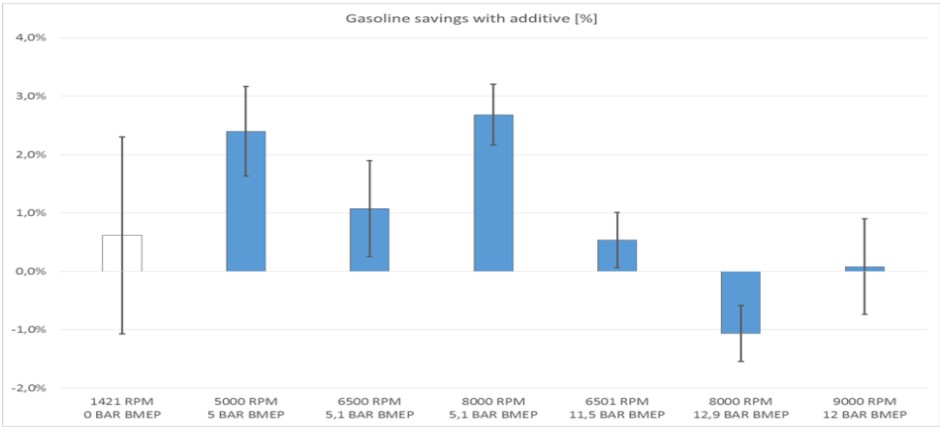

Figure 2.4: Comparative Gasoline Specific Fuel Consumption

Diesel results showed that 125 ppm wt./wt. of cetane improver LZ 8090 did not improve the specific fuel consumption significantly at load. However idle consumption was apparently improved by 5-10%.

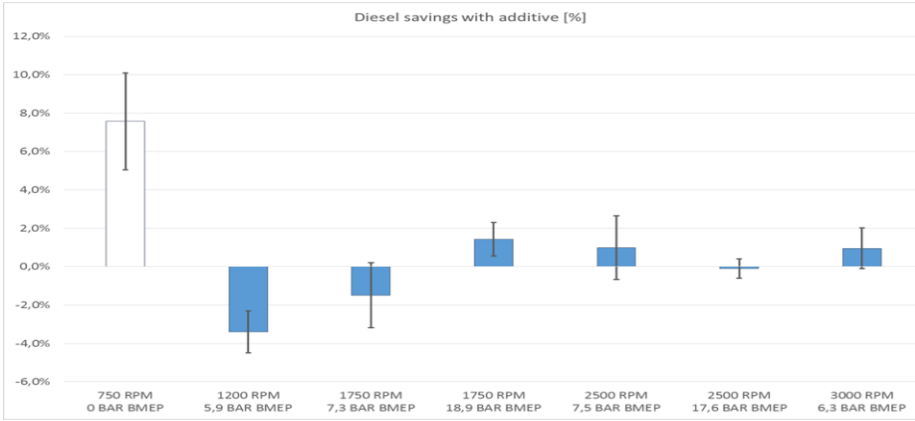

Figure 2.5: Comparative Diesel Specific Fuel Consumption

Overall, the benefits in terms of fuel consumption were quite small and not entirely consistent. The test results do not justify a recommendation for widespread use.

2.4) Conclusion

In summary, the specific friction modifier additive and general Cetane Improver additive in gasoline and diesel fuel respectively, show insignificant effect on fuel economy improvement. The experiment was conducted on conventional gasoline and diesel enginesunder steady-state engine test conditions. Regarding the real vehicle application, the overall friction loss from other systems: transmission, driveline, transfer and wheel will contribute more to friction than just the inside of the engine. Therefore, the few percent fuel economy gain from the engine may not impact directly to the car owner.

Work Program III:

Fuel Reforming by Thermo-chemical Recuperation

Faculty of Mechanical Engineering
Research Center for Energy Engineering and Environmental Preservation
Internal Combustion Engines Laboratory
Technion, Israel Institute of Technology

Fuel reforming by thermo-chemical recuperation

Leonid Tartakovsky and Arnon Poran

Final Report for AMF
Annex 52

Haifa, Israel

Nomenclature

δR	*uncertainty of calculated parameter R*
δX_i	*accuracy of measured value* X_i
ΔH	*enthalpy of reaction*
e_b	*burned zone energy*
e_s	*sensible energy*
e_u	*unburned zone energy*
E_i	*emissions of pollutant i*
h_a	*air enthalpy*
h_{av}	*enthalpy available for reforming*
h_f	*fuel enthalpy*
$h_{f,i}$	*injected fuel enthalpy*
m	*in-cylinder mass*
m_a	*air mass*
$\dot{m}_a$	*air flow rate*
m_b	*burned zone mass*
m_f	*fuel mass*
$\dot{m}_f$	*fuel flow rate*
$m_{f,i}$	*injected fuel mass*
m_u	*unburned zone mass*
$\dot{m}_f$	*fuel mass flow rate*
M_C	*molecular weight of carbon*
M_i	*molecular weight of pollutant i*
p	*cylinder pressure*
Q	*heat transfer rate*
Q_b	*burned zone heat transfer rate*
Q_u	*unburned zone heat transfer rate*
V	*cylinder volume*
V_b	*burned zone volume*
V_d	*displaced volume*
V_u	*unburned zone volume*
$W_{i,g}$	*gross indicated work*
$W_{i,g}$	*gross indicated power*

x_i	*mass fraction of species i*
$y_{c,fuel}$	*fuel's carbon mass fraction*
y_i	*molar fraction of pollutant i*
y_j	*$CO/CO_2/CH_{1.85}$ molar fraction*

Greek Symbols

η_c	*combustion efficiency*
η_i	*gross indicated efficiency*
θ	*crank angle (360 firing top dead center)*
θ_{50}	*Anchor angle, the CAD of 50% fuel mass burned*
θ_{0-10}	*flame development angle, CAD difference ignition and 10% of the fuel mass is burned*
θ_{10-75}	*CAD difference between 10% and 75% of the fuel mass burned*
θ_{10-90}	*Rapid burning angle - CAD difference between 10% and 90% of the fuel mass burned*
Λ	*excess air ratio*
σ_{IMEP}	*IMEP standard deviation*

Acronyms

BTE	*brake thermal efficiency*
CAD	*crank angle degrees*
COV	*coefficient of variation in the IMEP*
DI	*direct injection*
ED	*ethanol decomposition*
EOI	*end of injection*
HC	*Hydrocarbons*
HRR	*heat release rate*
ICE	*internal combustion engine*
IMEP	*indicated mean effective pressure (gross)*
LHV	*lower heating value*
MD	*methanol decomposition*
MSR	*methanol steam reforming*
PN	*particle number concentration*
SI	*spark ignition*
SOI	*start of injection*
TCR	*thermochemical recuperation*

TDC	*top dead center*
WHR	*waste heat recovery*
WOT	*wide-open throttle*

3.1) Introduction

In recent decades, there has been a continuous effort to reduce global environmental pollution and fossil oil consumption. As the main power source for transportation, internal combustion engines (ICE) are a major source of both environmental pollution and oil consumption. Thus, the reduction of pollutant and greenhouse gas (GHG) emissions generation as well as petroleum depletion can be achieved by increasing the ICEs' efficiency and using alternative low-carbon-intensity fuels. Ethanol and especially methanol are low-carbon-intensity fuels that are considered by many as good alternatives to petroleum because of their availability from various sources such as bio-mass, coal, natural gas and renewable energy-derived hydrogen [1], [2], [3], [4]. In this article, we consider using these alcohols as the primary fuel in an ICE-reformer system with waste heat recovery (WHR) through high-pressure thermochemical recuperation (TCR).

It is known that in ICE, approximately 1/3 of the energy introduced with the fuel is wasted along with the hot exhaust gases [5]. Thus, partial utilization of this energy, also known as waste heat recovery, can lead to a significant increase in the overall ICE efficiency [6]. One possible method of WHR is utilizing the energy of hot exhaust gases to sustain endothermic fuel reforming reactions. This method is known as thermochemical recuperation [7]. TCR has two main benefits. First, it increases the fuel's LHV due to the WHR process through endothermic fuel reforming reactions — see Eq. 1 - 3. Second, the mixture of gaseous reforming products (reformate) usually has a high hydrogen content, resulting in the

increased burning velocity, higher octane number and wider flammability limits [8] and [9]. Thus, TCR allows improvement in the ICE efficiency, not only due to the WHR process but also lean-burn operating possibilities, which approach the theoretical Otto cycle and the possibility of increasing the engine compression ratio.

Aside from their previously mentioned advantages, methanol and ethanol are also excellent primary fuels for reforming since they can be reformed at relatively low temperatures (approximately 250-300°C [3], [10]) to produce hydrogen-rich reformate. Commonly investigated reforming reactions for ICE applications are methanol decomposition — MD (Eq. 1), methanol steam reforming — MSR (Eq. 2), and low-temperature ethanol decomposition — ED (Eq. 3) [11], [12], [13].

$$CH_3OH_{(g)} \rightarrow CO + 2H_2 \qquad \Delta H = 90\ kJ/mol \qquad (1)$$

$$CH_3OH_{(g)} + H_2O_{(g)} \rightarrow CO_2 + 3H_2 \qquad \Delta H = 50 kJ/mol \qquad (2)$$

$$C_2H_5OH_{(g)} \rightarrow CH_4 + CO + H_2 \qquad \Delta H = 50 kJ/mol \qquad (3)$$

In this work, we focused mainly on MSR and ED due to the problems of catalyst stability and deactivation that are frequently observed in the MD process [14], [15]. It is possible that newly developed catalysts will make MD a beneficial option in the future [16].

Methanol reforming schemes investigated in the past showed up to 40% brake thermal efficiency (BTE) improvement compared to their gasoline counterparts but have also exhibited serious problems [17]. The main problems reported include uncontrolled combustion, catalyst deactivation, cold start and engine maximal power loss due to reduced volumetric efficiency. The latter is a result of supplying gaseous reformate into the intake system that reduces the partial pressure of the air in the intake manifold, and the absence of an evaporative cooling effect compared to the case of a liquid fuel port injection.

More recent studies have reported on a high-efficiency, low-emission hydrogen-fueled ICE, for which the problems of reduced power and uncontrolled combustion were solved by the direct injection (DI) of hydrogen [18]. Hagos et al. [19], [20] studied the combustion of syngas (H2 + CO) derived from biomass gasification in a DI SI engine and reported on the possibility of CO and HC emissions reduction together with NOx emissions increases at higher loads. Li et al. [21] and Shimada & Ishikawa [22] studied the onboard reforming of hydrous ethanol with a reformate supply to the intake manifold. Both reformate gas and unreformed ethanol were burned for power production. They reported on engine efficiency improvement up to 18%, together with a substantial decrease in NOx, CO and THC emissions. Yoon [23] studied reformer design limitations for the steam reforming of methanol. He [24] proved that H_2 and CO participation in the combustion process of ICE results in the increase of O, H and OH radicals' concentration and hence improves the flame propagation and combustion process. Recent studies propose solving the cold start problem by integrating the reforming system in an electric-hybrid vehicle and keeping a small on-board pressurized vessel with reformate for start-up or injection of some of the primary fuel with a port fuel injector [20], [25]. In a previous study [26], we suggested the high-pressure TCR concept and showed that performing the reforming reactions at high pressure is essential to enabling direct injection of the reformate. Otherwise, a significant fraction of the engine power would be required to compress the reformate prior to its injection [26]. In [27], Peppley showed that a commercial $CuO/ZnO/Al_2O_3$ catalyst was able to support MSR reactions without a significant deactivation problem up to a pressure of 40 bar. Since no evidence of catalyst stability at high-pressure MD was reported, we focused our research on MSR. Assuming that an MD catalyst will prove to be stable at high pressures, this reaction may be beneficial because there will be no need to carry, preheat and evaporate water in the reformer; the reformate heating value will be greater; and lower injection pressure will be required. An advantage of MSR over MD is that the presence of CO_2 in the reformate greatly contributes to the

decrease of the in-cylinder temperature and thus leads to the reduction of NOx formation.

Previously [26], we conducted a simulation of ICE with a high-pressure TCR system based on methanol steam reforming and showed that the BTE improvement of 14% can be achieved at a rated power regime compared to the gasoline-fed counterpart. Previous simulations also showed that engine feeding with MSR and ED products results in reduced pollutant emissions compared to gasoline [25]. BTE — in the case of ICE feeding with MSR products — was predicted to be higher compared to ED and gasoline [25].

3.2) Objectives

The research reported in this article aimed at an experimental proof of previous theoretical findings and demonstrated that a DI SI ICE fed by MSR reforming products can efficiently operate at an injection pressure proven to be feasible for high-pressure TCR as a milestone to creating a complete system of ICE with high-pressure thermochemical recuperation.

Another important aim was to study the influence of the injection pressure and timing on the engine efficiency and pollutants formation at a constant engine operation mode. The latter investigation was essential because of a need to find the lowest injection pressure, which allows efficient operation of a DI SI ICE fed by MSR reforming products, as a milestone on the way towards creating a complete system of ICE with high-pressure TCR.

An additional goal was to assess the available enthalpy of the exhaust gas needed for fuel reforming and to analyze the influence of the injection timing on this important parameter.

3.3) Methodology

3.3.1 Experimental set-up

The experimental setup is based on a single-cylinder, direct-injection SI engine designed to operate with the direct injection of various gaseous fuels such as MSR, ED, methane etc., as well as a carburetor gasoline-fed engine (baseline configuration). The engine was built as a part of the laboratory system of ICE with high-pressure TCR aimed at proving the feasibility of the system. Fig. 3.1 shows a schematic of the experimental setup.

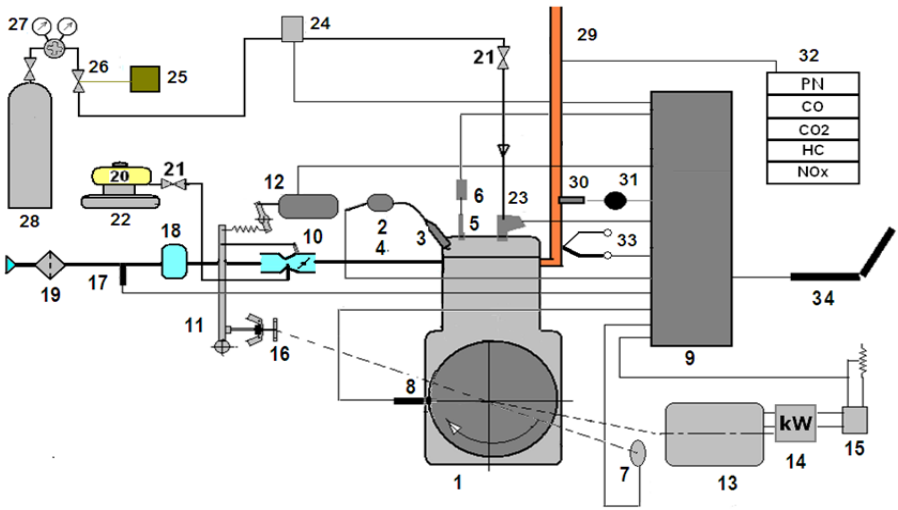

Figure 3.1 Schematic of the experimental setup. 1 - Robin EY20-3 single cylinder ICE; 2 - ignition coil; 3 - spark plug; 4 - air intake system; 5 - pressure transducer; 6 - charge amplifier; 7 - crankshaft encoder; 8 - TDC proximity sensor; 9 - data acquisitor and controller; 10 - throttle; 11 - centrifugal speed governor; 12 - linear actuator; 13 - generator; 14 - power gauge 15 - trace driven generator load; 16 - crankshaft driven gear of the engine speed governor; 17 - air flow meter; 18 - pressure wave damper; 19 - air filter; 20 - gasoline tank; 21 - valve; 22 - electronic scales; 23 - DI gas

injector; 24 – gas flow meter; 25 – hydrogen detector; 26 – emergency self-acting stop cock; 27 – pressure regulator; 28 – gas cylinder; 29 – exhaust line; 30 – O2 sensor; 31 – air to fuel ratio gauge; 32 – exhaust gas analyzers; 33 – thermocouple; 34 – computer [38]

The laboratory engine was based on a Robin-EY20-3 4-stroke spark ignition (SI) air-cooled, single cylinder ICE (1) coupled with a Sincro GP100 2.2kW AC 230 V generator (13). This engine was selected as the basis for the first prototype of a DI MSR-fed engine because of the extra space in the cylinder head that enabled the relatively easy addition of a gas-DI injector and a pressure transducer. The main parameters of the baseline engine are listed in Table 1.

Table 3.1 Specifications of Robin EY-20 ICE

Bore x Stroke, mm	*67x52*
Displacement, cm^3	*183*
Compression ratio	*6.3*
Power, kW @ speed, rpm	*2.2 @ 3000*
Continues BMEP @ 3000 rpm, bar	*4.8*
Gasoline feed system	*Carburetor*

The original ICE ignition system was replaced by an AEM 30-2853 coil (2) and a Denso IWF 24 Iridium spark plug (3) to enable a spark charge and spark timing variation.

Engine control and data logging were carried out with a dSPACE DS 1104 controller board (9) connected to a computer (34). In-cylinder pressure and crank angle measurements for a combustion process analysis were performed with a Kistler crankshaft encoder 2613B (7) at a resolution of 0.5^o mounted on the free end of the generator shaft; a Kistler 6061B water-cooled pressure transducer (5) and a Kistler 5018 charge amplifier (6). The pressure transducer was installed in the cylinder head according to the manufacturer instructions.

The desired engine speed was regulated by varying the spring load of the governor with a linear actuator (12) in the case of gasoline-fed operating

and by changing the quantity of the injected fuel and load for the case of gaseous wide-open-throttle (WOT) operation. The engine load was controlled via resistors and a rheostat, which were connected to the gen-set generator.

The gaseous fuel flow was measured by a Bronkhorst F111-AI-70K-ABD-55-E mass flowmeter (24). Conversion between various gas types was performed using FLUIDAT software based on the constant pressure heat capacities of the mixtures. Gasoline consumption was measured using the digital scales GF-12K from A&D Ltd. (22).

Gaseous fuels were supplied to the engine from premixed compressed gas vessels (28) with a mix accuracy of 1% of the lowest concentration species that was provided by a supplier of gas mixtures. The desired injection pressure was set by a pressure regulator.

The CO_2 and CO concentrations were measured from a dried exhaust gas sample line with a California Analytical Instrument (CAI) 600 series NDIR analyzer. The NO_x was measured from the same sampling line using a Thermal Converter 501x and NO_x chemiluminescent analyzer 200EH from Teledyne Instruments. Total hydrocarbons (HC) were measured directly from the exhaust line with a CAI 600 series FID HC analyzer. The nanoparticle number concentration (PN) and size distribution were measured with an Engine Exhaust Particle Sizer 3090 (EEPS) equipped with a 379020A rotating disk thermodiluter; both are produced by TSI (32).

The intake air flow was measured by a VA-420 flow sensor and was verified by the calculation of an exhaust gas carbon balance and by using a wide-band Lambda sensor kit LC-1 from Innovate Motorsports, which was based on a Bosch LSU 4.2 O_2 sensor (30).

In the research, we used an in-house-developed direct gaseous fuel injector. The injector was developed based on a commercial Magneti Marelli IHP072 gasoline DI injector. The modification was made to the

nozzle to allow higher volumetric flow rates required for gaseous fuel injection. The flow diameter of the injector was 0.85 mm^2, and its discharge coefficient was in the range of 0.87 ± 0.07. Further details regarding the injector can be found in [28]. The relative location of the injector, spark plug and pressure transducer can be seen in Fig. 2. The optimization of the location and orientation of the gas DI injector was beyond the scope of this work and is not discussed hereinafter.

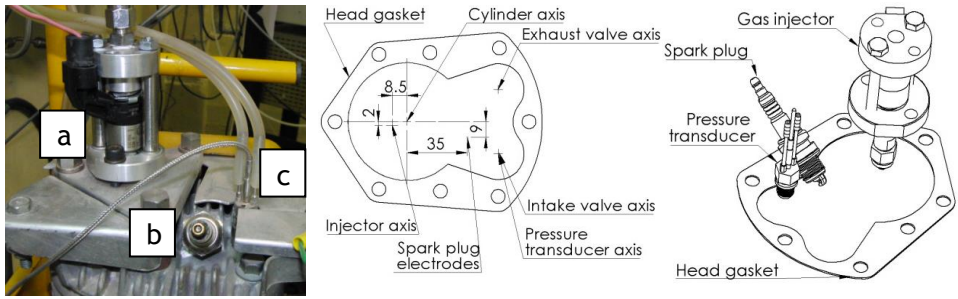

Figure 2.2 On the left: a picture of the gas injector (a) spark plug (b) and pressure transducer (c) as installed on the cylinder head. In the middle: a drawing of the same components' orientation with the cylinder head omitted to enable a clear view of the components. On the right: the relative location of the spark plug, injector and pressure transducer (dimensions are shown in mm). The spark plug electrodes and injector nozzle are located 12 mm and 0.3 mm above the gasket plane, respectively [38]

The ignition timing for each fuel was constant and set as the MBT value for the specified speed at WOT and the mid-range of the air excess factor: for MSR, @ λ=2; for ED, @ λ=1.5; and for gasoline, @ λ=1. Obtaining the MBT ignition timing values for each studied engine operating mode was not possible due to limited amount of available MSR and ED gases.

3.3.2 Data Processing

The measured data were processed to obtain the results as described in the following section. The gross indicated mean effective pressure (IMEP) is defined following Eq. 4:

$$IMEP = \frac{\int pdV}{V_d} = \frac{W_{i,g}}{V_d} \qquad (4)$$

Where as V_d is the displaced volume; V is the cylinder volume; p is the cylinder pressure; and $W_{i,g}$ is the gross indicated work.

The IMEP was calculated by integrating the in-cylinder pressure values over the cylinder volume for the compression and expansion strokes only (gross). The integration was performed numerically using the trapezoidal method. For every engine regime shown in this work, approximately 100 cycles were measured, and the IMEP shown is that of the average cycle for the considered regime. An important parameter of the engine is the IMEP coefficient of variation (COV). It is defined as the standard deviation of the IMEP divided by the mean IMEP (Eq. 5) [30]:

$$COV = \frac{\sigma_{IMEP}}{IMEP} \qquad (5)$$

Where as σ_{IMEP} is the IMEP standard deviation and IMEP is the average IMEP of all cycles.

The gross indicated efficiency (η_i) was calculated following Eq. 6 [30]:

$$\eta_i = \frac{W_{i,g}}{m_f \cdot LHV_f} \qquad (6)$$

Where as m_f is the fuel mass supplied to the cylinder per cycle and LHV_f is the lower heating value of the fuel.

For the case of reforming products, the indicated efficiency was calculated based on the primary fuel mass that is required to produce the reforming products and the primary fuel's LHV. For example, the indicated efficiency for the MSR products was calculated according to Eq. 7.

$$\eta_{MSR} = \frac{W_{i,g}}{\frac{n_M \cdot M_M}{n_W \cdot M_W + n_M \cdot M_M} \cdot m_{MSR} \cdot LHV_M} \qquad (7)$$

Where as $W_{i,g}$ is the gross indicated work; m_{MSR} is the MSR products mass supplied to the cylinder per cycle; n_M is the number of methanol moles participating in the MSR reaction; n_W is the number of water moles participating in the MSR reaction; M_M is the molar mass of the methanol; M_W is the molar mass of water; and LHV_M is the lower heating value of the methanol.

The burned mass fraction and heat release rate (HRR) results were obtained by processing the measured values of the in-cylinder pressure and piston position using GT-Power software. Pressure pegging was performed using the least squares method as described in [31]. Because the injection of gaseous fuel started soon after the inlet valve close, in these cases, the method was applied for the compression period after the end of the injection and before the ignition. Moreover, all pegging results were double-checked using another method, where the error between the measured and simulated (using GT-Power) pressure values during 40 CAD after the intake valve closing in the compression stroke is minimized by applying a pressure offset shift. An advantage of this approach is that it uses extra measured values, such as fuel mass and fresh air contents in the cylinder. Both methods produced similar results in the considered range of engine operating modes. A two-zone combustion methodology was used by applying the first law for control volume — Eq. 8 and 9 [32].

$$\frac{d(m_u e_u)}{dt} = -p\frac{dV_u}{dt} - Q_u + \left(\frac{dm_f}{dt}h_f + \frac{dm_a}{dt}h_a\right) + \frac{dm_{f,i}}{dt}h_{f,i} \qquad (8)$$

$$\frac{d(m_b e_b)}{dt} = -p\frac{dV_b}{dt} - Q_b - \left(\frac{dm_f}{dt}h_f + \frac{dm_a}{dt}h_a\right) \qquad (9)$$

Where as m_u is the unburned zone mass; e_u is the unburned zone energy; p is the in-cylinder pressure; V_u is the unburned zone volume; Q_u is the unburned zone heat transfer rate; m_f is the fuel mass; h_f is the fuel enthalpy; m_a is the air mass; h_a is the air enthalpy; $m_{f,i}$ is the injected fuel mass; $h_{f,i}$ is the injected fuel enthalpy; m_b is the burned zone mass; e_b is the burned zone energy; V_b is the burned zone volume; and Q_b is the burned zone heat transfer rate.

Following the applied two-zone model, at the beginning of the combustion, the entire cylinder content is in the unburned zone, and at any time step, a certain amount of unburned mixture is transferred to the burned zone. In the burned zone, the equilibrium of 11 possible combustion products is assumed; thus, the temperature and pressure are obtained. Iterations for the amount of unburned mixture that transferred to the burned zone are made until the obtained pressure matches the measured pressure. Additional information that was required for the burned mass fraction calculation is the heat transfer to the cylinder walls and a residual gas fraction in the cylinder. The heat transfer was calculated using the Woschni engine model without swirl or tumble. A convection heat transfer multiplier was applied to match the measured pressure results and measured exhaust gas temperatures assuming that 100% of the fuel mass is burned. The residual gas fraction was calculated by creating an engine model in GT-Power software and calibrating it to the measured results, and then re-applying the residual gas fraction to the combustion analysis. Based on the obtained instantaneous values of the burned mass fraction, the following parameters were calculated and analyzed: flame development angle θ_{0-10}, rapid burning angle θ_{10-90} and $\theta_{10-75}-$ CAD difference between 10% and 75% of the fuel mass burned.

The heat release rate was calculated using the same assumptions but with a single-zone first law Eq. 10 for control volume [30].

$$HRR = -p\frac{dV}{d\theta} - Q - \frac{d(m \cdot e_s)}{d\theta} \quad (10)$$

Where as V is the cylinder volume; θ is the crank angle; Q is the heat transfer rate; m is the in-cylinder mass; and e_s is the sensible energy of the cylinder content.

The maximum pressure was calculated for the averaged and filtered engine cycle for each operating mode. The available exhaust enthalpy was calculated based on the measured fuel flow rate, air-to-fuel ratio and exhaust gas temperature assuming an ideal gas mixture and the exhaust gas composition of complete fuel combustion for specific heat calculations. The reference state for enthalpy availability was chosen as 200°C. This reference temperature was chosen to provide a sufficient temperature gradient for a heat exchange between the exhaust gases and the primary fuel that is expected to enter the reformer after preheating it at approximately 150°C.

The combustion efficiency η_c was calculated according to Eq. 11 [30]:

$$\eta_c = 1 - \frac{\left(\dot{m}_a + \dot{m}_f\right)\left(\sum_i x_i \cdot LHV_i\right)}{\dot{m}_f \cdot LHV_f} \quad (11)$$

Where as $\dot{m}_f$ is the fuel flow rate; $\dot{m}_a$ is the air flow rate; x_i is the mass fraction of species i; LHV_i is the LHV of species i; and LHV_f is LHV of the fuel.

The heating value of 44 kJ/kg was assumed for HC. The hydrogen content in the exhaust gases was not measured and was thus omitted from the calculation, which introduces some upward bias in the obtained values of combustion efficiency.

A conversion of the measured pollutant concentrations to specific pollutant emissions (in g/kWh) was performed based on a carbon balance analysis, measured fuel flow rates and the assumption that the lube oil burn and particulate formation effects on the carbon balance are negligible (Eq. 12).

$$E_i = \frac{\dot{m}_f \cdot y_{c,fuel} \cdot y_i \cdot M_i}{M_C \cdot \sum y_j \cdot \dot{W}_{i,g}} \qquad (12)$$

Where as E_i is the specific pollutant emission of pollutant i; $\dot{m}_f$ is the fuel mass flow rate; $y_{c,fuel}$ is the fuel's carbon mass fraction; y_i is the molar fraction of pollutant i; M_i is the molecular weight of pollutant i; M_C is the molecular weight of carbon; y_j is the CO/CO$_2$/CH$_{1.85}$ molar fraction; and $\dot{W}_{i,g}$ is the gross indicated power.

The uncertainty of the calculated parameters was assessed using Eq. 13 [33]:

$$\delta R = \left(\sum_{i=1}^{N} \left(\frac{\partial R}{\partial X_i} \delta X_i \right)^2 \right)^{1/2} \qquad (13)$$

Where as δR is the uncertainty of calculated parameter R; $\frac{\partial R}{\partial X_i}$ is the partial derivative of R with respect to measured value X_i ; and δX_i is the accuracy of measured value X_i .

It is known that the IMEP calculation is insensitive to random noise and absolute pressure referencing errors but is very sensitive to crank phasing errors [34]. The calculation also involves numerical integration. Thus, COV and IMEP uncertainty were calculated by applying the approach suggested by Moffat [33] for computing uncertainty when a computer program is used for the results analysis. An angle phase error of ±0.5^o was used in this calculation (equal to the encoder resolution). The average IMEP error was

found to be 2.5% with a maximal error of 5% that was observed at idle and engine feeding with a gaseous fuel. Table 3.2 summarizes the accuracy of the measured data and uncertainty of the calculated parameters. The uncertainty values calculated for COV; indicated efficiency, combustion efficiency; and NO_x, HC, CO and CO_2 emissions are shown as error bars in Figs. 3.3 and 3.6 - 3.11. The uncertainty values are shown for all measurement results presented in Figs. 3.3 and 3.6 - 3.11. However, in some cases, due to the wide range of values shown in one graph, error bars may not be seen due to their relatively small absolute values.

Table 3.2 Accuracy of measured data and uncertainty of calculated parameters.

Accuracy of measured parameters	
Device	*Manufacturer, (Accuracy)*
Crankshaft encoder 2613B	*Kistler Instrument A.G., (Resolution 0.5º, Dynamic accuracy +0.02º at 10000 rpm)*
Charge Amplifier Type 5018	*Kistler Instrument A.G., (<±0.3% at 0-60˚C)*
Water cooled pressure transducer 6061B	*Kistler Instrument A.G., (Max. linearity ≤±0.29% FS*)*
Mass flow meter F111-AI-70K-ABD-55-E	*Bronkhorst High-Tech B.V., ±(0.5% of MV*+0.1% of FS*)*
Air flow sensor VA420 with integrated measuring unit	*CS Instruments GmbH, (±1.5% of MV*)*
Wide-band Lambda sensor LC-1 kit	*Innovate Motorsports based on Bosch LSU 4.2 O_2 sensor, (at λ=1: ±0.007; at λ=1.7: ±0.05)*
NO_x analyzer 200EH	*Teledyne Instruments, (0.5% of MV*)*
HC analyzer 600 series	*California Analytical Instruments, (±0.5% of FS*)*
CO, CO_2 analyzer 600 series	*California Analytical Instruments, (±1% of FS*)*

Exhaust Engine Particle Sizer 3090	*TSI, NA*, ***
Rotating Disk Thermodiluter 379020A	*TSI, (±10%)*
Power gauge (Wattmeter) DW-6060	*Lutron Electronics Company, (±1%)*
Digital scales GF-12K	*A&D Ltd, (±0.1 g)*
Maximal uncertainty of calculated parameters	
IMEP	*±5%*
Indicated Power	*±5%*
COV	*±4%*

*FS – full scale, MV – Measured value, NA – Not available.

*** It was found in [29] that the new SOOT matrix recently developed by TSI to improve the EEPS PN concentration and size distribution measuring accuracy (which was used in our study) provides PN concentration readings in the range of 84% to 96% of those obtained with a scanning mobility particle sizer (SMPS) across a wide range of diesel engine operating conditions.*

3.3.3 Available Enthalpy of Exhaust Gas

When considering an onboard fuel reforming system, it is important to make sure that the exhaust gas possesses enough energy to sustain the endothermic reforming reactions. In our previous work [35] we showed that full conversion of methanol is not necessarily beneficial because the non-reformed methanol can be reused relatively easily – Fig. 3. In order to achieve higher flow rate through the injector, cooling of the reformate before its injection is required. On the other hand, the enthalpy of the reformate as it exits the reformer can be utilized to preheat the incoming methanol-water mixture before it enters the reformer. Thus, in our approach we use a heat exchanger to serve both of these purposes (Fig 3).

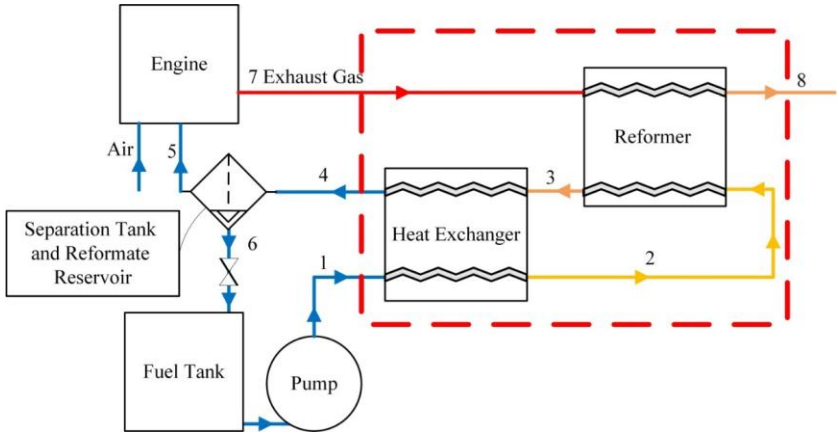

Figure 3. Schematic of the considered high-pressure TCR system. 1 - methanol and water mix (1:1 molar ratio) at high pressure; 2 - preheated methanol and water mix; 3 - hot reforming products with residues of unreformed methanol and water; 4 - cooled reforming pro ducts with condensed unreformed methanol and water; 5 - cooled gaseous reformate; 6 - condensed unreformed methanol and water; 7 - hot exhaust gas; 8 - cooled exhaust gas [45]

At steady-state conditions, the flow rates of the primary fuel that enters the reformer (1), of the gaseous reformate that enters the engine (5) and of the exhaust gas (7) are interrelated. The relationship between (5) and (7) depends on λ. The relationship between (1) and (5) can be expressed by the methanol conversion fraction f:

$$f = (\dot{n}_{M,1} - \dot{n}_{M,4}) / \dot{n}_{M,1} \qquad (1)$$

Where $\dot{n}_{M,1}$ is the methanol molar flow rate at the entry to the heat exchanger (1) and $\dot{n}_{M,4}$ is the methanol molar flow rate at the heat exchanger outlet (4) [mol/s].

It is useful to normalize both the heat required for reforming and the exhaust gas available enthalpy by the available enthalpy of the fuel that enters the engine. Thus, the overall fuel flow rate is canceled when dividing and the resulting expressions allow simpler analysis unaffected by

the fuel flow rate and hence the engine power. The normalized heat (in %) required for reforming ($\bar{q}$) was calculated according to Eq. (15):

$$\bar{q} = \frac{f\left(h_{CO_2}(T+\Delta T)+3\cdot h_{H_2}(T+\Delta T)\right)+(1-f)\left(h_{H_2O,l}(T+\Delta T)+h_{M,l}(T+\Delta T)\right)-\left(h_{H_2O,l}(T)+h_{M,l}(T)\right)}{4\cdot f\cdot LHV_f}\cdot 100\%$$

Where: $h_i(T)$ - total enthalpy (sum of the enthalpy of formation and the sensible enthalpy) of species i at temperature T [J/mol]; LHV_f - lower heating value of MSR reformate per mole ($181.37\cdot 10^3$ [J/mol]); ΔT - temperature difference between heat exchanger inlet (1) and outlet (4) [K]. Subscript l denotes liquid phase.

The normalized available enthalpy ($\bar{h}_{av}$) was calculated by subtracting the enthalpy of the cold exhaust gas (8) from the enthalpy of the hot exhaust gas (7) and dividing it by the available enthalpy of the fuel entering the engine (5), while assuming exhaust gas is an ideal gas and its composition is that of complete combustion products (Eq. 16):

$$\bar{h}_{av}(\lambda, T_7, T_8) = \frac{\left(1+\lambda\left(\frac{\dot{n}_a}{\dot{n}_f}\right)_{st}\right)\left(\sum y_i \int_{T_8}^{T_7} c_{p,i}\,dT\right)}{LVH_f}\cdot 100\% \qquad (3)$$

Where: T_8 - exhaust gas temperature at the reformer inlet (8) - Fig. 3 [K]; T_7 - exhaust gas temperature at the reformer outlet (7) [K]; $\dot{n}_f$ - fuel flow rate at the engine inlet (5) [mol/s]; $\dot{n}_a$ - air molar flow rate [mol/s]; y_i - molar fraction of species i based on complete combustion stoichiometry; $c_{p,i}$ - specific heat of species i at constant pressure [J/mol/K].

3.4) Results and Discussion

This section consists of three main parts. The first part discusses the reformate influence on the combustion process in an ICE and provides a comparison with gasoline and methane. The second part discusses the effects of engine feeding by reforming products based on its performance in terms of the indicated efficiency and pollutant emissions. The third part deals with an available exhaust gas enthalpy to necessary to sustain the endothermic reforming reactions.

3.4.1 Combustion Process

Cycle-to-cycle variation is an important parameter indicating the quality of the combustion process for two main reasons. First, the optimum spark timing is normally set for an average cycle. Thus, for a fast burning cycle, the ignition is actually over-advanced, and for a slow burning cycle, it is over-retarded. This results in the loss of power and efficiency. Second, fast burning cycles lead to high in-cylinder pressure, high pressure rise rates, and high NO_x formation and may also lead to knock appearance. These fast cycles limit the engine's compression ratio and affect the possibility of tuning optimization [30]. Cyclic variations in the cylinder are caused by a mixture motion variation, especially in the vicinity of the spark plug because they change the early flame development and thus affect the fuel burning behavior and the heat release rate. The fuel burning velocity has significant influence on the cycle-to-cycle variability since it influences the early flame development and thus affects the overall heat release rate. The higher burning velocity of a fuel-air mixture reduces the cyclic variations and hence has a beneficial effect on engine efficiency and emissions. Fig. 3.4 shows the COV of MSR and ED as function of λ at constant ignition timing and WOT compared to the reference cases of gasoline and methane.

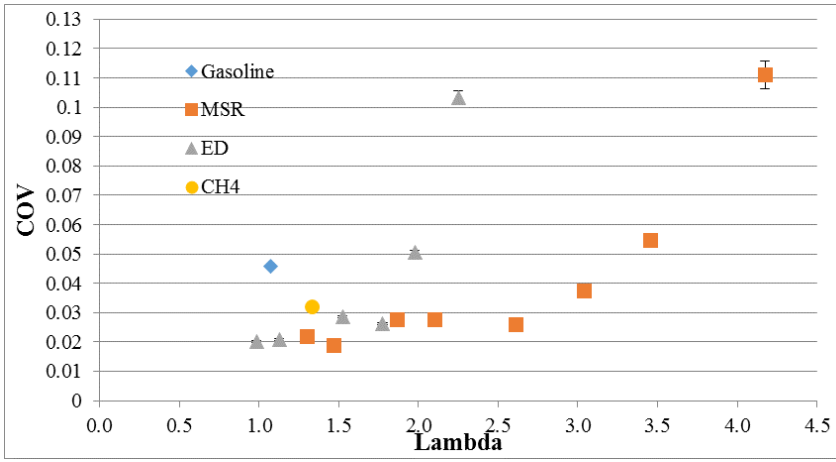

Figure 3.4 Cycle-to-cycle variation as a function of Lambda for various fuels. Engine speed 2800 rpm; the MSR and ED operated at WOT, and the injection pressure was at 40 bar. The gasoline and methane were at IMEP 3.6 bar. The ignition timing for gasoline MSR and ED was constant at 333, 347 and 339 CAD, respectively. The error bars show the uncertainty of the calculated COV values [38]

As expected, the COV for ED and MSR was substantially lower than in the cases of engine feeding with gasoline and methane thanks to the presence of hydrogen in the reformate that increases the mixture laminar burning velocity [35]. Moreover, the COV values in the cases of engine feeding with reforming products do not exceed 0.05 up to λ=3.5 and λ=2 for MSR and ED, respectively. COV ≤0.05 is widely accepted as a sign of stable, well-tuned engine operation [2]. Thus, in the case of ICE feeding with reformates, efficient operation is possible at very lean fuel-air mixtures, especially for MSR reformate fuel. The MSR reformate allows stable operation for a wider range than ED due to the higher molar fraction of hydrogen in the mixture (75% compared to 33.3%). It is important to underline that the ICE was able to work unthrottled with both MSR and ED reformates up to low idle. However, for ED, the COV at high idle reached an unacceptably high value of 0.37 due to the misfire appearance, which resulted in poor combustion efficiency and high HC emissions (Fig. 3.7, 3.10). *Thus, for this*

setup, unthrottled operation with ED in the entire load range was not recommended. However, this may not be true for an engine with a higher compression ratio, different injector nozzle, optimized spark timing for WOT idle, and a different injector and spark plug relative location. It should be noted that for MSR reformate, even with the negative influence of all of the above mentioned circumstances, the COV value at the WOT idle operating mode did not exceed 0.11.

The fuel burning velocity has also a significant effect on the heat release process. A high burning velocity leads to an increase of HRR. The latter results in thermal efficiency improvement because the engine working cycle approaches the theoretical Otto cycle. However, at the same time, the maximal in-cylinder pressure, pressure rise rate and heat transfer losses increase due to higher in-cylinder temperatures. An example of a few typical HRR curves for the different fuels considered in this work is shown in Fig. 3.5

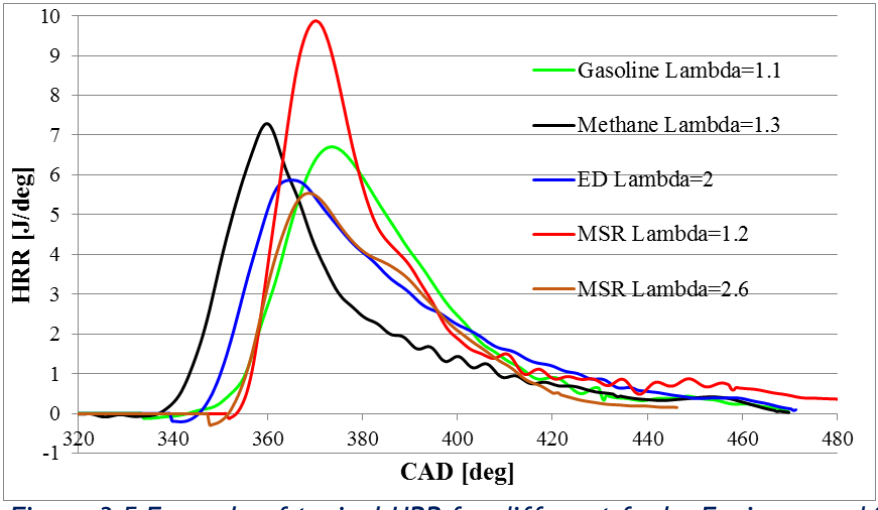

Figure 3.5 Example of typical HRR for different fuels. Engine speed 2800 rpm; measured power 800 W; gas injection pressure, 40 bar [38]

As seen from Fig. 3.5, the HRR of MSR products is significantly higher than those of gasoline and methane, but can be moderated by increasing λ to a

degree where their HRR is comparable. Since the brake power for all shown cases is the same, the highest brake thermal efficiency is achieved for the case where the least heat is released (i.e., the least area under the HRR-CAD graph). The highest BTE is obtained for engine feeding with MSR reformate at λ=2.6. This is a result of the positive effect of reduced pumping and heat transfer losses that overcome the negative effect of lower HRR. At the considered engine operating mode (800 W @ 2800 rpm) in case of ICE feeding with MSR reformate, the highest efficiency is achieved at the highest possible λ. When power is kept constant, the maximal pressure p_{max} does not change substantially as the air-fuel ratio varies. For example, when λ changes from 1.2 to 2.6, the values of p_{max} change from 17.5 to 16.9 bar only. This is a result of two contradicting effects. The HRR decreases at higher air excess factors, thus aiming at maximal pressure reduction. At the same time, cylinder pressure at the start of compression increases with λ rise, as a result of throttle opening, thus acting toward the maximal pressure increase. Fig. 3.6 shows a comparison of flame development (θ_{0-10}) and rapid burning angle (θ_{10-90}) parameters for different fuels and air-fuel ratios.

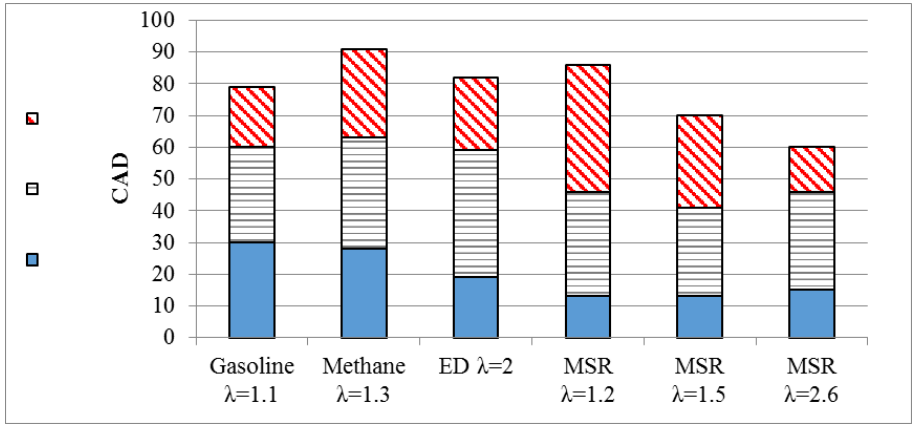

Figure 3.6 Flame propagation angles for different fuels and air excess ratios. Engine speed 2800 rpm, measured power 800 W, injection pressure 40 bar; θ_{0-10} - flame development angle; θ_{10-75} – CAD difference between 10% and 75% of fuel mass burned; θ_{75-90} - CAD difference between 75% and 90% of fuel mass burned [38]

The flame development angle (θ_{0-10}) for MSR products is much lower than those of methane, ED and gasoline – Fig. 3.6. This explains the lower COV of MSR at a wide range of excess air ratios (Fig. 3.4). It can also be seen that in the case of MSR with λ=1.5 and especially λ=1.2, the rapid burning angle (θ_{10-90}) is much higher than expected. This is a result of the insufficient flow rate through the injector, which resulted in a longer injection duration (until 15 CAD after ignition) and thus led to late end of combustion and reduced combustion efficiency. The non-optimized injector positioning (a relatively large distance between the gas injector and the spark plug) also contributed to the retarded combustion of the portion of the fuel that was injected late. In the case of a higher mass flow rate through the injector, it is expected that the rapid burning angle may be further reduced because of the shorter injection duration, which enables more time for fuel-air mixing.

The exhaust gas temperature is also an important parameter when considering a TCR system since the exhaust energy is used for the fuel reforming. Although the temperature of the exhaust gas decreases as the air-to-fuel ratio increases, the exhaust mass flow rate increases (as a result of throttle opening) and heat transfer losses to the cylinder walls decrease. Thus, the reduction of available enthalpy (when it is considered as a percentage of the fuel's energy) with Lambda increase is quite moderate compared to the observed decrease in the exhaust gas temperature (Table 3.3). It is useful to consider the available enthalpy of exhaust gas as a percentage of the energy introduced to the engine with the fuel ($\dot{m}_f \cdot LHV_f$) since this enthalpy is used to reform the same fuel and flow rates of the fuel and the exhaust gas are interrelated. For the case of MSR with λ=1.2, the enthalpy availability is exceptionally high due to the late injection that leads to fuel burning late in the expansion stroke (Figs. 3.4 and 3.5; Table 3.3). A detailed discussion on exhaust gas enthalpy is provided in section 3.4.3.

Table 3.3. Exhaust gas temperatures and available enthalpy, $\dot{W}_{i,g}$ = 1.5 kW

	Gasoline λ=1.1	Methane λ=1.3	ED λ=2	MSR λ=1.2	MSR λ=1.5	MSR λ=2.6
T_{exh} [°C]	583	454	450	634	502	396
h_{av} [kW]	1.03	0.8	1.11	1.68	1.17	0.88
Available enthalpy, % of fuel energy	16	14	19	22	18	18

3.4.2 Engine Performance

As explained in the previous section, the beneficial properties of hydrogen-rich ED and MSR fuels, together with the WHR advantages, allow for much better efficiency, especially at low loads. Fig. 3.7 shows the engine-indicated efficiency when fed with the various fuels as a function of engine load (IMEP)

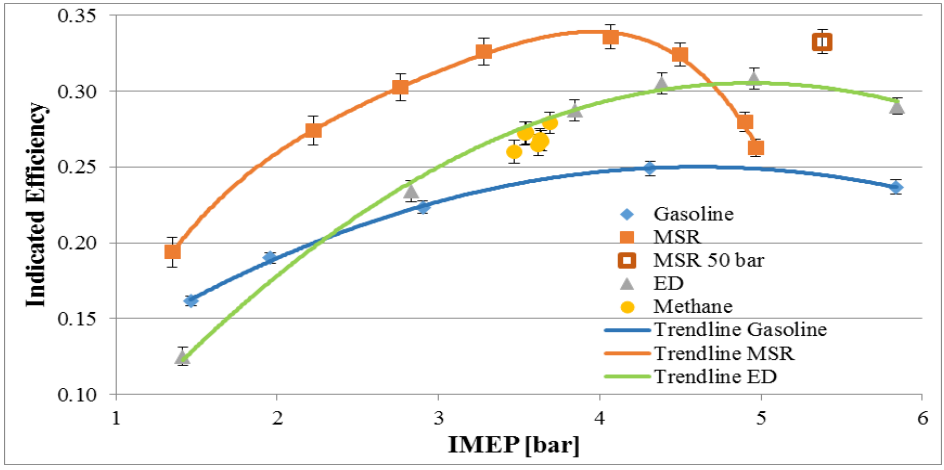

Figure 3.7 Engine-indicated efficiency at various load regimes. Engine speed 2800 rpm; ED and MSR at WOT; injection pressure at 40 bar; injection start at 230 CAD. The ignition timing for gasoline, MSR and ED was constant at 333, 347 and 339 CAD, respectively. The error bars show uncertainty for the calculated indicated efficiency values [38]

As seen from Fig. 3.7, the thermal efficiency of the engine fueled by MSR products was improved by 18-39% (relative) compared to the engine operating with gasoline. At higher loads (IMEP > 4 bar), there was an insufficient MSR reformate flow rate through the injector. This required late end of injection (up to 5 CAD before ignition) and along with a non-optimized positioning of the injector resulted in fuel combustion late in the expansion stroke (see Figs. 3.5 & 3.6) and, as a result, lower efficiency - Fig. 3.7. This problem can be resolved by increasing the injector flow area or injection pressure. In our case, the latter solution was easier, and by increasing the injection pressure up to 50 bar, we have achieved an indicated efficiency of 0.33 at an IMEP of 5.4 bar. Fig. 3.7 reveals that the reformate flow rate problem was less severe for the case of ED due to the higher energy density of the ED products compared to the MSR reformate. Although ED has this advantage over MSR, for most of the engine operating range, MSR showed superior efficiency. At low loads (close to idle), the indicated efficiency of the engine fed with MSR and ED reformates reduced rapidly, also because we worked at WOT, which led to high Lambda values and, as a result, high COV (Fig. 3.4) and non-optimized ignition timing for these regimes (which was constant throughout this experiment). In the case of engine feeding with ED, it also led to poor combustion efficiency (Fig. 3.8). This effect was less obvious for gasoline, where Lambda remained constant. However, when operating with the MSR reformate, the engine efficiency remained substantially higher compared to gasoline, even at the lowest engine loads.

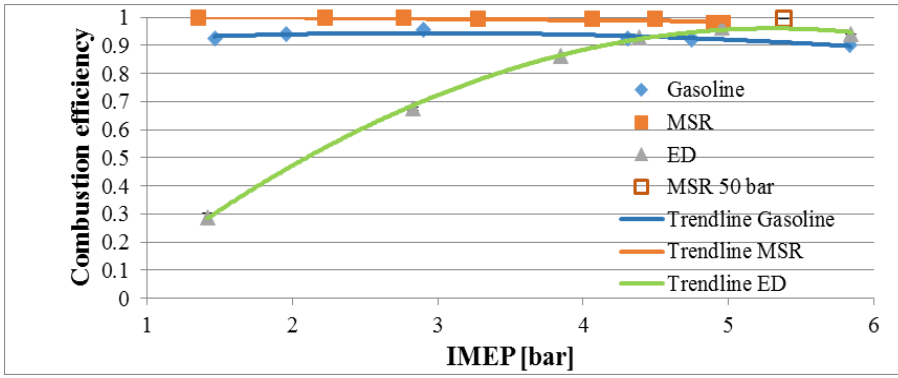

Figure 3.8 Combustion efficiency at various load regimes. Engine speed 2800 rpm; ED and MSR at WOT; injection pressure at 40 bar; injection start at 230 CAD. The ignition timing for gasoline, MSR and ED was constant at 333, 347 and 339 CAD, respectively. The error bars show uncertainty in the calculated combustion efficiency values [38]

Fig. 3.8 shows that even though it is possible to work unthrottled with the ED reformate up to idle, the combustion efficiency in this case decreases to unacceptably low values, which makes throttling the beneficial option. It is expected that this problem would be less severe for higher compression ratio engines. For MSR, a reduction in combustion efficiency is not apparent because of the wider flammability limits of the hydrogen-rich mixture (the lack of H_2 content measurement in the exhaust gas can result in some overestimates of the calculated combustion efficiency values). The reduction in indicated efficiency for the case of engine feeding with MSR may be mainly attributed to the reasons offered earlier (high COV, non-optimal ignition timing). Throttling, to some extent, may also be beneficial for MSR at low loads because of the need to reduce cycle-to-cycle variability and to ensure the available enthalpy required for primary fuel reforming.

One of the most important advantages of reformates over gasoline is the possibility of pollutant emissions mitigation due to the efficient combustion of low carbon intensity and hydrogen-rich gaseous fuel. Figs.

9-12 show a comparison of pollutant emissions between gasoline, ED and MSR reformates.

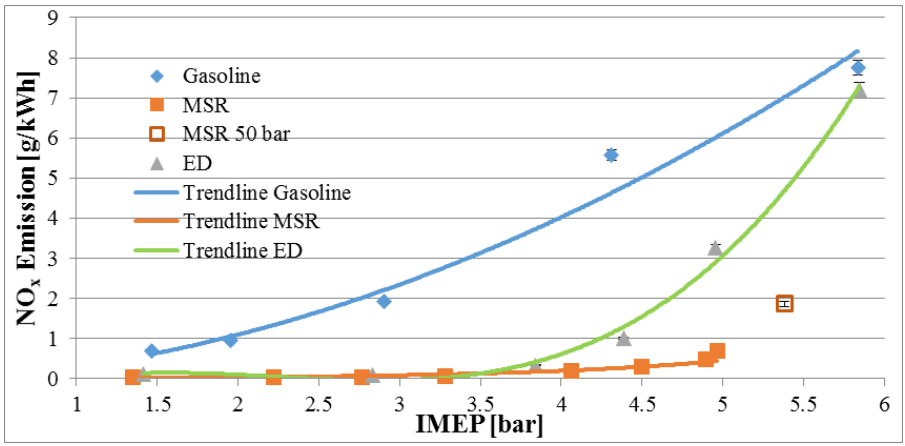

Figure 3.9 NO_x emission for gasoline, ED and MSR products as function of IMEP. Engine speed 2800 rpm; ED and MSR at WOT; injection pressure at 40 bar; injection start at 230 CAD. The ignition timing for gasoline, MSR and ED was constant at 333, 347 and 339 CAD, respectively. The error bars show uncertainty for the calculated NO_x emission values [38]

As expected, substantially lower NO_x emissions were measured for reformate fuels compared to those of gasoline-fed engines, which is due to the lean burn of reformates that allowed substantially lower maximal in-cylinder temperatures and, as a result, weaker NO_x formation. As the load increases and the mixture becomes richer, the NO_x formation process intensifies. However, in the case of engine feeding with MSR products, the fuel injected into the cylinder contains a substantial amount of CO_2 (it constitutes 17% wt. of a stoichiometric air-MSR fuel mixture). The latter works as an inherent EGR: reduces the in-cylinder temperatures and as a result leads to lower NO_x formation. The obtained results show that ICE operating with MSR products leads to a reduction of NO_x emissions by 73-94% in the entire tested range of engine loads.

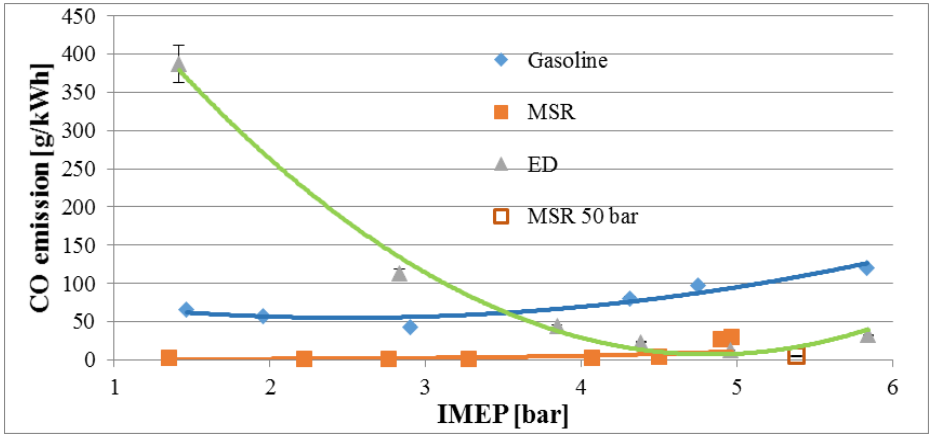

Figure 3.10 CO emission for gasoline, ED and MSR products as function of IMEP. Engine speed 2800 rpm; ED and MSR at WOT; injection pressure at 40 bar; injection start at 230 CAD. The ignition timing for gasoline, MSR and ED was constant at 333, 347 and 339 CAD, respectively. The error bars show uncertainty for the calculated CO emission values [38]

The CO emissions of direct-injection SI ICE fed with MSR products remain lower than 5 g/kWh for most of the tested operating range. For the IMEP higher than 4.5 bar, there is a significant increase attributed to the lower air excess factor, late injection and combustion, which leads to freezing CO oxidation chemistry. It is important to note that for injection pressure of 50 bars, when a more optimal fuel injection strategy can be realized, CO emissions remained below 5 g/kWh up to an IMEP of 5.4 bar. The obtained results show that the engine operating with MSR reformate leads to a reduction in CO emissions by 70-97% in the entire tested range of engine loads. The high CO emissions for the case of gasoline are influenced, of course, by the fuel supply method (carburetor). The reason for the significant CO emission increase at low loads in case of engine feeding with ED products is the work with WOT (at high λ values up to 2.7), which resulted in the poor and incomplete combustion of the ED reformate fuel (Fig. 3.8). This problem is clearly reflected in the high level of HC emissions when the ICE is fed with ED products operating unthrottled at low-load regimes (Fig. 3.11).

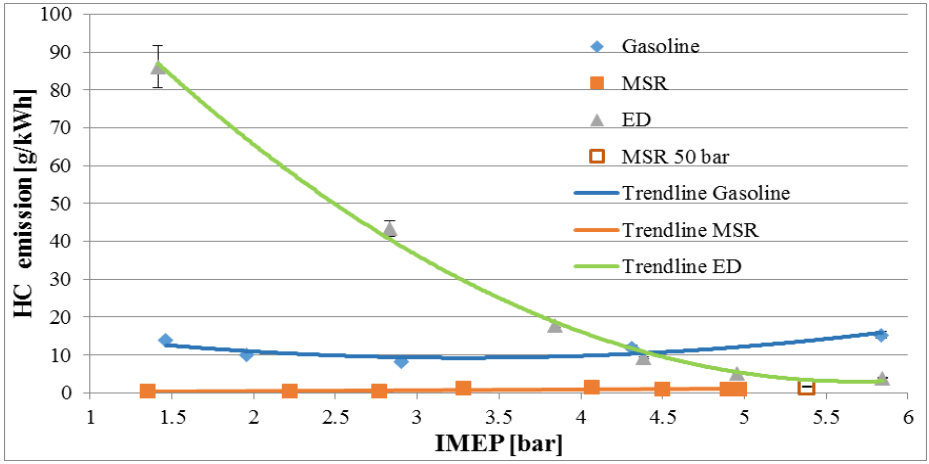

Figure 3.11 HC emission for gasoline; ED and MSR products as functions of IMEP. Engine speed 2800 rpm; ED and MSR at WOT; injection pressure at 40 bar; injection start at 230 CAD. The ignition timing for gasoline, MSR and ED was constant at 333, 347 and 339 CAD, respectively. The error bars show uncertainty for the calculated HC emission values [38]

As seen from Fig. 3.11, the HC emissions of the engine fed by MSR products are extremely low because the only source of HC formation in this case is lubricating oil. For gasoline, the emissions are higher as a result of combustion of the much richer mixture created in the carburetor compared to the reformate fuels. ICE operating with MSR products leads to a reduction in HC emissions by 85-97% in the entire tested range of engine loads. The extremely high HC emissions at low loads in the case of engine feeding with ED reformate are due to the poor combustion efficiency, as explained above (Fig. 8). The incomplete combustion of ED reformate at low loads is also misleading when CO_2 emissions are considered. As seen from Fig. 12, CO_2 emissions of the engine fed with ED reformate seem to be beneficially low, but this is only because a high percentage of carbon introduced to the cylinder with the fuel is emitted as HC or CO (Figs. 3.8, 3.10 & 3.11).

Even though our testing procedure did not exactly meet the requirements of the EPA standard CFR-40 part 1054 for non-handheld engines, we have performed a comparison with the standard limits, as shown in Table 3.4, for the purpose of relative assessment of the engine performance when fed by gasoline and MSR products.

Table 3.4 Comparison of emissions calculated according to CFR-40 part 1054 phase 3 (class I engines) based on maximum IMEP 5.4 bar for the ICE fed with gasoline and MSR products

	MSR	Gasoline	Standard limits
NO_x+HC [g/kWh]	1.1	13.5	10
CO [g/kWh]	3.5	67	610 (5 for marine generator engines)

As seen from Table 4.4, the emissions of the baseline ICE fed with gasoline exceed the standard limits, whereas in case of engine feeding with MSR products, it emits almost an order of magnitude less NO_x + HC emissions than the regulation prescribes. The obtained results give an indication of the good potential of MSR-fed ICE in achieving a substantial reduction of pollutant emissions. However, because the experiments reported in this article were conducted with a low compression ratio engine (meaning low efficiency, but also low temperature and NO_x formation) at constant speed and ignition timing, it is too early to indicate whether there will be a need for exhaust gas aftertreatment in the case of MSR-fed ICE at an automotive scale.

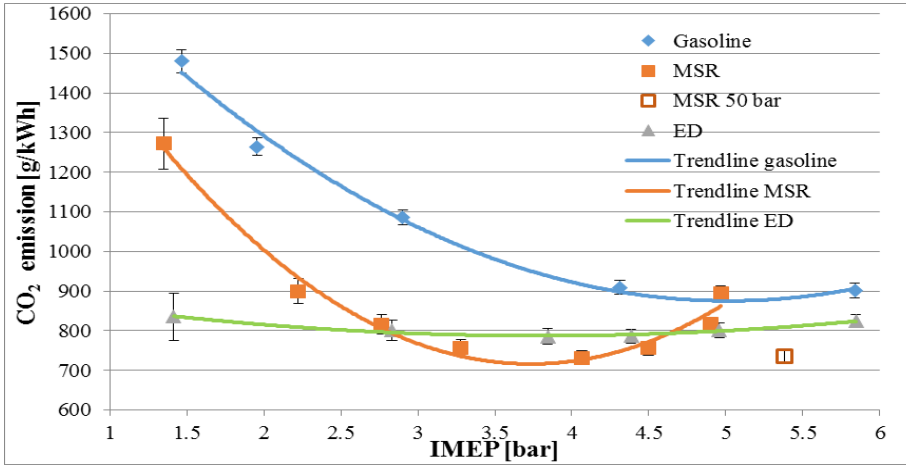

Figure 3.12 CO_2 emissions for gasoline, ED and MSR products as a function of IMEP. Engine speed 2800 rpm; ED and MSR at WOT; injection pressure at 40 bar; injection start at 230 CAD. The ignition timing for gasoline, MSR and ED was constant at 333, 347 and 339 CAD, respectively. The error bars show uncertainty in the calculated CO_2 emission values [38]

CO_2 emissions, in the cases of engine feeding with reforming products, are lower compared to gasoline in most of the operating range thanks to the increased efficiency and low carbon intensity of the alcohol primary fuels. The only exception is at the highest IMEP regime for MSR, and this is due to the reduced efficiency caused by the late end of injection that was necessary to achieve the required power at an injection pressure of 40 bars. When the injection pressure was raised to 50 bar, the CO_2 emission was reduced substantially to 735 g/kWh at IMEP of 5.4 bar as a result of the engine efficiency improvement. For comparison purposes, CO_2 emissions at the same IMEP when the engine was fed with gasoline were measured to be approximately 900 g/kWh (Fig. 3.12).

The particle number (PN) emissions proved to be much harder to assess. We did not find any clear relationship between engine operating regime and PN emissions. Even for the same operating regime, the measured PN concentrations were extremely unstable, showing different types of

behavior. Fig. 3.13 shows an example of two measurements taken for the same operating mode.

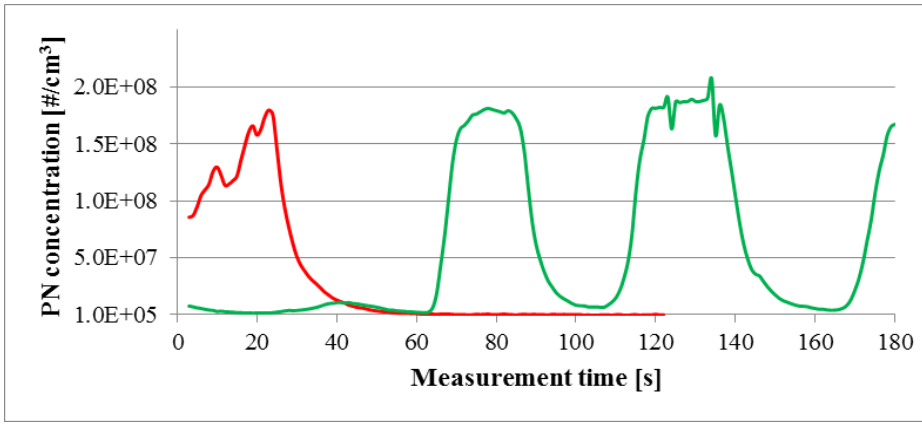

Figure 3.13 Total PN concentrations. Engine speed 2800 rpm; MSR products at WOT; λ=2.5; measured power, 850 W; injection pressure at 40 bar [38]

It is possible to distinguish a number of different patterns from the observed PN emission behavior. The red line shows a case where low PN concentrations were measured most of the time with a single sharp spike where the PN level rises above the baseline level by more than two orders of magnitude. The green line demonstrates the multiple-spike behavior of PN emissions. Measurements with low PN concentrations (close to 10^5 cm^{-3}) that are stable along the 2-3 min measurement period were recorded as well. Similar behavior in measured PN concentrations was reported previously for an SI engine [36]. The authors of this publication related these spikes to combustion chamber deposit breakup. In our measurements, the baseline level of the measured PN concentrations was found to be in the range of 10^5 - 10^6 cm^{-3}, which is close to the PN concentrations observed for a hydrogen-fueled engine where lubrication oil was the only reason for PN formation [37]. We suppose that in our case, the main sources of PN emissions are both the breakup of combustion chamber deposits and lubricant combustion. Further research is required

to better understand the mechanism and physical reasons for the observed phenomena.

3.4.3 Available Enthalpy of Exhaust Gas

Even though a possibility of unthrottled operation of ICE fueled with MSR products was demonstrated for the case of onboard methanol reforming, it is important to ensure that the exhaust gas possesses enough available enthalpy to sustain the endothermic reforming reactions. To calculate the heat required for the reforming reactions ($\bar{q}$) and the available enthalpy of the exhaust gas ($\bar{h}_{av}$), Eq. (15) and (16) were used. Fig. 3.14 shows the normalized heat required for reforming ($\bar{q}$) as a function of conversion fraction (f) and temperature difference (ΔT) between the heat exchanger inlet and outlet.

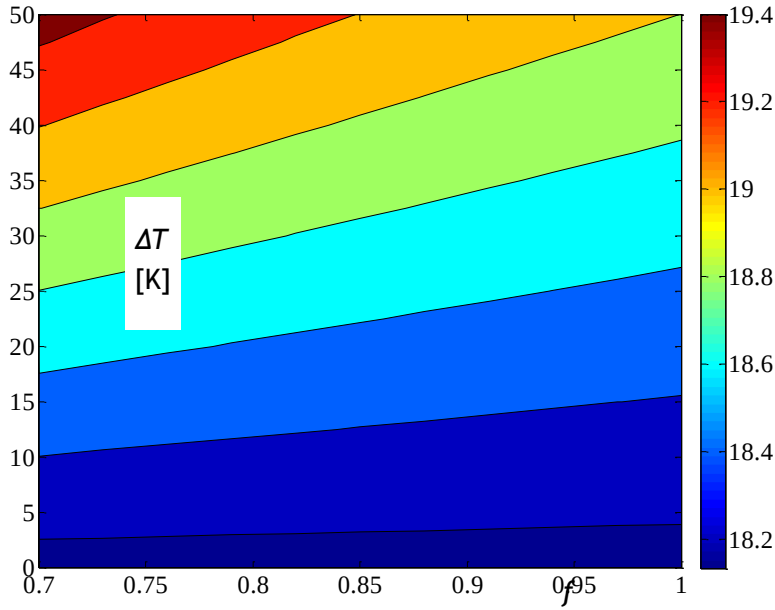

Figure 3.14 Percentage of the fuel energy delivered to the engine, which is required for reforming, as a function of the methanol conversion fraction (f) and the temperature difference (ΔT) between heat exchanger inlet (1) and outlet (4) [45]

As seen from Fig. 3.14, the required normalized heat $\bar{q}$ varies in the range of 18.2-19.4%. It is fair to assume that methanol conversion fraction (f) higher than 0.7 and ΔT lower than 50K can be safely achieved. Moreover, since there are no special limitations on the heat exchanger (Fig. 3.3) design (i.e. no need in a catalyst, relatively low temperatures and flow rates of fluids whereas one side is liquid), we believe that ΔT in the range of 10 to 20K is realistic. Thus, $\bar{q}$ will be around 18.5% with conversion fraction having only a minor effect on $\bar{q}$ - Fig. 3.14. The latter assessment makes sense because in the suggested configuration of the high-pressure TCR system where unreformed methanol and water are condensed in the heat exchanger - Fig. 3, the unreformed liquids cause parasitic losses only due to their temperature rise by ΔT. For this reason, the partial derivative $\left(\frac{\partial \bar{q}}{\partial f}\right)$ vanish for ΔT =0 and increases as ΔT increases - Eq. (15).

By using Eq. 16 and assuming that the exhaust gas leaves the reformer at 500K, we calculated $\bar{h}_{av}$ as a function of λ and the exhaust gas temperature – Fig. 15. An assumption of the cooled exhaust temperature of 500K was chosen. The latter was assumed to ensure that the temperature of the cooled hot stream (exhaust gas 8) is above the temperature of the heated cold stream (methanol-water mixture entering the reformer after pre-heating 2) and provides a sufficient temperature gradient for heat transfer – Fig. 3.3 We also plotted on Fig. 3.15 the experimental results obtained for WOT engine operation in the wide range of loads with λ varying from 1.55 to 4.2 (idle).

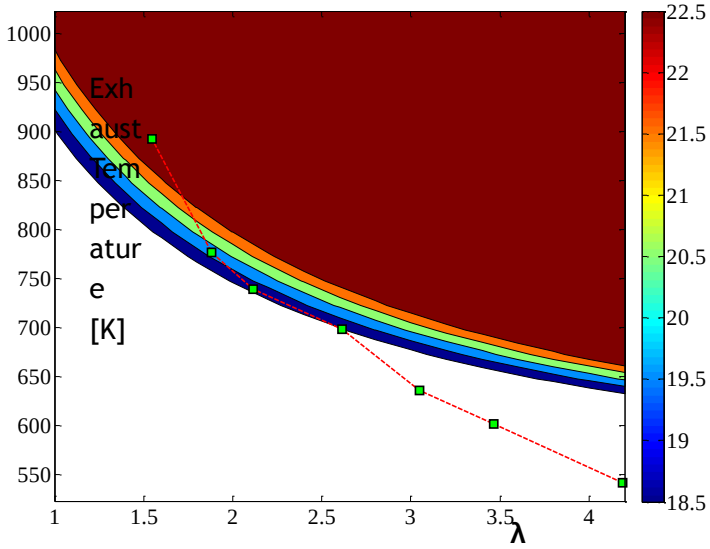

Figure 3.15 $\bar{h}_{av}$ as a function of λ and the exhaust gas temperature. Engine speed 2800 rpm; SOI 127 CAD BTDC; injection pressure at 40 bar; exhaust gas outlet temperature 500K [45]

As seen in Fig. 3.15, at high load and λ=1.5 the available enthalpy of the exhaust gas is sufficient to sustain the reforming reactions. As the load is decreased and excess air ratio is increased (at wide-open throttle) the amount of available enthalpy becomes marginal (2< λ <2.5) and then insufficient (λ>2.5). Thus, the possibility of unthrottled operation at λ>2 is dependent on the reforming system design characteristics such as ΔT, heat transfer losses through the system boundaries and the minimal possible exhaust gas temperature at the reformer outlet. The latter has a strong effect mainly at high excess air ratios because of the low exhaust gas temperatures and the relatively high flow rates at these operating modes. Considering the experimental point of λ=4.2 and T_{exh} = 540K as an example, the normalized available exhaust gas enthalpy ($\bar{h}_{av}$) is increased from 5.5% to 12.3% and 19.1% when the temperature of the cooled exhaust gas decreases from 500K to 450K and 400K, respectively. In the considered case of the high-pressure TCR system, the exhaust gas temperature at the

reformer outlet also depends on the reforming pressure. Lower reforming pressure will cause the water-methanol mixture to enter the reformer at a lower temperature due to partial evaporation at the pre-heating stage. Evaporation at the pre-heating stage becomes impossible with pressure increase. Hence, methanol-water temperature at the reformer inlet (2) increases and, as a result, the possible outlet temperature of exhaust gas increases as well. Engine operation at λ>2 may be achieved by using a reformate reservoir which is filled while working at low excess air ratios or by delaying combustion through late ignition or injection to increase exhaust gas temperatures. The effect of injection timing and pressure on engine efficiency and emissions was investigated and is discussed hereinafter.

3.4.4 Injection Strategy

It is clear that engine performance and emissions are dependent on the strategy of reformate injection, which affects the fuel-air mixing quality and thus influences combustion process. When a DI ICE with high-pressure TCR is considered, the injection pressure is a very important parameter because either the reformate has to be compressed prior to injection or the reforming has to be performed at high pressure [26, 38]. Since compressing the reformate prior to its injection is an energy consuming process, it is beneficial to perform the reforming reactions at high pressure thus compressing the methanol and water at their liquid state and substantially reducing the energy required for compression. The drawbacks of high-pressure reforming are more severe requirements to the mechanical strength of the reforming system and a concern of catalyst deactivation due to coke formation. Another drawback of high-pressure reforming related to heat exchange process in the reformer and heat exchanger was discussed in the previous section. Thus, it is desirable to inject the fuel at the lowest possible injection pressure that allows sufficient reformate flow rate to meet engine power and efficiency requirements. It is important to remember that the required injection

pressure is strongly influenced by the injector design and its fuel flow area. As the flow through the injector is choked during most of the injection period and at most of the injection pressures, the necessary injection pressure is inversely related to the injector flow area and injection period. An example presented in Fig. 3.16 for the engine operating mode at 2800 rpm, WOT and λ=1.5 illustrates such a dependence and shows how the pressure required to allow sufficient fuel flow rate varies with the injection timing and injector flow area. The calculation was based on the assumption of ideal gas flow and experimentally obtained data for the same operating regime with the in-house developed injector (CD=0.79, A=0.85 mm^2).

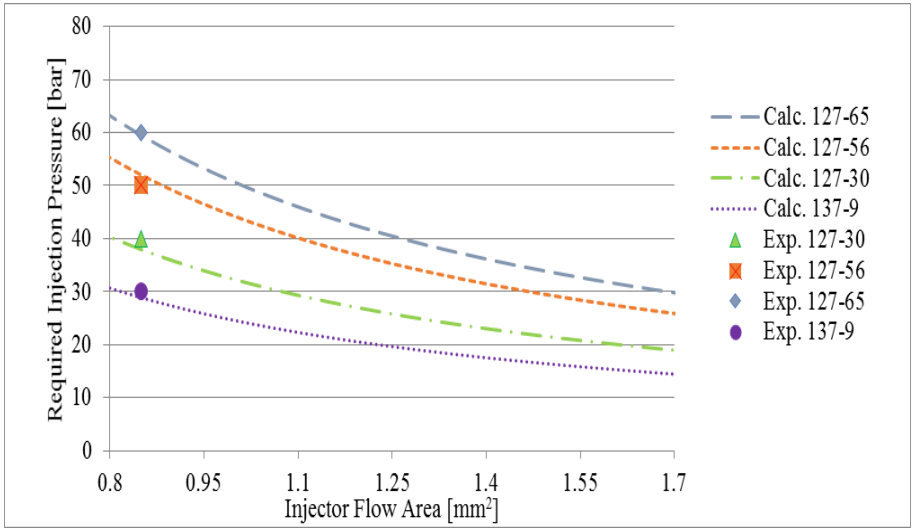

Figure 3.16 Required injection pressure as a function of the injection timing and the injector flow area. Engine speed 2800 rpm, WOT, λ=1.5, CD=0.79, fuel mass per cycle 22.5 mg. Numbers in the legend: SOI-EOI CAD BTDC [45]

Since the injector is based on an available commercial injector, we tried to maximize the flow area by maximizing needle lift and concentric hole area to a degree that still allowed good sealing. Thus, we had no possibility to further increase the injector flow area. So, the parameters

we varied in our experiments were injection pressure and injection timing only.

The injection pressure was varied from 30 to 60 bar and the SOI timing was varied from 137 to 97 CAD BTDC for WOT operation at an engine speed of 2800 rpm and excess air ratio of 1.5. The ignition timing was set as an MBT value (13 CAD BTDC) for the given speed and λ at injection pressure of 40 bar and SOI timing of 127 CAD BTDC. The ignition timing was kept constant in the studied range of injection timings and pressures due to limited amount of available MSR gas.

When the engine indicated efficiency values are plotted as a function of SOI timing and injection pressure, the indicated efficiency seems to be clearly dependent on the injection pressure (Fig. 3.17).

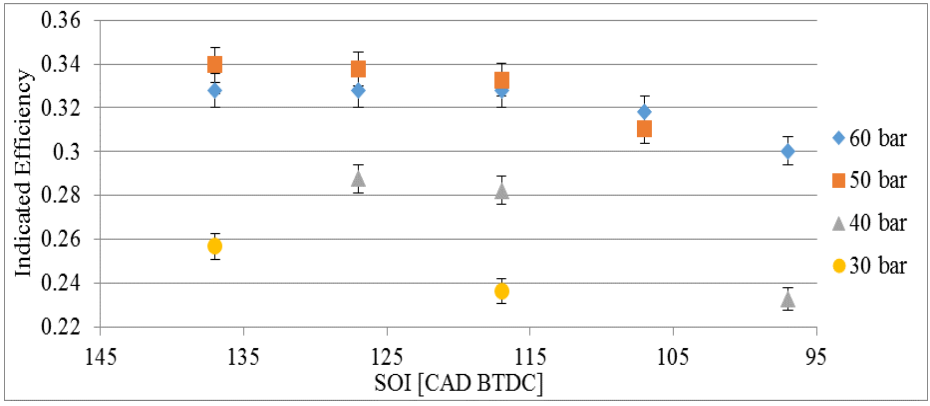

Figure 3.17 Indicated efficiency as a function of injection pressure and SOI timing. WOT, engine speed 2800 rpm and λ=1.5. Error bars show the uncertainty of the calculated indicated efficiency values [45]

The lower engine efficiency in the case of the lower injection pressures (30 and 40 bar) and late SOI is a result of the late end of injection (EOI) that results in lower HRR and late end of combustion due to retarded mixing and late mixture formation (Fig. 3.18).

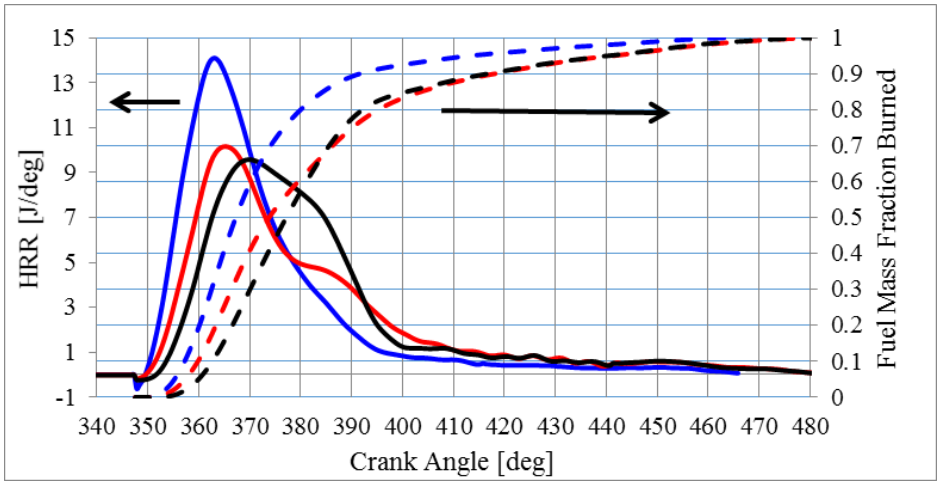

Figure 3.18 HRR and fuel mass fraction burned for 3 typical cases: injection period 117-23 CAD BTDC, 40 bar (red lines); injection period 117-54 CAD BTDC, 60 bar (blue lines); injection period 97-33 CAD BTDC, 60 bar (black lines). Engine speed 2800 rpm, WOT, λ=1.5. Solid lines – HRR; dashed lines – fuel mass fraction burned [45]

For the three cases shown in Fig. 3.10, the highest efficiency was achieved for early reformate injection at the higher pressure (blue line). In the latter case, injection ended early (65 CAD BTDC) allowing good fuel-air mixing before ignition. For this reason, the flame development angle ($\theta_{0\text{-}10}$) was the lowest (10 CAD) in this case and only a relatively small fraction of the reformate was burned late in the expansion stroke (θ_{90}=391 CAD). It also led to reduced cycle-to-cycle variation – Fig. 3.19. As SOI is retarded or the injection pressure is lowered, the end of injection is delayed allowing less time for mixture formation and thus causing an increase in the flame development angle (Fig. 18) and resulting in a higher fuel fraction that is burned late in the expansion stroke (θ_{90}=417 CAD). Such a late and a slower combustion leads, as anticipated, to a more substantial cycle-to-cycle variation and is reflected in higher COV values – Fig.3.19. In the shown cases (Fig. 3.18) the late high-pressure injection is more efficient than the early low-pressure injection because at 23 ATDC

both cases has the same mass fraction burned, but for the low-pressure injection a higher portion of the fuel is burned later in the expansion stroke or too early BTDC. As can be seen from Fig. 3.18, for all the considered cases, the flame termination phase is relatively long due to the combustion chamber geometry of the tested engine (side-valve configuration).

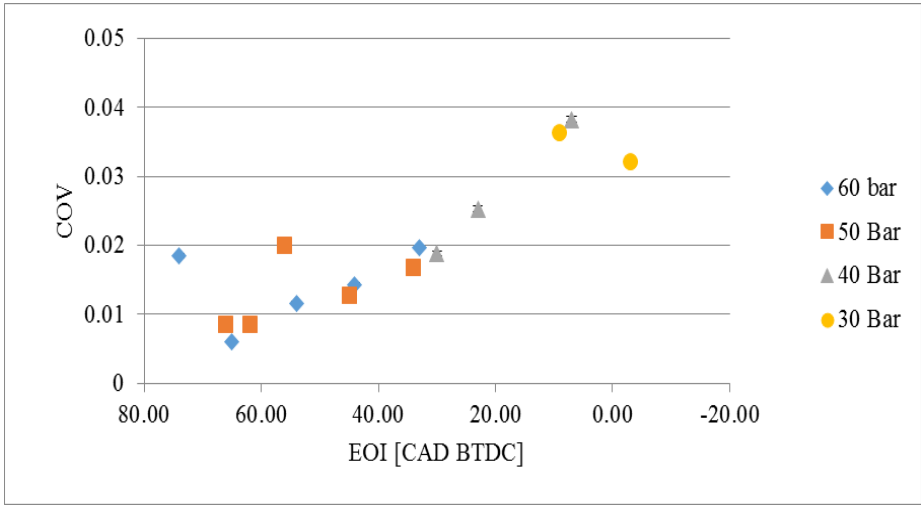

Figure 3.19 COV dependence on injection timing (EOI - end of injection). Error bars show the uncertainty of the calculated COV values [45]

Cycle-to-cycle variation is an important engine performance parameter because the optimum ignition timing is normally set for an average cycle [30]. Thus, for slow burning cycles the ignition is over-retarded and for fast burning cycles it is actually over-advanced resulting in loss of power and efficiency. Fast burning cycles lead to high in-cylinder pressure, high pressure rise rate, high NOx formation and may also lead to knock appearance. These fast cycles limit the engine's compression ratio and affect a possibility of tuning optimization [30]. Cyclic variations in the cylinder are caused by mixture motion and excess air ratio variations especially in the vicinity of the spark plug, because they change the early

flame development and thus affect the fuel burning behavior and the heat release rate. Hence, improved mixture formation leads to reduced cycle-to-cycle variations and has a beneficial effect on engine efficiency and emissions. As seen in Fig. 3.19, early EOI reduces the COV and hence has a beneficial effect on the efficiency. The data shown in Fig. 19 clearly indicate that cycle-to-cycle variation strongly depends on EOI timing, and hence the time available for fuel-air mixing, and almost insensitive to the injection pressure. When the end of injection is retarded from 65 towards 5 CAD BTDC, the obtained COV values rise from 1% to almost 4%, respectively.

Since the engine efficiency depends on injection timing through reformate-air mixture formation with the subsequent variation in COV and HRR, when we plot indicated efficiency vs. EOI, the different pressure lines of Fig. 3.17 almost merge into a single trend line (Fig. 3.20). This is explained by the mutual influence of the SOI timing and the injection pressure (which determines the flow rate through the injector and thus the injection duration) on the finally achieved end of injection. As expected, the late combustion resulted in higher available energy of exhaust gas (Fig. 3.20). The latter fact should be taken into account when an ICE with TCR is considered.

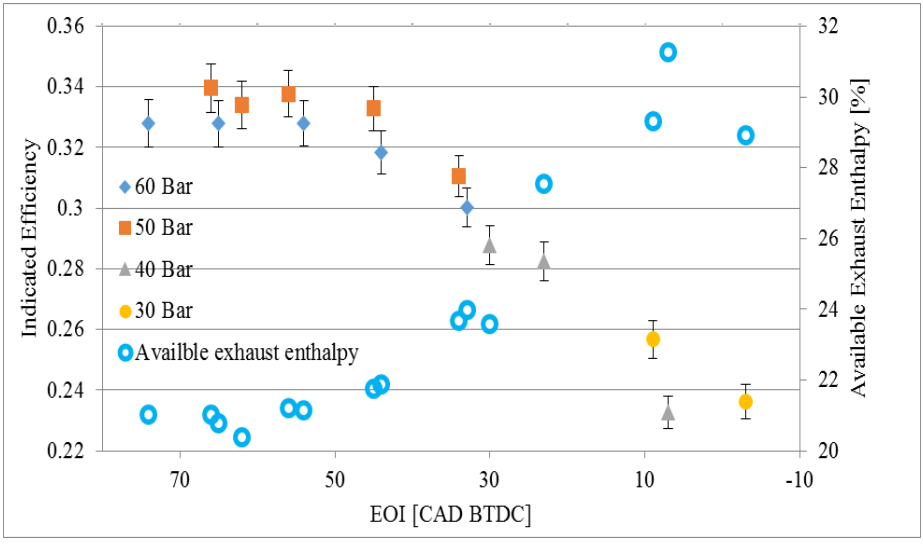

Figure 3.20 Indicated efficiency and available exhaust energy as a function of EOI timing and injection pressure. WOT, engine speed 2800 rpm and λ=1.5. The temperature of the cooled exhaust gas assumed to be 500K. Error bars show the uncertainty of the calculated indicated efficiency values [45]

As seen in Fig. 3.20, if EOI is retarded beyond 50 CAD BTDC an increase in the available exhaust gas enthalpy ($\overline{h}_{av}$) and a sharp decrease in efficiency are observed, which is attributed to late combustion and increased cycle-to-cycle variation. The efficiency decrease is observed at much earlier EOI values than reported in [39] where the performance of a DI ICE fed with pure hydrogen was studied. This finding may be addressed to the fact that in our case the baseline engine was not a DI engine and the process of reformate-air mixing within the cylinder was not optimized (this important task lies out of the scope of the reported research). The combustion chamber shape and the fact that the applied injector has a single injection axis, which was relatively far from the spark plug, delays mixture formation in the vicinity of the spark plug and leads to slower and delayed combustion. Another reason of the observed differences between the reformate and pure hydrogen combustion in a DI engine that in the case of methanol reformate combustion, the latter contains substantial amount (up to 25%) of a diluent gas CO_2. The higher specific heat of carbon dioxide compared to diluent air (by 5-8% in the temperature range 1000 – 2500 K) leads to combustion temperature reduction and, as a result, to lower burning velocities. Thus, the same EOI retarding results in a bigger combustion shift into the expansion stroke with the subsequent efficiency reduction.

A slight increase in efficiency as EOI is retarded was expected from previous simulations (carried out under assumption of negligible changes in mixing quality with EOI retarding) due to reduction of compression work (about 1.5% absolute improvement for 60 CAD retard for an engine with compression ratio of 10) [26]. The obtained experimental results show a possible appearance of a mild efficiency maximum (in the range of

the uncertainty) as a function of EOI timing, which most probably reflects joint effect on efficiency of opposite influencing factors, like compression work, fuel-air mixing quality and combustion phasing. The experimental data show (Fig. 20) that for the studied conditions (engine speed 2800 rpm, λ=1.5), the minimal reformate injection pressure, which is required to achieve the highest possible engine efficiency is 50 bar. It can be seen from Fig. 3.20 that if EOI could be advanced by 20 CAD (from approximately 30 towards 50 CAD BTDC), even injection pressure of 40 bar could be sufficient to achieve the highest possible efficiency. This would require SOI slightly before intake valve closing (IVC) and is possible, if backflow prevention could be achieved.

Similarly to engine efficiency, also pollutant emissions were found to be dependent mainly on EOI timing – Figs. 3.21- 3.25. Specific emissions of various gaseous pollutants, as well as particle number concentrations, obtained at different injection pressures are almost merged into a single line when plotted vs EOI timing. This finding can be expected because CO_2 emissions are inversely related to engine efficiency; NO_x and CO - are related to the HRR and late combustion, which have been shown previously to be linked to EOI timing. Similarly to the indicated efficiency behavior, for all studied injection pressures, the pollutant emissions data merge into a single trend line. This implies that pollutant formation is mainly affected by the fuel-air mixing process. Figs. 3.21- 3.24 show the CO_2, NO_x, CO and HC emissions as a function of the EOI, respectively.

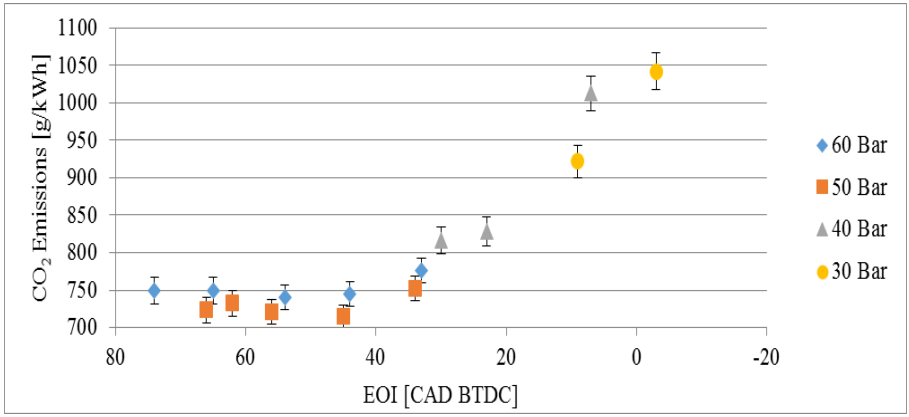

Figure 3.21 CO_2 emission as a function of EOI timing and injection pressure. WOT, engine speed 2800 rpm and λ=1.5. Error bars show the uncertainty of the CO_2 emission values [45]

CO_2 emissions (Fig. 3.21) show a possible appearance of a mild minimum at EOI timing of 50-60 CAD BTDC (in the range of the uncertainty) that matches the maximum of engine's efficiency.

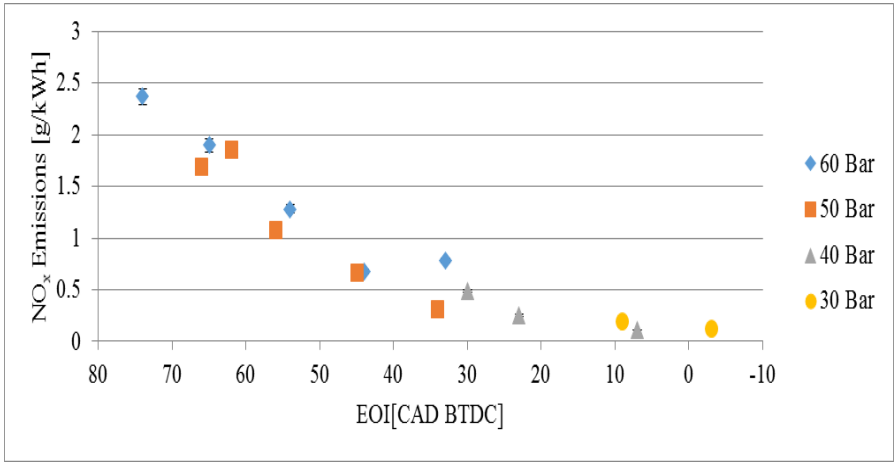

Figure 3.22 NO_x emission as a function of EOI timing and injection pressure. WOT, engine speed 2800 rpm and λ=1.5. Error bars show the uncertainty of the NO_x emission values [45]

As seen from Fig. 3.22, NO_x emissions decrease with EOI retarding due to late mixing and combustion that reduces in-cylinder temperatures. For some of the range it is at the cost of reduced efficiency but still there is a range between EOI of 74 and EOI of 50 CAD BTDC where indicated efficiency is almost constant and NO_x emissions drop by a factor of 2.5. This finding can be explained by the fact that at an advanced EOI timing compression work rise prevents increase in indicated efficiency, whereas high maximal in-cylinder temperatures lead to intensified NO_x formation. Another possible reason is linked to the ignition timing that was set at MBT value for the injection pressure of 40 bar and SOI timing of 127 CAD BTDC. For earlier EOIs with higher HHR, ignition was over-advanced thus resulting in higher temperatures and increased NO_x formation, but not higher efficiency.

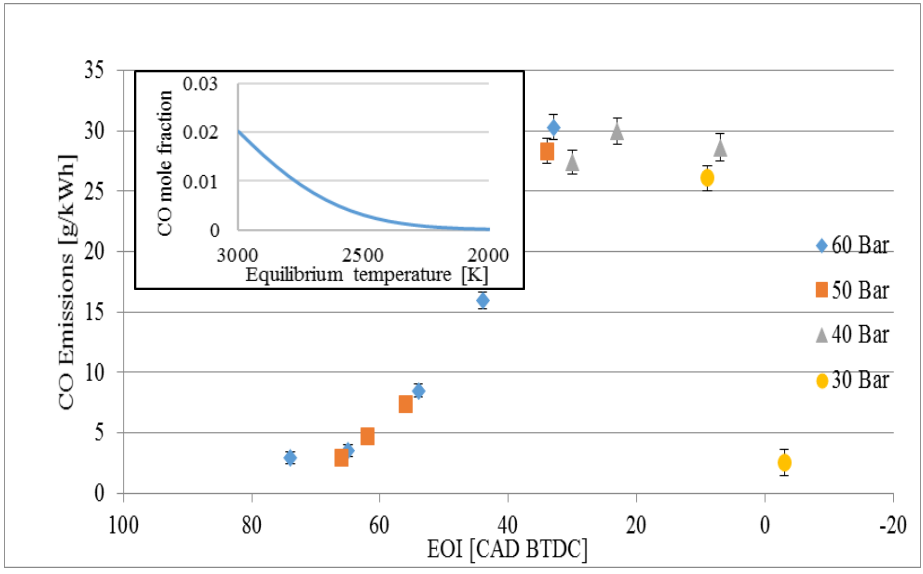

Figure 3.23 CO emission as a function of EOI timing and injection pressure. WOT, engine speed 2800 rpm and λ=1.5. Error bars show the uncertainty of the CO emission values. Insert - CO equilibrium mole fraction vs temperature [45]

As can be seen from Fig. 3.23, EOI retarding leads to significant increase in CO emissions. At some value of EOI timing (in our experiments at approximately 35 CAD BTDC) the measured levels of CO emission achieve a mild maximum and significantly decrease with further EOI retarding. The observed dependence of CO emission on EOI timing is defined by changes in chemical kinetics of CO_2 dissociation to CO affected by variations in combustion temperature and cooling rate. It is known that at high temperatures CO_2 dissociates to CO and the CO chemistry is assumed to be in equilibrium [30]. As the burned gas is cooled during the expansion stroke, CO mole fraction remains significantly higher than its equilibrium value due to the relatively slow kinetics. Furthermore, CO oxidation reactions are highly dependent on the cooling rate and actually freeze as the gas passes through the exhaust valves [30] and [40].

It is important to note that in the case of engine fueled with MSR reformate, CO_2 is introduced to the combustion process together with the fuel (hydrogen), and is not formed as a result of a hydrocarbon fuel combustion. In the considered case, as EOI is retarded, two opposing factors influence CO formation. First, the maximal combustion temperatures are decreased (which is reflected also in lower NO_x emissions with EOI retarding) leading to lower equilibrium CO concentrations – see the insert on Fig. 3.23 (equilibrium CO molar fractions were calculated for p = 20 bar and λ=1.5 using [41, 42]). Second, combustion is delayed, thus leading to higher temperatures later on in the expansion stroke. This can be clearly seen from the higher available exhaust gas enthalpy values with EOI retarding - Fig. 3.20. This leaves less time for CO oxidation before exhaust valve opening, reduces temperature relaxation time (increases cooling rate) and thus leads to higher CO emissions. We believe that as EOI is retarded from 75 to 35 CAD BTDC, the effect of increased cooling rate is more significant than the reduction of peak cylinder temperatures. This results in a rise of the measured CO emission. As EOI is further retarded, the effect of these phenomena becomes comparable, and with later EOI - the effect of temperature

reduction begins to be dominant. This behavior is reflected in a mild maximum and a substantial reduction of CO emission that was measured at the most retarded EOI timing.

Dependence of HC emission on EOI timing is shown in Fig. 3.24. Since the only source for HC formation is lubrication oil [43], HC emissions decrease as combustion process is prolonged thus allowing more complete oil combustion. The obtained results show a good potential of the DI engine with high-pressure TCR to achieve ultra-low emissions without any need in exhaust gas aftertreatment. In this case, a reformer will replace the currently used catalytic converter. However, further investigation of this subject is required to make definite conclusions about a possibility of engine operation without aftertreatment.

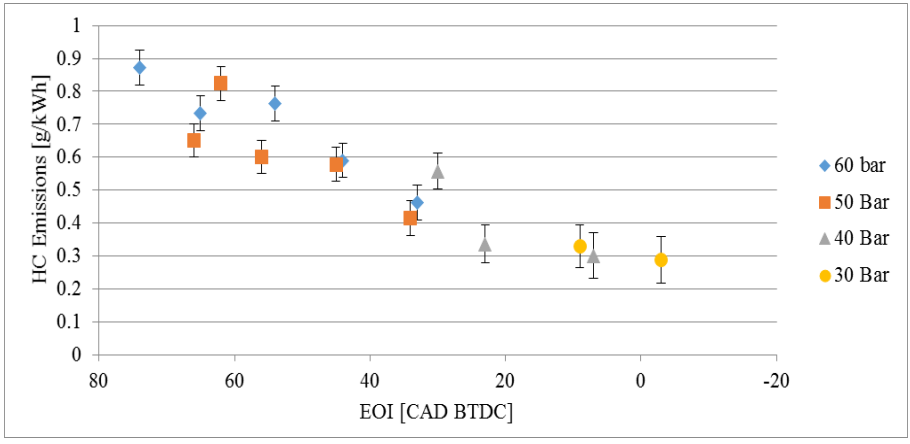

Figure 3.24 HC emission as a function of EOI timing and injection pressure. WOT, engine speed 2800 rpm and λ=1.5. Error bars show the uncertainty of the HC emission values [45]

PN concentrations were much harder to measure due to the spiky nature of PN emission in SI engines [44]. This spiky nature was also observed in our measurements with spikes occurring every 30-60 seconds and spike

duration between 5 to 20 seconds. Thus, it was decided to compare time-averaged PN emissions with measurements duration of at least 120 seconds at a measuring frequency 10 Hz. Even though the spiky nature of PN emission increases the measurement uncertainty, the trend of PN emission reduction with EOI retarding is clear (Fig. 3.25).

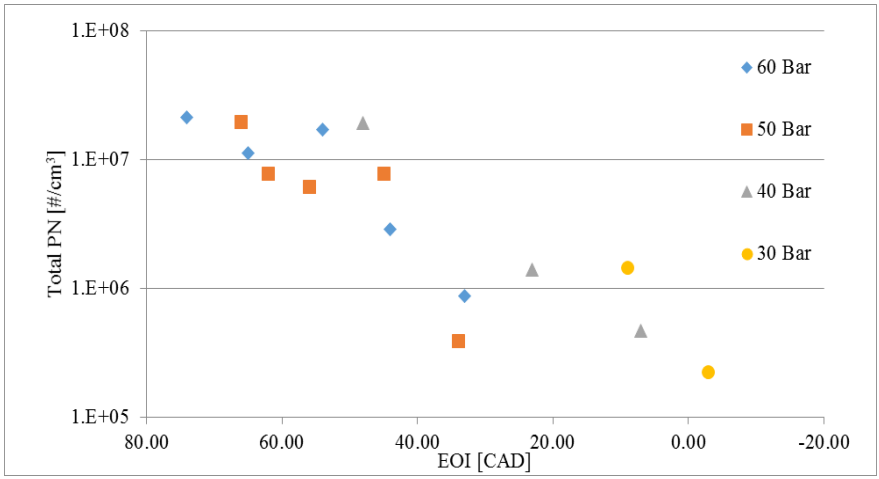

Figure 3.25 PN emission as a function of EOI timing and injection pressure. WOT, engine speed 2800 rpm and λ=1.5 [45]

Although in the case of PN emission the scatter around the average emission line is higher than for other pollutants (notice the logarithmic scale) this may be due to the spiky nature of the PN emissions. The level of measured PN emissions is similar to that one observed earlier in [43] where particles formation in a hydrogen-fed ICE was investigated. Lubrication oil and deposits breakup are believed to be the source of PN emission. This explains the reduction in PN emission as the combustion is prolonged for retarded EOI timings. The latter, similarly to HC emission, allows more time for completer combustion of particles formed at earlier combustion stages. It is also possible that the lower temperatures at retarded EOI timing result in smaller amounts of burned lubricant and thus - lower HC and PN emissions.

3.5) Summary and Conclusions

An experimental setup — based on a single-cylinder SI ICE with the ability to operate as a DI engine fed by gaseous fuels — was built. It was used to conduct experiments with two of the most widely investigated alcohol reforming schemes, which include low temperature ethanol decomposition and methanol steam reforming products as well as gasoline (as a reference case).

It was shown that for both studied reformate types, the engine can work unthrottled up to idle, but at the expense of an increased COV, reduced combustion and indicated efficiency. The problems of combustion efficiency and cycle-to-cycle variability and the consequent efficiency reduction were much more severe with the ED reformate because of the smaller hydrogen content in the mixture. COV values, in the case of engine feeding with the MSR reformate, did not exceed 0.05 up to λ=3.5. Engine feeding with the MSR reformate resulted in much higher heat release rates, which is reflected in substantially shorter flame development angles (13-15 CAD) compared to gasoline (30 CAD) or methane (29 CAD).

The thermal efficiency of the engine fueled by MSR products was improved by 18-39% compared to the engine operating with gasoline. The results of the experiments showed that with the current gaseous direct injector (flow area of 0.85 mm^2), injection pressure of 40 bar is insufficient to achieve IMEP pressures higher than 4.5 bar with high efficiency. An option of increasing the injector flow area or the injection pressure should be considered and analyzed. This, in turn, may require an increase of the reforming pressure.

The MSR reformate showed much lower pollutant emissions compared to ED products and gasoline. Engine feeding with MSR resulted in emissions reductions of 73-94%, 90-96%, 85-97%, and 10-25% in NO_x, CO, HC and CO_2 emissions, respectively, compared to gasoline feeding.

Overall, the reformate fuels have showed great improvement over gasoline in terms of combustion behavior, such as reduced COV for a wide range of excess air ratios and a faster heat release rate. These fundamental benefits are reflected in a significant improvement of engine thermal efficiency and a dramatic reduction in pollutant emissions. It is expected that further improvement can be achieved if ignition timing, throttling and injector positioning & orientation are optimized. The potential of meeting future emission legislation without a need for exhaust gas after-treatment should be explored. ED has an advantage over MSR in terms of primary fuel energy density, reformate energy density and required heat transfer area for the reformer, but has major disadvantages in thermal efficiency and pollutant emissions. Both schemes show good prospects for further development.

It was shown that although unthrottled engine operation with lean burning is possible, the available enthalpy of exhaust gas for methanol reforming becomes marginal at $\lambda>2$ and insufficient at $\lambda>2.5$ for the considered configuration of the high-pressure thermochemical recuperation system (Fig. 3.3) and at assumptions as were outlined earlier.

The experimental results show that for the studied conditions the minimal reformate injection pressure, which is required to achieve the highest possible engine efficiency is 50 bar. In the case that EOI could be advanced by 20 CAD (from approximately 30 towards 50 CAD BTDC), even injection pressure of 40 bar can be sufficient to achieve the highest possible efficiency. This would require SOI slightly before intake valve closing (IVC) and is possible, if backflow prevention could be achieved. Another

possibility to reduce the required injection pressure is to increase the injector flow area.

The trends of reduction in NO_x, HC, PN emission and increase in CO emission were observed with EOI retarding. End-of-injection timing is shown to be the main influencing factor on engine efficiency and pollutant emissions. The obtained results indicate that there is a range of EOI timing where indicated efficiency is almost constant and NO_x emissions drop by a factor of 2.5. Particle number emissions can be reduced in this range by a factor of 4. Further investigation on the nature of particles formation and size distribution in an engine fueled with MSR reformate is required.

3.6) References

[1] *Wang, Z., Liu, H., Long, Y., Wang, J., & He, X. (2015). Comparative study on alcohols–gasoline and gasoline–alcohols dual-fuel spark ignition (DFSI) combustion for high load extension and high fuel efficiency. Energy 82: 395-405.*

[2] *Wang, X., Ge, Y., Zhang, C., Tan, J., Hao, L., Liu, J., & Gong, H. (2016). Effects of engine misfire on regulated, unregulated emissions from a methanol-fueled vehicle and its ozone forming potential. Applied Energy 177: 187-195.*

[3] *Sá S., Silva H., Brandão L., Sousa J.M. & Mendes A. (2010), Catalysts for methanol steam reforming—A review. Applied Catalysis B: Environmental 99: 43-57*

[4] *Lorenzut B., Montini T., De Rogatis L., Canton P., Benedetti A. & Fornasiero P. (2011), Hydrogen production through alcohol steam reforming on Cu/ZnO based catalysts. Applied Catalysis B: Enviromental 101(3-4): 397-408*

[5] *He, M., Zhang, X., Zeng, K., & Gao, K. (2011). A combined*

thermodynamic cycle used for waste heat recovery of internal combustion engine. Energy 36(12): 6821-6829.

[6] Shu, G., Zhao, M., Tian, H., Wei, H., Liang, X., Huo, Y., & Zhu, W. (2016), Experimental investigation on thermal OS/ORC (Oil Storage/Organic Rankine Cycle) system for waste heat recovery from diesel engine. Energy 107: 693-706.

[7] Chakravarthy, V. K., Daw, C. S., Pihl, J. A., & Conklin, J. C. (2010). Study of the theoretical potential of thermochemical exhaust heat recuperation for internal combustion engines. Energy & Fuels 24(3): 1529-1537.

[8] Verhelst, S. (2014), Recent progress in the use of hydrogen as a fuel for internal combustion engines. International Journal of Hydrogen Energy 39: 1071-1085.

[9] Verhelst, S. & Wallner, T. (2009), Hydrogen-fueled internal combustion engines. Progress in Energy & Combustion Science 35: 490-527.

[10] Morgenstern D.A. & Fornango J.P (2005), Low-Temperature Reforming of Ethanol over Copper-Plated Raney Nickel: A New Route to Sustainable Hydrogen for Transportation. Energy and Fuels 19: 1708-1716

[11] Wheeler, J. C., Stein, R. A., Morgenstern, D. A., Sall, E. D., & Taylor, J. W. (2011). Low-temperature ethanol reforming: A multi-cylinder engine demonstration SAE Technical Paper No. 2011-01-0142.

[12] Liao C.H. & R.F. Horng (2016), Investigation on the hydrogen production by methanol steam reforming with engine exhaust heat recovery strategy. International Journal of Hydrogen Energy 41(9): 4957–4968.

[13] Wijaya W.Y. (2013), Methanol steam reforming for hydrogen production: concept and evaluation of integrated advanced energy system. PhD Thesis, Tokyo Institute of Technology, Tokyo, Japan, 102 pp.

[14] Twigg M.V. & M.S. Spencer (2003), Deactivation of copper metal catalysts for methanol decomposition, methanol steam reforming and methanol synthesis. Topics in Catalysis 22(3–4): 191-203

[15] Cao W., G. Chen, S. Li & Q. Yuan (2006), Methanol-steam reforming over a ZnO–Cr2O3/CeO2–ZrO2/Al2O3 catalyst, Chemical Engineering Journal 119: 93–98.

[16] Marbán, G., López, A., López, I., & Valdés-Solís, T. (2010). A highly active, selective and stable copper/cobalt-structured nanocatalyst for methanol decomposition. Applied Catalysis B: Environmental 99(1): 257-264.

[17] Pettersson, L. & Sjostrom, K. (1991). Decomposed Methanol as a Fuel—A review. Combustion Science and Technology 80(4-6): 265-303.

[18] Matthias, N. S., Wallner, T., & Scarcelli, R. (2012). A hydrogen direct injection engine concept that exceeds US DOE light-duty efficiency targets. SAE International Journal of Engines 5: 838-849.

[19] Hagos, F. Y., Aziz, A. R. A. & Sulaiman, S. A. (2014). Syngas (H_2/CO) in a spark-ignition direct-injection engine. Part 1: Combustion, performance and emissions comparison with CNG. International Journal of Hydrogen Energy 39: 17884—17895.

[20] Hagos, F. Y., Aziz, A. R. A., & Sulaiman, S. A. (2015). Investigation of deposit formation in direct-injection spark-ignition engine powered on syngas. International Journal of Automotive Technology 16(3): 479-485.

[21] Li, G., Zhang, Z., You, F., Pan, Z., Zhang, X., Dong, J., & Gao, X. (2013). A novel strategy for hydrous-ethanol utilization: Demonstration of a spark-ignition engine fueled with hydrogen-rich fuel from an onboard ethanol/steam reformer. International Journal of Hydrogen Energy 38(14): 5936-5948.

[22] Shimada, A. & Ishikawa, T. (2013). Improved thermal efficiency using hydrous ethanol reforming in SI engine. SAE Technical Paper No. 2013-24-0118

[23] Yoon, H. C., Otero, J., & Erickson, P. A. (2007). Reactor design limitations for the steam reforming of methanol. Applied Catalysis B: Environmental 75(3): 264-271.

[24] He, Z., Gao, Z., Zhu, L., Li, S., Li, A., Zhang, W., & Huang, Z. (2016). Effects of H_2 and CO enrichment on the combustion, emission and

performance characteristics of spark ignition natural gas engine. Fuel 183: 230-237.

[25] Tartakovsky, L., Baibikov, V., & Veinblat, M. (2013). Comparative Performance Analysis of SI Engine Fed by Ethanol and Methanol Reforming Products. SAE Technical Paper No. 2013-01-2617.

[26] Poran, A., & Tartakovsky, L. (2015). Energy efficiency of a direct-injection internal combustion engine with high-pressure methanol steam reforming. Energy 88: 506-514.

[27] Peppley, B. A., Amphlett, J. C., Kearns, L. M., Mann, R. F., & Roberge, P. R. (1997, July). Hydrogen generation for fuel-cell power systems by high-pressure catalytic methanol-steam reforming. In Energy Conversion Engineering Conference, 1997. IECEC-97., Proceedings of the 32nd Intersociety (pp. 831-836). IEEE.

[28] Tartakovsky, L., Amiel, R., Baibikov, V., Fleischman, R., Gutman, M., Poran, A., & Veinblat, M. (2015). SI Engine with Direct Injection of Methanol Reforming Products–First Experimental Results. SAE Technical Paper No. 2015-32-0712.

[29] Wang, X., Grose, M. A., Caldow, R., Osmondson, B. L., Swanson, J. J., Chow, J. C., Watson, J.G., Kittelson, D.B., Li, Y., Xue, J. & Jung, H. (2016). Improvement of Engine Exhaust Particle Sizer (EEPS) size distribution measurement–II. Engine exhaust particles. Journal of Aerosol Science 92: 83-94.

[30] Heywood, J. B. (1988). Internal Combustion Engine Fundamentals. New York: McGraw-Hill.

[31] Lee, K., Yoon, M., & Sunwoo, M. (2008). A study on pegging methods for noisy cylinder pressure signal. Control Engineering Practice, 16(8), 922-929.

[32] Shavit, A., & Gutfinger, C. (2008). Thermodynamics: from concepts to applications. Boca Raton: CRC Press.

[33] Moffat, R. J. (1988). Describing the uncertainties in experimental results. Experimental thermal and fluid science, 1(1), 3-17.

[34] Brunt, M. F., & Pond, C. R. (1997). Evaluation of techniques for absolute cylinder pressure correction. SAE Technical Paper No.

970036.

[35] Omari A, M. Shapiro, & L. Tartakovsky (2015), Laminar burning velocity of alcohol steam reforming products and effects of cellularity on flame propagation. SAE Technical Paper No. 2015-01-0775.

[36] Graskow, B. R., Kittelson, D. B., Abdul-Khalek, I. S., Ahmadi, M. R. & Morris, J. E. (1998). Characterization of exhaust particulate emissions from a spark ignition engine. SAE Technical Paper No. 980528.

[37] Miller, A. L., Stipe, C. B., Habjan, M. C., & Ahlstrand, G. G. (2007). Role of lubrication oil in particulate emissions from a hydrogen-powered internal combustion engine. Environmental Science & Technology 41(19): 6828-6835.

[38] Poran A., Tartakovsky L. (2017). Performance and emissions of a direct injection internal combustion engine devised for joint operating with high-pressure thermochemical recuperation system. Energy 124: 214-226.

[39] Mohammadi, A., Shioji, M., Nakai, Y., Ishikura, W., & Tabo, E. (2007). Performance and combustion characteristics of a direct injection SI hydrogen engine. International Journal of Hydrogen Energy 32(2): 296-304.

[40] Creighton, J. R. (2000). Dependence of CO emissions on the rate of product cooling. Combustion and Flame 123(3): 402-411.

[41] Turns, S. R. (2012). An introduction to combustion concepts and application. New York: McGraw-Hill.

[42] Olikara, C., & Borman, G. L. (1975). A computer program for calculating properties of equilibrium combustion products with some applications to IC engines. SAE Technical Paper 750468.

[43] Miller, A. L., Stipe, C. B., Habjan, M. C., & Ahlstrand, G. G. (2007). Role of lubrication oil in particulate emissions from a hydrogen-powered internal combustion engine. Environmental Science & Technology 41(19): 6828-6835.

[44] Graskow, B. R., Kittelson, D. B., Abdul-Khalek, I. S., Ahmadi, M. R. & Morris, J. E. (1998). Characterization of exhaust particulate emissions

from a spark ignition engine. SAE Technical Paper 980528.

[45] Poran, A., Tartakovsky, L. (2017). Influence of methanol reformate injection strategy on performance, available exhaust gas enthalpy and emissions of a direct-injection spark ignition engine. International Journal of Hydrogen Energy 42: 15652-15668.

Work Program IV:

Performance Assessment of Various Paraffinic Diesel Fuels

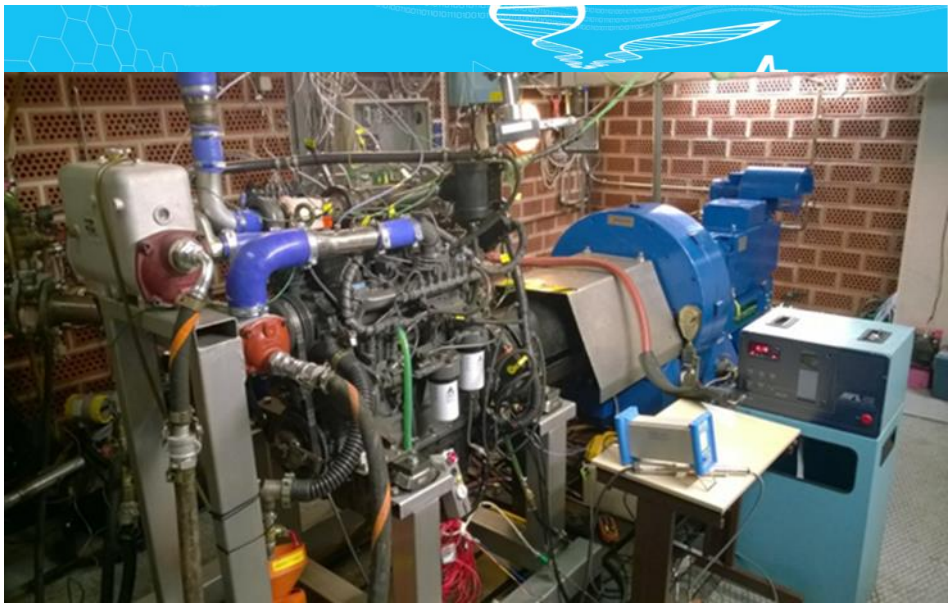

Authors:

Rasmus Pettinen, Timo Murtonen and Petri Söderena

Reprinted from: VTT Research and Technology, Finland

VTT-R-02129-17

Report's title	
Performance Assessment of Various Paraffinic Diesel Fuels	
Customer, contact person, address Somnuek Jaroonjitsathian PTT Public Company Limited 71/1 Moo 2, Pahonyothin KM 78, Sanabtueb Wangnoi, Ayutthaya 13170, Thailand	**Order reference** IEA-AMF Annex 52
Project name	**Project number/Short name**
Author(s) Rasmus Pettinen, Timo Murtonen and Petri Söderena	**Pages** 22
Keywords Paraffinic, Diesel, Efficiency	**Report identification code** VTT-R-02129-17

Summary

Global energy politics sets demands on both engine manufacturers and fuel developers to produce sustainable, high efficient and environmental friendly solutions. New fuel compounds are continuously presented to improve tail pipe emissions and increase engine overall efficiency. Paraffinic diesel fuels have become common within the past decade, representing modern, high efficient and clean burning fuels. It seems that paraffinic diesel fuels may improve engine attributes in various manners. Paraffinic diesel fuels are produced from diverse feedstock through the Fisher-Tropsch process or by utilizing hydrotreatment.

This report consists of both a literature research and an experimental study concerning paraffinic diesel fuels and their general combustion behaviour in relation to engine efficiency and tailpipe emissions. The literature includes analysis of following paraffinic diesel fuels: Hydrotreated vegetable oil, Crude Tall Oil based diesel fuel and Gas-To-Liquids diesel fuel. The experimental study concerning paraffinic fuel efficiency and emission behaviour was executed in VTT facilities.

Summary (Continue)

Two different types of test strategies were used: experiments with OEM parameters and tests with optimized engine parameters for one type of paraffinic fuel. The goals for the research related to optimized parameters were to attain as high engine efficiency as possible without exceeding predefined boundaries of tail pipe emissions. Both transient and steady state driving cycles were used.

Based on both literature research and experiment results, paraffinic diesel fuels may be used for improving engine attributes and/or emission formation. Depending of paraffinic fuel type, improvements in CO, THC and PM emission are achievable with OEM injection parameters. Using optimized engine parameters, a maximum gain on approximately 4% in engine efficiency were experienced using paraffinic diesel fuels without drawbacks in emissions when compared to conventional diesel fuel.

Confidentiality	Public

Espoo 26.10.2017

Written by	**Reviewed by**	**Accepted by**
Rasmus Pettinen, Scientist	Nils-Olof Nylund, Research Professor	Jukka Lehtomäki, Research Team Leader

VTT's contact address

Biologinkuja 5, 02015 Espoo, Finland

Distribution (customer and VTT)

4.1) Introduction

Fuel quality serves a significant role regarding combustion quality and tailpipe emissions. Furthermore, utilizing the full potentiality of modern engine technology sets certain demands on fuel properties. Efficient and clean fuels may remarkably affect engine performance while reducing the formation of greenhouse gases and harmful local emissions such as particulate matter (PM). Paraffinic diesel fuels are being developed as alternative, high efficient and low-emission fuels compared with the traditional diesel. Paraffinic diesel fuels are virtually free from aromatics, clean burning and may therefore generate less regulated emissions. In addition, if injection parameters are optimized, moderate engine efficiencies may be attained by using paraffinic high cetane fuels. Paraffinic diesel fuels tend to have high cetane number (CN), contributing improved combustion behavior and less combustion noise.

Paraffinic diesel fuels are generally divided into three subcategories [1]: gas-to-liquids (GTL), hydrotreated vegetable oil (HVO) and biomass-to-liquids (BTL). These fuels share deviant attributes, affecting differently on both engine performance and emission behavior. In order to specify the behavior of these fuels, standardized experimental tests were carried out at VTT during autumn 2016. The emission and combustion characteristics of four different fuels were studied: fossil diesel and three different paraffinic diesels. The experiments were carried out using a commercial common-rail diesel engine, AGCO 44AWIC, designed for offroad use. Measurements were performed with original equipped manufacturer (OEM) injection parameters and parameters optimized with one of the paraffinic fuels. Aim was to find out whether a parameter set optimized with one paraffinic fuel would work equally with other paraffinic fuels. Optimization strategy was to increase engine efficiency without increase in emissions above the defined reference level. Emissions and engine performance were measured using steady-state and transient test cycles.

4.2) Survey of Paraffinic Diesel Fuels

Paraffinic diesels are high quality, sulfur and aromatics free synthetic fuels. Paraffinic fuels are generally suitable as drop-in fuels for diesel engines, intended for reducing regulated emissions. Due to the deviant attributes, the greatest benefits of paraffinic fuels are however attained through specific engine recalibration and injection parameters optimization. The paraffinic diesels are commonly categorized depending of the raw material and production strategy. GTL is produced from natural gas through the Fisher-Tropsch process, meanwhile HVO and crude tall oil (CTO)-based fuels are renewable fuels hydrotreated from vegetable oils and/or animal fats. BTL can be produced from various biomass-feedstock through gasification and the Fischer-Tropsch process. Several projects concerning BTL are globally ongoing, yet the commercialisation of paraffinic BTL is still in progress [2].

Remarkable leaps in paraffinic diesel fuel development has been made during the last decade. Neste Oy has introduced its newest HVO-concept (Neste MY [3]), UPM a renewable fuel based on CTO - BioVerno [4], and Shell has lauched a commercial GTL-project (Shell GTL) [5]. Several studies prove all above mentioned parrafinic diesel fuels being adaptive with modern diesel engines. These fuels can generally either be used as blends together with conventional diesel or completely alone.

The commercial diesel fuels on the markets follows standardized regulations concerning fuel specifications. The standardization of fuel quality has generally forced the engine distributrors to optimize the engine geometry and parameters based on these standardized specifications. The quality of European diesel fuels follows the specifications of the EN 590:2013 standard. The EN 590 standard includes requirements in i.e. CN, sulfur content and maximum allowed FAME biodiesel content [6]. Due to the deviant attributes does paraffinic diesel

fuels not meet the current European diesel fuel specification. Instead, paraffinic diesel fuels follows the European paraffinic diesel fuel standard EN 15940:2016. The EN 15940 standard divides paraffinic diesel fuels in two classes depending on the given CN: A - high cetane paraffinic fuel and B - normal cetane paraffinic fuel. The main differences between these standards are presented in Table 1.

Table 4.1. Central specifiactions for standardizied conventional diesel fuel (EN 590) and paraffinic diesel fuels (EN 15940). [6]

	EN 590	EN 15940, Class A	EN 15940, Class B
Cetane number	> 49	> 70	> 51
Density at 15 C (kg/m^3)	820 - 860	765 - 800	780 - 810
Viscosity at 40 C (mm^2/s)	2.0 - 4.5	2.0 - 4.5	2.0 - 4.5
Flash point (^oC)	> 55	> 55	> 55
Water content (mg/kg)	< 200	< 200	< 200
Carbon residue (10% btms)	< 30	< 30	< 30
Oxidation stability (g/m^3)	< 25	< 25	< 25
Total aromatics (wt-%)	-	< 1.1	< 1.1
Polyaromatics (wt-%)	$\leq$ 8.0	-	-
Sulfur content (mg/kg)	< 2	< 5	< 5
FAME content	< 7	< 7	< 7

The general fuel attributes of diesel and paraffinic fuels are shown in Table 4.2. All renewable paraffinic diesel fuels have a virtually non-aromatic content, generally leading in significant reduction of soot formation. CN of paraffinic fuels tend to be high, hypothetically improving the combustion attributes concerning both ignition delay time (IDT) and combustion efficiency. The incresed combustion efficiency leads generally in lower CO and THC tailpipe emissions. High CN also reduces the time for fuel premixing, lowering the premixed combustion phase of diesel

combustion, reducing combustion noise and high heat release peaks causing excess NO_x. The energy density (lower heating value, LHV) of paraffinic fuels and EN 590 in relation to fuel mass are very similar. Compared with EN 590, density of both HVO and GTL seems however to be significantly lower and the density of CTO somewhat lower. These attributes may according to litterature research increse the volumetric fuel consumption in some extent.

Table 4.2 Typical fuel specifications of different diesel fuels based on literature studies. [7][8][9]

Properties	EN 590 (summer grade)	HVO	CTO based paraffinic diesel	GTL
Density at 15 C (kg/m^3)	835	775 - 785	814*	770 – 785
Viscosity at 40 C (mm^2/s)	3.5	2.5 - 3.5	3.5	3.2 - 4.5
Cetane number	53	>70	65	>70
Distillation range (°C)	180 - 360	180 - 320		190 – 330
Cloud point (°C)	-5		-5,4	0 - -25
Heating value, lower (MJ/kg)	42.7	44.0	43.27	43.0
Heating value, lower (MJ/l)	35.7	34.4	35.2	34.0
Total aromatics (wt-%)	30	0	**	0
Polyaromatics (wt-%)	4	0	**	0
Oxygen content (wt-%)	0	0	**	0
Sulfur content (mg/kg)	< 10	< 10	< 5	< 10
Lubricity HFRR at 60 C (µm)	< 460	< 460	228	< 460
Storage stability	Good	Good	Good	Good

*marginally outside the EN 15940 specification

** Information not available in articles

4.2.1 Hydrotreated Vegetable Oil

Hydrotreated vegetable oil (HVO) is produced from triglyceride (vegetable oil or animal fat) through removing the oxygen using a hydrotreatment process. The triglyceride forms paraffinic hydrocarbons - a mixture of normal- and iso-paraffins [10]. Likewise all other paraffin fuels, HVO contains no aromatics or sulphur [7]. Compared to EN 590, HVOs CN is remarkably high. Seen from Table 4.2, the heating value of HVO in relation to fuel volume is ~4% lower than EN 590. Furthermore, Sugiyama et al. suspects in their paper [10] that due to HVOs higher viscosity combined with a lower density, the fuel spray atomization may in some cases be deviant from normal diesel spray behaviour.

Engine emission formation is severely dependent of both engine parameters and operation load. Using non-adapted injection parameters, similar performance and brake specific fuel consumption (BSFC) figures has been experienced between conventional diesel fuel and HVO. Despite HVO has a lower volymetric energy density, the energy flow through the injectors seems to remain equal. HVOs lower viscosity increases the volumetric flow (approx. 3-4% higher compared to diesel), compensating the difference in energy density. Figure 4.1 illustrates optical experiments

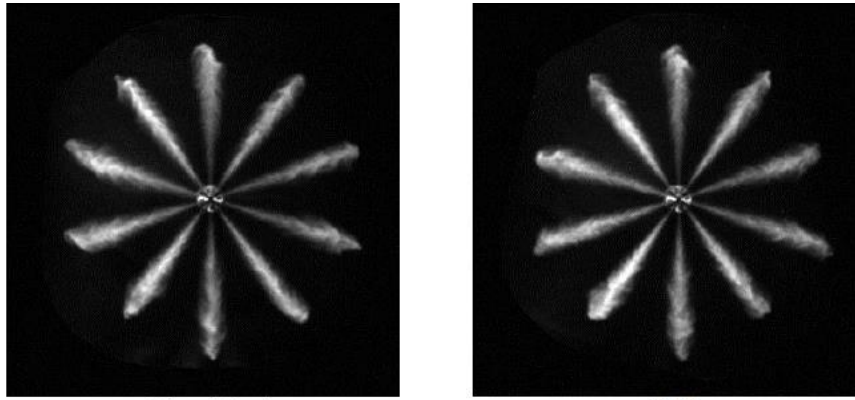

Figure 4.1. Comparison of fuel spray behaviour. [10]

regarding fuel spray behavior with both diesel and HVO. These experiments indicated no general differences in penetration, droplet size (Sauter mean diameter) or spray diameter. In addition, equal spray behaviour in terms of diffusion were noted with both fuels. [10]

Both NO_x reduction and improvements in PM formation has been experienced using HVO [7]. On medium or high load conditions, up to 65% of soot reduction has been recorded [11]. On low and part load, 80% reductions of indicated specific carbon monoxide emissions (ISCO) and indicated specific hydrocarbon emissions (ISHC) are achievable. According to Sugiyama et al., improvements up to 4 - 5% of fuel consumption may be attained by optimizing the diesel parameters for HVO though advancing fuel injection timing without a penalty in smoke or combustion noise [10].

The improved emission outcome can be explained through examining the fuel specification. Due to the low aromatic content, HVO combustion generates less soot. High CN in the other hand affects combustion characteristics i.a. through improving fuel evaporation and decreasing the ignition delay. Shorter ignition delay time decreases the magnitude of the premixed diesel combustion phase. The premixed diesel combustion phase is generally responsible for causing high heat release peaks, rapid pressure rise rate (PRR), affecting both NO_x formation and combustion noise. High CN also improves the fuel reactivity, causing lower ISCO and ISHC emissions. CN affects particularly the combustion quality in lower loads, as combustion chamber temperatures are remarkably lower. [11]

In 2011, VTT performed a long term study concerning usage of HVO and 30% HVO in commercial diesel fuelled buses [12]. Conclusions for effect of emission reductions using 100 % HVO were 10 % for NO_x, 30% for PM, 30 % for CO and 40 % for THC. Based on the results, the effect on engine aftertreament using HVO is excellent. Due to the lower density of HVO, a 5,2 vol-% increase in fuel consumption (100% HVO) was estimated. The energy consumption was however estimated equal due to HVOs lower volumetric

energy density. The tests confirms pure HVO being suitable as a drop-in fuel in conventional diesel applications without any risks of causing technical issues.

4.2.2 Crude Tall Oil based Renewable Fuel

A production strategy to refine renewable paraffinic diesel fuel from crude tall oil (CTO) has recently been developed. A total GHG reduction of 80% may be achieved in the transport field by using CTO-based renewable fuel as a substitute for traditional diesel fuels. CTO is a liquid wood-based residue that can be converted into paraffinic diesel through a hydrotreatment process. CTO is separated from "black liquor", a chemically versatile liquid extracted from softwood during a cellulosic chemical pulping process. CTO contains 36-58% of carbon chains of 16 to 20 carbon containing fatty acids, 10-38% of rosin acids and 10-38% of sterols. CTO may also contain neutral substances, mainly consisting of β-sitosterol. The chemical composition of CTO varies depending on several factors, such as raw material (tree species, growing cycle, age etc.) and geographic location (Table 4.3.). For instance: CTO extracted from trees growing in the South-eastern parts of US are acid rich (fatty acid, 50 wt% and resin acid 40 wt%), meanwhile in Scandinavia, share of acids are milder (fatty acid, 42 wt% and resin acid, 39 wt%). [13]

Table 4.3. Composition of CTO. [13]

	South eastern US	Northern US and Canada	Scandinavia
TAN	172	135	155
Saponification number	172	166	142
Resin acids (wt%)	40	30	42
Fatty acids (wt%)	50	40	39
Usaps (wt)	8	15	10

Due to the large composition of impurities, solid particles, elements and metals CTO must be purified before the hydrotreatment. CTO is commonly hydrotreated in a plug flow reactor. The plug reactor is responsible of hydrodeoxigenation, hydrosulphurization, isomerization, hydrogenation and cracking. The raw hydrotreated CTO consists both of light and mid-distillate diesel components. These are later separated through general fractionation methods. [13]

Several tests indicates CTO-based paraffinic diesels being fully compatible both as blend- or drop-in fuels for modern direct injected CI-engines. Mixing 30% of CTO-based paraffinic diesel with traditional diesel in non-adapted diesel engines indicates minimal changes in performance and emission characteristics [13]. Figure 4.2 illustrates combustion characteristics of a 30% CTO-based fuel blend (B30UPM). The combustion behaviour on part load is almost identical compared with the reference fuel. On high load, a small increase in indicated mean effective pressure (IMEP) has been experienced. Equal combustion behaviour has also been detected on higher CTO-based blends. Figure 3 represents full load heat release characteristics of three different fuel mixtures (100% diesel, 50/50 diesel/CTO, and 100% CTO). Barely no difference in heat release speed or magnitude can be noted [8].

Increasing the share of CTO-based renewable fuel in the fuel blend, improved CO and THC emission trends are found. The high CN and low aromatic content promotes the fuel reactivity throughout the combustion process. The higher the CTO-based fuel share, the greater effect on PM, CO and THC is seen. Optimizing the engine parameters on pure CTO-based fuel in NO_x-PM trade off to "high-NO_x strategy", very low PM-emission levels may be reached. [8]

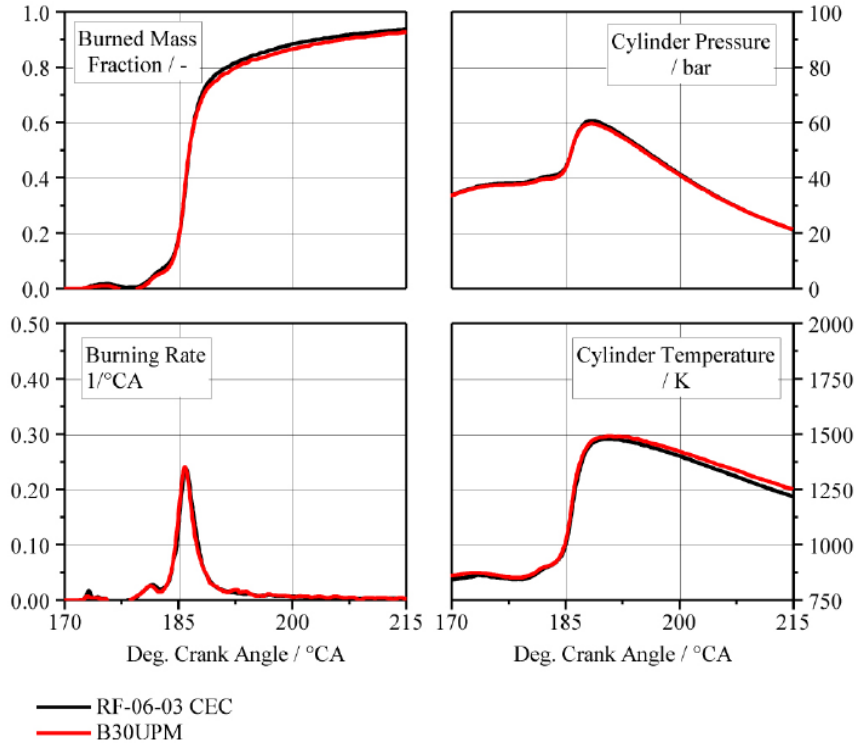

Figure 4.2 Combustion characteristics of both EN590 and B30UPM. [13]

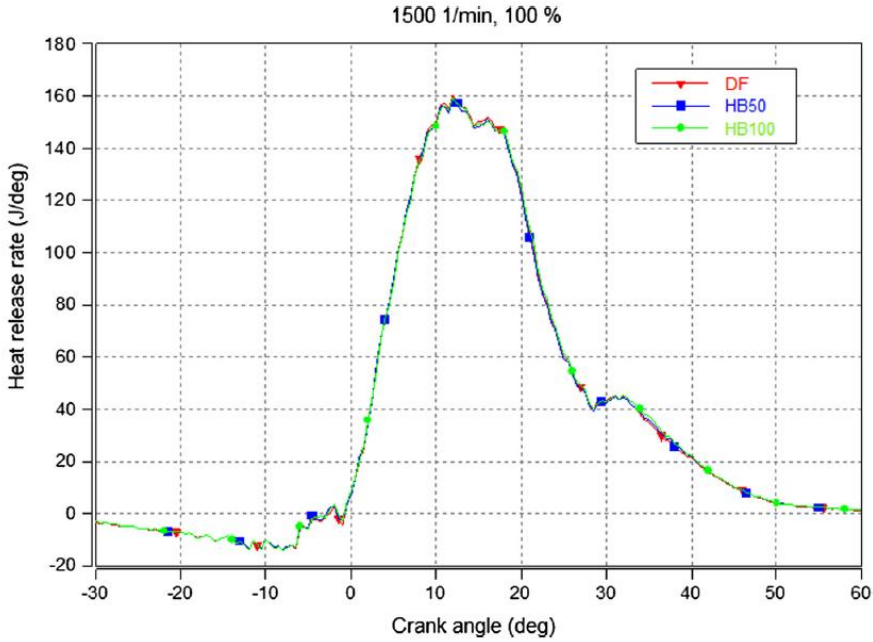

Figure 4.3 Heat release rate of three different fuel blends (diesel, 50/50 diesel CTO, and 100% CTO). [8]

In 2014, VTT performed a long-term fuel test concerning CTO-based paraffinic fuels. The purpose of the experiment was to study the impact of using CTO-based diesel fuels in a larger time scale. The fuel blend contained 20 % CTO-based renewable fuel. No notable difference in engine or emission after-treatment ageing was be found. The emission trends concerning CO, CO_2 and THC for both conventional and CTO-based (20% CTO) diesel fuels were very similar. The experiment indicated CTO-based paraffinic diesels being suitable for drop-in purpose [14].

4.2.3 Gas-to-liquids

Gas to liquids (GTL) is paraffinic diesel fuel produced through a low temperature Fischer-Tropsch process. The Fischer-Tropsch process utilizes catalytic reactions to synthesize paraffinic hydrocarbons from shorter organic chemicals, such as methane.

GTLs attributes shares similarities with HVO. Compared with traditional fossil based diesel fuel, GTL has a high CN and higher hydrogen to carbon ratio. GTL is also virtually free from sulphur and aromatics. The combustion of GTL paraffin improves emission similar to HVO. PM emissions can be significantly reduced depending on the operating conditions and engine configuration. Highest PM reduction rates are often experienced on higher loads. Due to the high CN, combustion quality is improved in form on reduced CO and HC. Particularly on lower loads, emission reductions up to 40% regarding CO and HC has been experienced. The combustion noise seems to be equal compared to conventional diesel. Figure 4.4 illustrates the difference in PM-NO_x trade-off between diesel and GTL in a non-adapted diesel engine. [15]

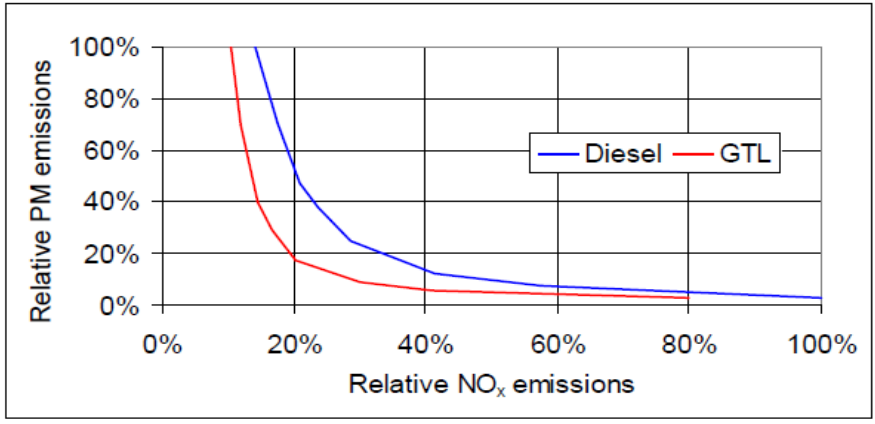

Figure 4.4 A typical improvement PM-NOx trade-off improvement using GTL in a non-adapted diesel engine. [15]

Although GTL is well compatible with non-adapted CI-engines as a drop-in fuel, the best benefits of the fuel are attained with recalibrated engine parameters. The method for optimizing the injection parameter using GTL is dependent of the desired after-treatment strategy. The optimization strategies concerns generally the PM-NO_x trade off. Maximizing NO_x reduction may lead to slightly increased CO and PM formation, although significantly lower (52%) NO_x emissions has been recorded. Aiming for constant NO_x, PM reductions up to 30-55% may be achieved. Also, a 20-40% HC reduction and 10-40% lower CO are possible. Optimizing parameters for lowest fuel consumption seems to serve a fair trade off between NO_x and PM formation. Greatest reductions in fuel consumption are reported as high as 7,5 wt%, while a reduction of 24% NO_x respectively 30% PM could be reached. [15]

4.2.4 Survey Summary

The general characteristics of the paraffinic fuels are somewhat different. It seems that HVO and GTL shares many similarities in combustion behavior concerning engine performance and emission characteristics. Compared with both traditional diesel and CTO-based renewable diesel, both HVO and GTL has significantly higher CN, yet lower density and viscosity. These attributes together raise the fuel reactivity, thus improving the combustion quality. Especially on low loads, significant improvements in CO and THC formation are expected. However, if the injection timing is not recalibrated, the short ignition delay may cause decrease in engine efficiency. The greatest benefits of these fuels may therefore be achieved through optimizing engine parameters. Additionally, fuels with high CN (higher fuel reactivity) would allow lower compression ratios (CR). Reducing CR will decrease the overall combustion temperature, thus resulting in lower NO_x.

Concerning performance and combustion, CTO-based renewable diesel seems to behave similar to traditional diesel. The combustion characteristics of the CTO-based fuel was close to identical compared with

the reference (EN 590) on all different fuel blends (CTO-based fuel 0-100wt-%). Higher shares of CTO-based fuels seem however to magnify the improvement of tail-pipe CO, THC and PM. The change in combustion efficiency is suspected to be a result of the slightly higher CN.

Combustion efficiency of a given fuel is highly dependent of the operation parameters for a specific engine. Due to the deviant attributes of all fuels included in the survey, optimization of parameters in relation to each fuel may be taken into consideration. Using OEM parameters, the lower fuel density of HVO and GTL may increase volumetric fuel consumption in some extent, while changes using CTO-based products seems to be smaller. Observing the general attributes of paraffinic fuels - such as higher CN - combustion and engine efficiency may through optimization however increase max. ~ 5%.

Figure 4.5 represents average CN of both conventional diesel and paraffinic diesel fuels included in the survey. Surprisingly, the reported CN of HVO varied between 70 and 88 depending of literature reference. The variation of CN is somehow large. It is highly suspected that the determination of HVO CN has become more precise over time. CN of HVO and GTL were both determined as >70, whereas CTO-based fuel may be between 60 and 70. Average CN of all paraffinic fuels included in the survey is 68.

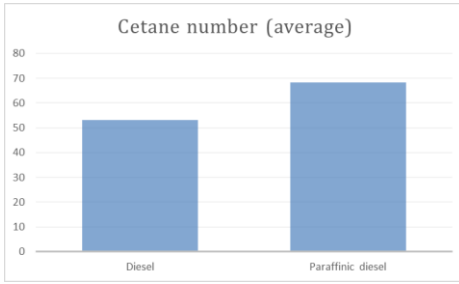

Figure 4.5 Average CN of both conventional and paraffinic diesel.

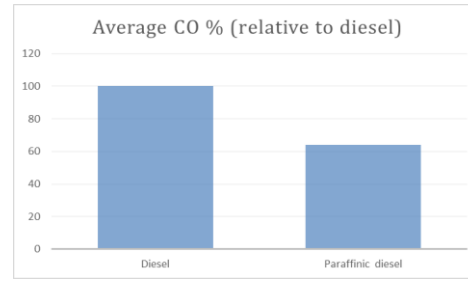

Figure 4.6 Average difference in CO% using non-adapted parameters.

Figures 4.6 – 4.9 represent typical emission trends collected from literature included in this chapter. The paraffinic fuel has been compared with the reference included in their own literature. The emission data and trends are then averaged in relation to the reference fuel. Due to different experiment methodology and uncertainties, the data and figures must be seen as directional conclusions. Concluded from figures 4.5 – 4.8, increasing CN on non-adapted parameters improve CO and THC emissions while NOx variation is low. Furthermore, significant (50%) improvements in PM formation can be attained through using non aromatic fuel compounds.

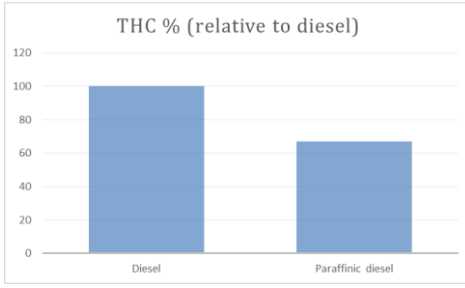

Figure 4.7 Average difference in THC% using non-adapted parameters.

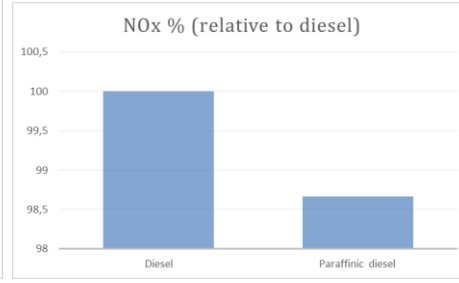

Figure 4.8 Average difference in NOx% using non-adapted parameters.

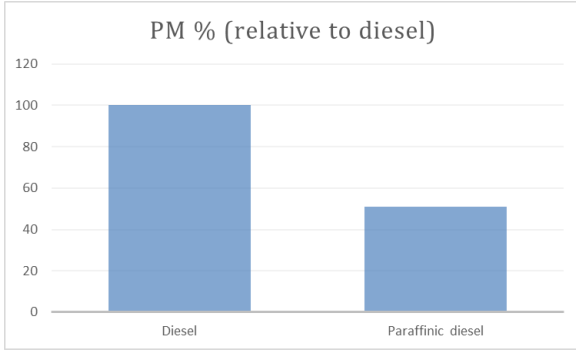

Figure 4.9 Average difference in PM-emission characteristics using non-adapted parameters.

As a conclusion: all of the introduced renewable paraffinic diesels affected positively on emission formation - particularly concerning CO, THC and PM-emissions. Least benefits were noted concerning NO_x-formation. Fuel consumption and performance using OEM parameters are in general expected to remain similar to the reference, EN 590. In addition, all of the fuels included in the survey seem to be applicable as a drop-in fuel. In order to attain full benefits from each fuel, an optimization of injection parameters should however be made.

4.3) Engine Optimization for Renewable Paraffinic Diesel

Paraffinic diesel fuels have been proven to decrease PM, CO, THC emissions compared to fossil diesels. In certain cases the emission reductions with different paraffinic diesels are equal when comparing results to fossil diesel. With current common-rail fuel injection technology this gives an opportunity to optimize engine parameters for better engine efficiency without increase in NOx emissions. The aim of this project was to optimize non-road diesel engine for one paraffinic diesel fuel and

compare the results with typical European grade diesel fuel measured with OEM engine parameters.

4.3.1 Tests Fuels

The measured fuels were supplied by fuel producers and all the fuels are in commercial production. The reference fuel was selected to meet the requirements of EN590:2013 standard. Fuel specifications are presented in table 4 which ***Fuel 1 (reference fuel) or fossil diesel, Fuel 2 is paraffinic renewable diesel, Fuel 3 is paraffinic fossil diesel and Fuel is paraffinic renewable diesel.***

Table 4.4: Fuel specifications.

Fuel Properties	Unit	Fuel 1 Reference	Fuel 2 Paraffinic	Fuel 3 Paraffinic	Fuel 4 Paraffinic
Density (15 degC)	kg/m3	845	780	778	813
Kin. Viscosity (40 degC)	mm2/s	2.99	2.92	2.69	2.81
Cetane number (IQT)	-	52.8	78.9	-	60.8
Sulphur content	mg/kg	6.9	< 1	< 5	< 1
Aromatics	wt-%	27,9	< 0.2	n.a.	n.a.
Polycyclic aromatics	wt-%	4.9	n.a	n.a	n.a
FAME content	vol-%	6.9	0	0	0
Lower heating value	MJ/kg	42.4	43.8	43.9	43.3
Lower heating value	MJ/l	35.8	34.2	34.2	35.2
Initial boiling point, IBP	°C	173	210	180	171
Distillation 10% recovered	°C	223	261	214	198
Distillation 90% recovered	°C	336	289	328	321
Final boiling point, FBP	°C	355	302	344	365

4.3.2 Research Methods

Specification of the engine used for the measurement is presented in the Table 4.5 Test engine was Tier 4 interim emission level Off-road diesel engine. Engine is utilizing SCR-only philosophy, thus there is no additional systems for emissions control such as EGR or DPF. Exhaust gas aftertreatment system was not installed on the engine. Engine ECU was open for parameter modification.

Table 4.5 Test engine specification.

Engine Detail	Unit	Specification
Engine type	-	Tier 4i Off-road Engine
Rated power	kW	95 @ 2200rpm
Maximum torque	Nm	550 @ 1500rpm
Swept Volume	[L]	4.4
Number of Cylinders	-	4
Valves per Cylinder	-	4
Fuel Injection Equipment	-	Bosch CRI 2 - 1600 bar
Turbocharger	-	pWG
Compression ratio	-	16.5:1
EGR	-	None
Exhaust Aftertreatment System	-	None

Measurements were performed with two engine calibrations:

1. *Engine OEM calibration*
2. *For paraffinic diesel "Fuel 2" optimized parameters*

Parameter calibration strategy for Fuel 2 was to maximize the combustion

efficiency while maintaining the NOx level that was measured with the reference diesel fuel and original parameters. Optimized calibration included optimizing of rail pressure by decreasing the pressure and by advancing the fuel injectors start of energizing (SOE) so that the center point of combustion was possible to move towards TDC. The change in the center point of combustion varied between 2°...2.5° CA depending of the load point.

Typically NO_x emission tends to increase while increasing the engine efficiency by advancing the phase of combustion. However with common-rail fuel injection system it is possible to partly compensate the increase in NO_x emission by decreasing the injection pressure. This tends to lead to increase PM emission which can be allowed with paraffinic fuels, since their PM emissions are on lower basis compared to fossil fuels. However, in addition to maintain the NO_x levels on reference level, also the goal for PM, CO and THC emissions was the same.

Test boundary conditions can be found in the Table 4.6 Boundary condition values in Table 6 were chosen according the engine installation guidelines and restrictions.

Table 4.6 Test boundary conditions.

Conditions	Unit	Specification
Exhaust back pressure @ rated power	mbar	230
Intake under pressure @ rated power	mbar	35
Charge air cooler pressure drop @ rated power	mbar	150
Charge air temperature in intake manifold @ rated power	°C	58
Intake air temperature	°C	25

Measurement were conducted in Non-Road Steady Cycle (NRSC) and Non-Road Transient Cycle (NRTC) test cycles. Only "hot" test cycles were measured. In Table 4.7 measurement matrix is shown. Transient test cycle was repeated three times and steady cycle two times with every test fuel.

Table 4.7 Measurement matrix.

Fuel	Engine Calibration	Test Cycles
Fuel1 (Reference)	OEM and optimized* parameters	3 x NRTC 2 x NRSC
Fuel2	OEM and optimized* parameters	3 x NRTC 2 x NRSC
Fuel3	Optimized* parameters	3 x NRTC 2 x NRSC
Fuel4	Optimized* parameters	3 x NRTC 2 x NRSC

Note: parameters optimized for Fuel 2

The emissions were measured using full flow dilution tunnel. Measurement devices are presented in Table 4.8

Table 4.8 Test measurement devices.

Measurement object	Measurement Device
NO and NO_2	CLD, ECO PHYSICS CLD 822 Mhr
HC	FID, JUM Heated FID 3-300A
CO	NDIR, Maihak Unor 610
PM	PM mass sampler
Fuel mass flow	Scale, AVL 733

4.3.3 Results

In this section results of the measurement are discussed. Measurement were conducted in NRSC and NRTC "hot" cycles. Results presented are average results and calcucated from the single measurement results of each test fuels presented in measurement matrix (Table 4.7).

a) NRSC cycle with OEM and optimized parameters

In Figure 4.10 the results with Fuel 1 (reference fuel) and Fuel 2 are presented with OEM and optimized engine parameters. The reference level was defined with Fuel 1 and OEM parameters. With the OEM parameters PM emission decreased significantly with Fuel 2, giving 32% lower PM emission compared to reference fuel. This is well in line with the test results of paraffinic fuel presented in the literature. The corresponding NO_x emissions decreased as well approximately 4%.

The total hydrocarbon emissions with Fuel 2 and OEM parameters were significantly lower (-51%) compared to reference fuel. This is due to zero aromatics content and much higher cetane number and thus better combustion characteristics. This was especially evident at part load conditions. The better combustion characteristics also decreased CO emissions by 24%.

Fuel 2 did not improve engine efficiency with OEM parameters in NRSC cycle (Figure 4.1). The volume specific fuel consumption increases with Fuel 2 and OEM parameters by 4.5% compared to reference fuel. This is explained with the lower energy content per volume (MJ/l) of Fuel 2 (app. -4.5%, see table 4.3), caused by the low density. The energy content of Fuel 2 as MJ/kg is higher compared to reference fuel.

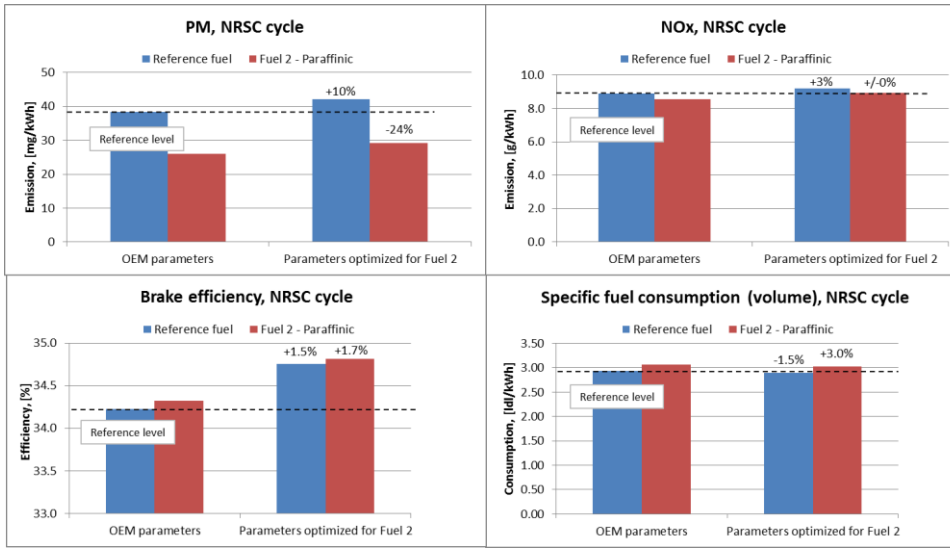

Figure 4.10. Reference fuel and Fuel 2 performance with OEM and Optimized parameters, percentages indicate the change compared to reference level. NRSC test cycle

In Figure 4.10 the results with optimized parameters are also presented. For Fuel 2 the optimized parameters improve engine efficiency in NRSC cycle by 1.7% compared to reference fuel with OEM parameters. Simultaneously PM emissions are still well (- 24%) under the reference level and the NO_x emissions do not increase above the reference level. Nevertheless, improvement in engine efficiency is not enough to decrease the volumetric fuel consumption on the same level with reference fuel. The optimized parameters also improve the engine efficiency with reference fuel but at the same time increase the NO_x emissions above the reference level by 3% and PM emissions by 10%.

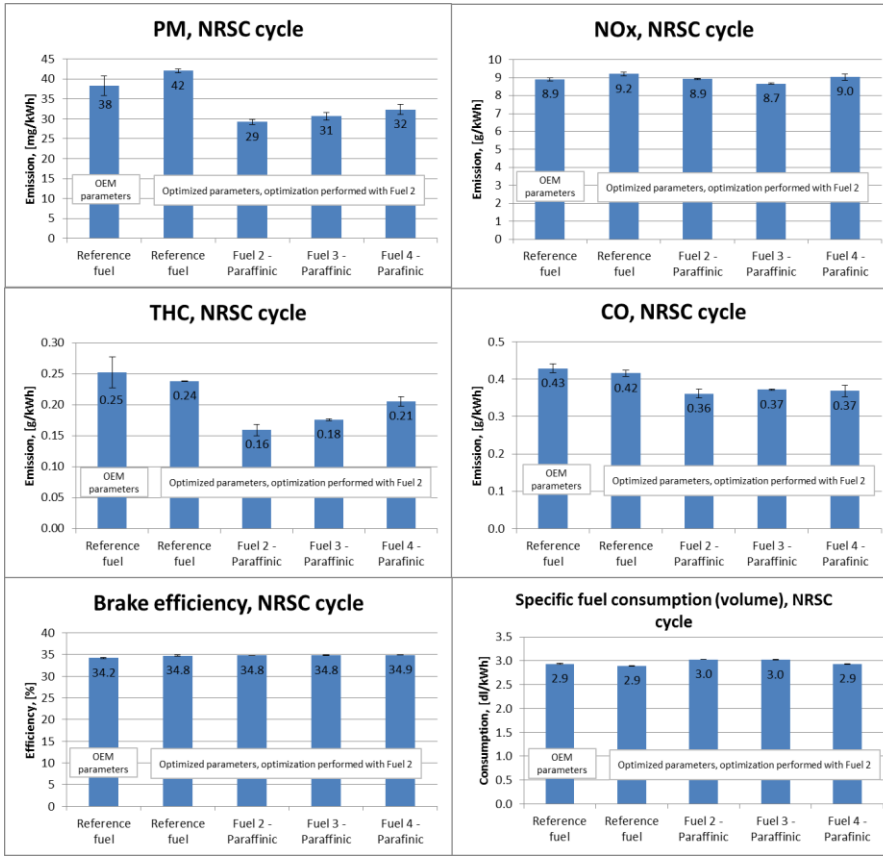

Figure 4.11 Test fuels performance in NRSC cycle

Figure 4.11 presents results with three paraffinic test fuels in comparison with reference fuel. The paraffinic fuels were measured with parameters optimized for Fuel 2. Based on the results it is possible to increase engine efficiency with paraffinic fuels while maintain the reference NO_x emission level. Over the test cycle the efficiency gain is in the range of 1.7 – 2.0% with paraffinic fuels. In individual test points the increase in efficiency altered from 1.0% to 4.3% being highest on 50 – 75% load conditions. At the same time with the efficiency increase, the PM, THC and CO emissions were

evidently below the results measured with the reference fuel. With the Fuel 4 and optimized parameters the volume specific fuel consumption was on a same level with reference fuel measured with OEM parameters. Corresponding fuel consumption with fuels 2 and 3 was somewhat higher. The engine efficiency increases also with reference fuel measured with optimized parameters but at the same time the NO_x and PM emissions also increase above the reference level defined with OEM parameters.

b) NRTC cycle with OEM and optimized parameters

Based on the parameter optimization on steady state engine loads, the parameters were re-written for the whole operation range of the engine. The method was quite rough and leaves room for further optimization.

Figure 4.12 presents the measurement results in transient NRTC cycle with reference fuel and Fuel 2 using OEM parameters and parameters optimized for Fuel 2. Results are very similar compared to the results with steady-state NRSC cycle. With Fuel 2 and optimized parameters the PM -emission stays well below the reference level and NO_x -emission does not increase significantly above the reference level while the engine efficiency increases. In NRTC cycle the engine efficiency increases by 1.4% with fuel 2 and optimized parameters compared to the reference level. With reference fuel and optimized parameters the efficiency increases a bit less compared to Fuel 2 and simultaneously the PM and NO_x -emissions increase some 10% above the reference level. The volumetric fuel consumption with Fuel 2 is higher compared to Fuel 1 as was the case also with steady-state cycle. The THC and CO emissions were 41% and 38% lower with Fuel 2 and optimized parameters compared to reference level.

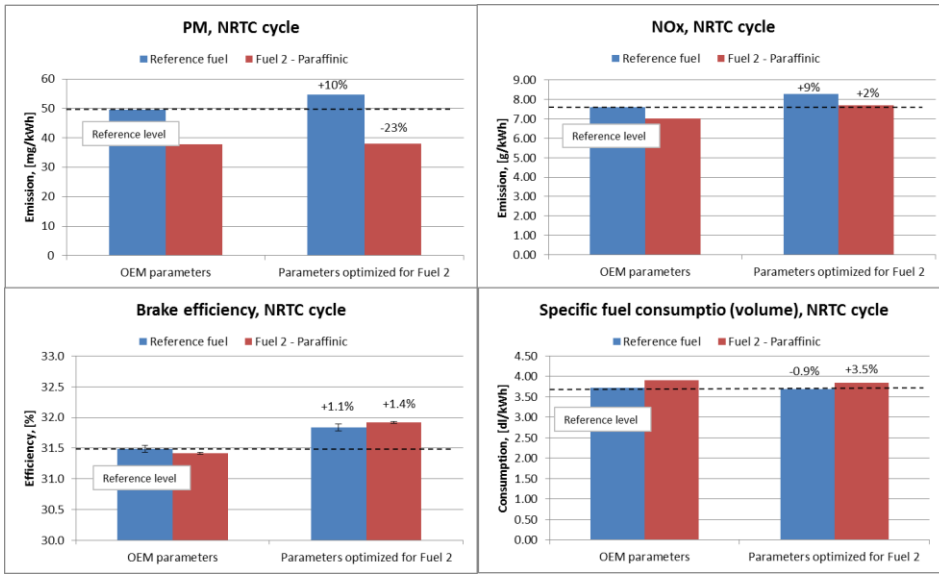

Figure 4.12. Reference fuel and Fuel 2 performance with OEM and Optimized parameters, percentages indicate the change compared to reference level. NRTC test cycle.

In Figure 4.13 the results measured with NRTC cycle are shown for all fuels. Paraffinic fuels were measured with parameters optimized for Fuel 2. Reference fuel was measured with both parameter sets. With Fuels 2 - 4 and optimized parameters engine efficiency is improved compared to reference fuel with OEM parameters. Corresponding PM, HC and CO emissions are also favourable for paraffinic fuels. The NO_x emissions with Fuel 3 are on the same level with reference fuel measured with OEM parameters. With Fuels 2 and 4 the NO_x emission are slightly above the reference level but on lower level compared to reference fuel with optimized parameters.

Improvement in the engine efficiency is in the range of 1.1 – 1.5% when paraffinic fuels are compared to reference fuel with OEM parameters. With Fuel 4 the volume specific fuel consumption is on the same level with reference fuel measured with OEM parameters. With Fuels 2 and 3 the corresponding consumption is somewhat higher. Engine efficiency is improved also with reference fuel when optimized parameters are used, but with penalty of having the highest PM and NO_x emissions.

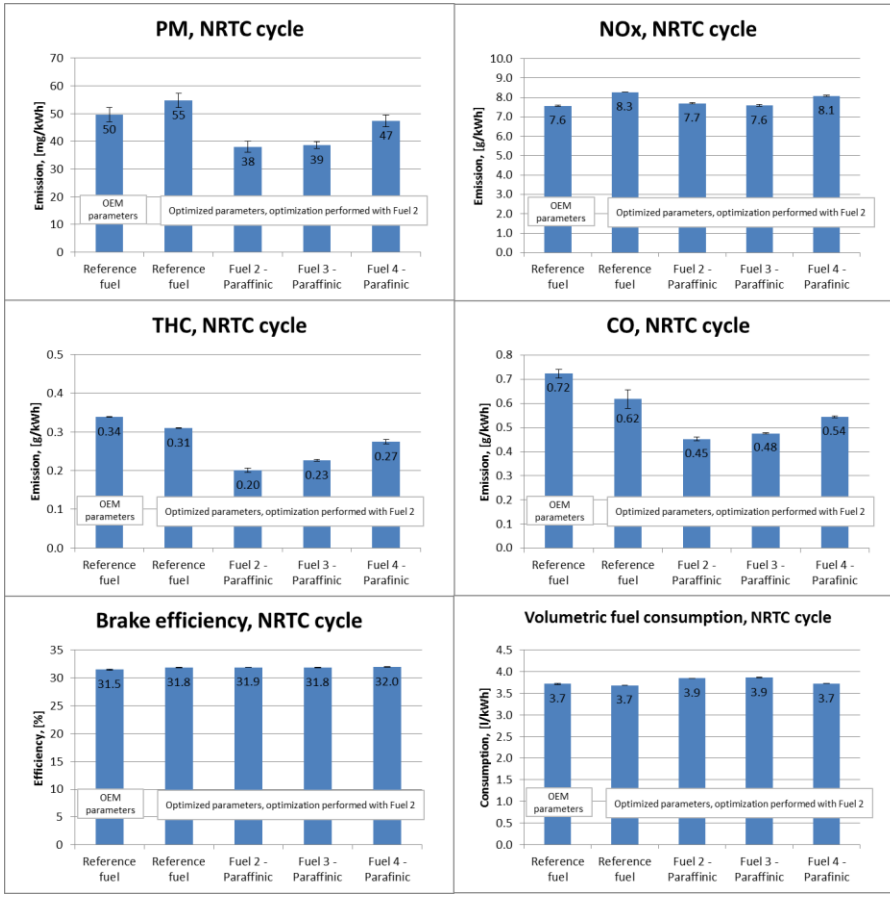

Figure 4.13. Test fuels performance in NRTC cycle.

4.3.4 Summary of the Measurements

The aim of this project was to optimize non-road diesel engine for one paraffinic diesel fuel and compare the results with typical European grade diesel fuel measured with OEM engine parameters. Optimization strategy was to increase the engine efficiency as high as possible without increase of emissions over the level defined with reference fuel and OEM engine parameters. Also two other paraffinic fuels were measured with parameters optimized for Fuel 2. This was done to find out if one set of optimized parameters work equally with a range of different paraffinic diesel fuels. Measurements were performed using steady-state and transient test cycles.

Measurements indicate that with the measured engine utilizing optimized parameters (rail pressure and fuel injector start of energizing) and paraffinic diesel fuel the engine efficiency can be increased up to 2% in steady-state cycle and up to 1.5% in transient test cycle. In individual load conditions of the steady-state cycle the increase in efficiency was even 4.0% in best case. The increase in engine efficiency was gained without any significant drawbacks in emissions when comparing results to reference fuel measured with OEM parameters. In transient test cycle some increase in NOx emissions was seen with fuels 2 and 4. However, those can be easily compensated with existing SCR systems without any hardware or software changes and with insignificant increase in combined cost for urea solution and fuel.

The engine efficiency with reference fuel and optimized parameters increased compared to reference level. The increase in efficiency came with the penalty of increased NOx and PM emissions. The NOx emissions increased 3 – 9% depending on test cycle and PM 10% in both test cycles compared to reference level.

4.4) References

[1] ASFE n.d. Paraffinic fuels and their benefits. , . http://www.synthetic-fuels.eu/paraffinic-fuels/about-paraffinic-fuels (accessed March 13, 2017)

[2] EBTP n.d. Biomass to Liquids (BtL). , . http://www.biofuelstp.eu/btl.html (accessed April 1, 2017)

[3] Neste 2017. Neste MY. , . https://nestemy.fi/ (accessed March 21, 2017)

[4] UPM 2017. UPM BIOVERNO - KOTIMAINEN JA UUSIUTUVA DIESEL. , . http://www.upmbiopolttoaineet.fi/upm-bioverno/Pages/Default.aspx (accessed March 21, 2017)

[5] Shell n.d. Shell Gas-To-Liquids. , . http://www.shell.com/energy-and-innovation/natural-gas/gas-to-liquids.html (accessed March 21, 2017)

[6] DieselNet 2015. Automotive Diesel Fuel. , . https://www.dieselnet.com/standards/eu/fuel_automotive.php (accessed March 20, 2017)

[7] Aatola, H., Larmi, M., Sarjovaara, T. & Mikkonen, S. 2008. Hydrotreated Vegetable Oil (HVO) as a Renewable Diesel Fuel: Trade-off between NOx, Particulate Emission, and Fuel Consumption of a Heavy Duty Engine. SAE Technical Paper 2008-01-2500. SAE Tech. Pap. (724), 12. doi:10.4271/2008-01-2500

[8] Niemi, S., Vauhkonen, V., Mannonen, S., Ovaska, T., Nilsson, O., Sirvi, K., et al. 2016. Effects of wood-based renewable diesel fuel blends on the performance and emissions of a non-road diesel engine. Fuel 186, 1–10. doi:10.1016/j.fuel.2016.08.048

[9] Hartikka, T. & Honkanen, M. n.d. "Engine optimization for paraffinic fuels .", 8–9.

[10] Sugiyama, K., Goto, I., Kitano, K., Mogi, K. et al. 2011. Effect of hydrotreated vegetable oil (HVO) as renewable diesel fuel on combustion and exhaust emissions in diesel engine. SAE Tech. Pap. 2011-01–19, 13. doi:10.4271/2011-01-1954

[11] Bhardwaj, O.P., Kolbeck, A.F., Kkoerfer, T. & Honkanen, M. 2013. Potential of Hydrogenated Vegetable Oil (HVO) in Future High Efficiency Combustion System. SAE Int. J. Fuels Lubr. 6(1), 157–169. doi:10.4271/2013-01-1677

[12] Nylund, N.O., Erkkilä, K., Ahtiainen, M., Murtonen, T., Saikkonen, P., Amberla, A., et al. 2011. Optimized usage of NExBTL renewable diesel fuel OPTIBIO.

[13] Heuser, B., Vauhkonen, V., Mannonen, S., Rohs, H. & Kolbeck, A. 2013. Crude Tall Oil-Based Renewable Diesel as a Blending Component in Passenger Car Diesel Engines. SAE Int. J. Fuels Lubr. 6(3), doi:10.4271/2013-01-2685

[14] Laurikko, J.K., Nylund, N.-O., Aakko-Saksa, P., Mannonen, S., Vauhkonen, V. & Roslund, P. 2014. Crude Tall Oil-Based Renewable Diesel in Passenger Car Field Test. SAE Tech. Pap. 2014–Octob, doi:10.4271/2014-01-2774

[15] Kind, M., Liebig, D., Doorn, R. Van, Lamping, M., Harrison, A., Clark, R., et al. 2010. Dedicated GTL Vehicle : A Calibration Optimization Study. SAE Int. J. Fuels Lubr. 3(1), 321–333. doi:10.4271/2010-01-0737

Work Program V:
Opportunity for Enhancing Fuel Efficiency by Ethanol Blended Gasoline Fuels (Thailand)

IEA/AMF ANNEX 52: Fuels for Efficiency

INTERNATIONAL ENERGY AGENCY:

ADVANCE MOTOR FUEL IMPLEMENTING AGREEMENT

PADOL SUKAJIT

ATSAWIN SALEE

SOMNUEK JAROONJITSATHIAN

PTT Research and Technology Institute

PTT Public Company Limited

5.1) Introduction

5.1.1 Introduction

Thailand has introduced several kinds of alternative fuels, e.g., ethanol, biodiesel, natural gas, etc. into transportation sector for several years. Although these could reduce the amount of imported crude oil, the impacts of fuels implementation on the national economics, environment and agriculture have to be considered carefully. PTT Public Company Limited or simply "PTT", as certified by the Ministry of Energy of Thailand, is a member of the Advanced Motor Fuels (AMF) program under the International Energy Agency (IEA). As a member, PTT has joined the Annex 52: Fuels for Efficiency working team under the WP6: Opportunity for Enhancing Fuel Efficiency by Ethanol Blended Gasoline Fuels. PTT has been studying on the performance of the gasoline engine using gasolines at different ratios of ethanol blending. In this work, the study was carried out by analyzing the combustion of ethanol-blended gasolines at different ethanol ratios inside the single cylinder research engine with direct injection and evaluating the engine performance. The work results will be shared and integrated with other works from the group members as well as utilized internally for the PTT product planning purpose.

5.1.2 Research Background

Thailand has promoted the use of ethanol-blended gasoline or gasohol in gasoline vehicles since 2001. It is typically known that some properties, e.g., heating value, density and chemical content, etc., of gasohol are different from those of gasoline. As a result, the combustion characteristic of gasohol inside the combustion chamber is different. Although the heating value of gasohol is approximately 35% lower than that of gasoline, the better antiknock property due to the higher octane index of gasohol is one of its superior property over the natural gasoline.

Therefore, the proper ethanol content in gasohol that enabling to obtain the highest engine performance, is the key factor to considered for market implementation.

Apart from the gasoline, gasohol is currently commercially available in Thailand as a major fuel for gasoline vehicles. There are three products of gasohol, namely E10, E20 and E85. An "E" prefix denotes gasoline blended with ethanol, while the following numbers denote the percentage of ethanol in that particular blend. For example, E10 has a mixture of 10 percent ethanol and 90 percent gasoline, while E20 has 20 percent ethanol and E85 has 85 percent of ethanol, respectively. In the future, gasoline and E10 are probably considered to be withdrawn from the list of products remaining E20 and E85 as a mainstream according to the study of the Energy Policy and Planning Office as shown in Fig. 1.1.

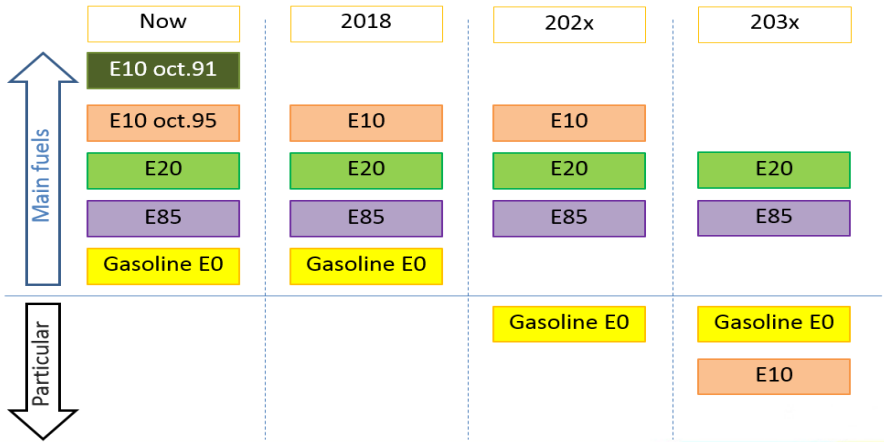

***Figure 5.1** Gasoline-base fuels planning timeline for Thailand market*

For the engine technology, the new gasoline engine typically equipped with the ignition controllable function. It was found that more torque generated by the engine could be obtained by advance the ignition timing or ignition at earlier time. In order to achieve that situation, high octane fuel is needed because the fuel have to sustain their state during

the compression stroke of the engine to avoid engine knock phenomenon and this could be realized by using high content of ethanol-blended gasoline.

Considering the gasoline engine technology timeline, there are two transitional stages of technology as can be seen in Fig. 5.2. The first stage is transition from carburetor to port fuel injection (PFI) and the second stage is transition from port fuel injection to direct injection (GDI). At this moment, Thailand market is in the latter stage, in which many car manufactures start launching the gasoline vehicles with GDI engine. The advantages of GDI technology comparing with PFI technology are, for example, intake valve deposit mitigation, high accuracy Air/Fuel ratio control, throttle loss reduction, fuel economy and CO_2 emission reduction improvement, etc.

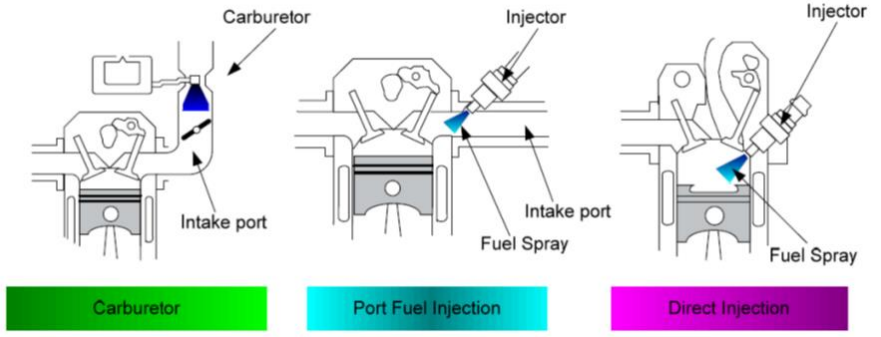

***Figure 5.2** The mixture formation systems in the gasoline engines [1]*

In GDI engines, the fuel is injected directly into cylinders at a high pressure. It is implemented the two basic charge modes, stratified and homogeneous charge as illustrated in Fig. 5.3. At the partial load conditions, stratified charge (late injection) is used. The fuel is injected during the compression stroke to supply the stratified charge. The engine can be operated at an air-fuel ratio exceeding 100 (lean condition) and fully unthrottled operation is possible. A homogeneous charge (early injection) is preferred for the higher load conditions. The fuel is injected

during the intake stroke so as to provide a homogeneous mixture. In most of this mode, the engine is operated under stoichiometric or a slightly rich condition at full load.

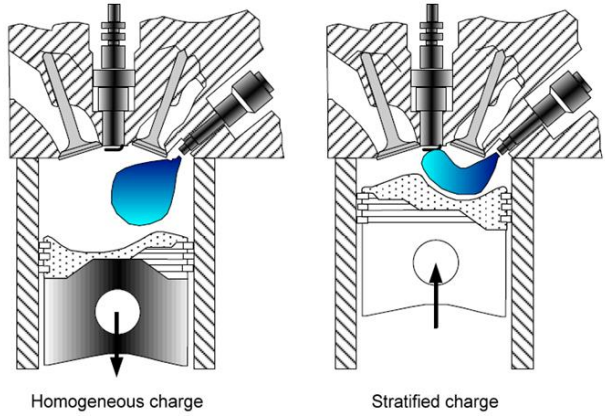

***Figure 5.3** Homogeneous and stratified charge mode [1]*

In the stratified operation, three combustion systems are used to form an ignitable mixture near spark plug at the instant ignition. These are the wall-guided, air-guided and spray-guided combustion systems, Fig. 5.4. The distinction between the different concepts is the used method with which the fuel spray is transported near the spark plug.

1. *Wall-Guided combustion system: The fuel is transported to the spark plug by using a specially shaped piston surface. As the fuel is injected on the piston surface, it cannot completely evaporate and, in turn, HC and CO emissions, and fuel consumption increase. To use this system alone is not efficient.*
2. *Air-Guided combustion system: The fuel is injected into air flow, which moves the fuel spray near the spark plug. The air flow is obtained by inlet ports with special shape and air speed is controlled with air baffles in the manifold. In this technique, fuel does not wet the piston and cylinder. In the air-guided and*

wall-guided combustion systems the injector is placed remote to the spark plug.

3. *Spray-Guided combustion system: In the spray-guided technique fuel is injected near spark plug where it also evaporates. The spray-guided technique theoretically has the highest efficiency. The spray guided combustion process requires advanced injector systems such as piezo injection. This technique has some advantages: reduced wall wetting, increased stratified operation region, less sensitive to in-cylinder air flow, less sensitive to cylinder to cylinder variation and reduced raw HC emissions. Reported disadvantages are spark plug reliability (fouling) and poor robustness (high sensitivity to variation in ignition & injection timing).*

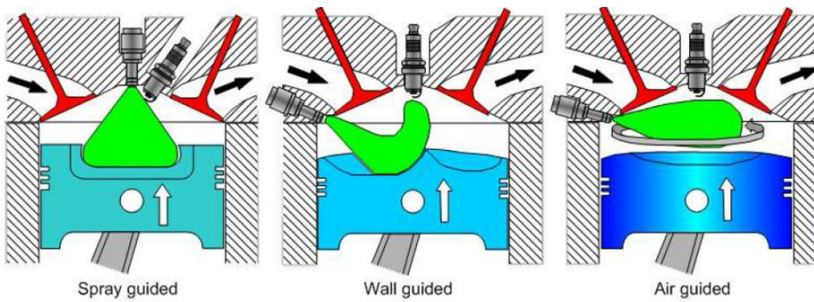

***Fig. 5.4** The wall-guided, air-guided and spray-guided combustion systems at stratified charge [1]*

In the article "Higher Ethanol Blends for Improved Efficiency" by Brian West from Oak Ridge National Laboratory, presented in the National Ethanol Conference at Texas in February 2015, the influences of ethanol content on the performance of the Ford's turbocharged gasoline direct injection engine was studied [2]. Fig. 5.5 (a) shows the effect of ethanol content on the octane (RON) number of fuel blends. It shows that as the ethanol content increased, the RON number increased towards the RON

number of neat ethanol. Fig. 1.5 (b) shows the performance test of the Ford engine when using several kinds of ethanol blended gasolines. It also shows that the engine thermal efficiency increased when the RON number increased.

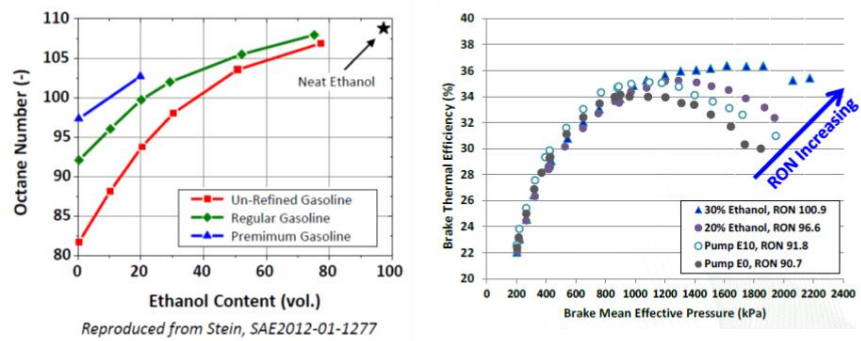

***Figure 5.5** (a) effects of ethanol content on octane number of fuel blend and (b) engine performance obtained from using several kinds of ethanol-blended gasolines [2]*

The research above is a part of Mid-level Ethanol Blends Program under the US Department of Energy during 2007-2012 with the budget 46 million US dollars. This ensures that blending ethanol at high content in gasoline is technically feasible and applicable, especially in Thailand where there is a goal to expand the use of ethanol as an alternative fuel in transportation sector. However, there still another technical concerns of ethanol that should be further studied and verified when mixing with gasoline, for example, heating value, evaporation and corrosive property, etc.

5.1.3 Objectives

1) *To develop the test method for conducting research on fuel impact with gasoline engine as well as to study the engine knocking parameters at given boundary conditions.*

2) *To determine the optimum ethanol content in gasoline to obtain the*

highest efficiency from gasoline direct injection engine.

3) *To gain the technical results not only for the IEA/AMF Annex 52 program commitment but also for PTT fuel product development.*

5.1.4 Hypothesis and Scope of Work

From the previous section, the information shows that if the engine can be fully controlled, using of high ethanol content in gasoline can enhance the engine performance. However, this work would like to extend the objective to the engine that has no special controlled, which can be representative of the commercial engine operation. This study would also verify the ability of the engine to adjust the ignition timing properly with the different blended fuel for antiknock and performing with high efficiency. Initially, knock measurement method and boundary conditions on the Ricardo GDI research engine were determined. After that the gasolines with different ratio of ethanol (E0-E85) were used to determine the optimum ratio of ethanol that gives the best engine performance.

5.1.5 Experimental Method

a. *Design the engine knock measurement method in Ricardo GDI research engine from the cylinder pressure signal using digital signal processing by AVL IndiCom. After that setting an operation matrix that covers all measurement ranges for measuring maximum brake torque when using all fuel blends.*

b. *Prepare and analyze the physical and chemical properties of ethanol blended gasolines at 0 (E0), 10 (E10), 20 (E20), 30 (E30) 50 (E50) and 85 (E85) percent of ethanol by volume.*

c. *Determine the octane numbers, i.e., research octane number (RON) and motor octane number (MON) of all fuel blends according to the ASTM D2699 and D2700.*

d. *Set the knock limit pressure and other parameters that related to the engine performance.*

e. *Conduct the experiment and summarize the results to determine the optimum ratio of ethanol in gasoline that the engine perform at the best efficiency.*

5.2) Combustion Characteristics and Engine Knock Investigation

5.2.1 Engine Knock and Antiknock Property of Engine Fuel

Engine knock is the result of an autoignition process of combustible mixture ahead of the frame front. Characteristic for the engine knock is the name giving knock sound that results from the high frequency oscillating cylinder pressure. This adversely affects output power and dramatically increases heat transfer to the piston and other combustion chamber surface.[3] If the knock is severe, it can cause damage to the engine. If not, it can generate noise which may be annoying to the users. Engine knock is caused by many factors, such as, fuel property, engine design or engine running conditions, etc.

The engine fails to operate at its best condition, i.e., at the ignition timing that obtains maximum torque at specific engine speed and throttle position due to the knock before it reaches that point or the engine has a condition called "Knock-limited". In modern engines, in which knock sensors are installed to prevent knock-limited condition. The knock signals were fed back to the engine control unit to adjust the ignition timing to prevent engine damage. This could result in reducing of engine performance.[4], [5], [6], [7] Therefore, the antiknock property of fuel is an important factor directly affecting the performance of new engines.

In order to qualify the antiknock property of fuel, the octane index (OI) is used. It defines as [8];

Octane Index, $OI = RON - KS$

Where RON = Research octane number,
MON = Motor octane number,
S = Sensitivity = RON – MON
K = Engine related parameter (Negative value)

This can be stated that in case there are two fuels with the same RON numbers, if one has higher sensitivity (Lower MON number), it will have higher octane index or higher knock resistance than another.

5.2.2 Fuel's Sensitivity

The key parameters of gasoline that are used to define the antiknock quality are research and motor octane number (RON and MON). RON and MON are determined by single cylinder CFR engine according to ASTM D2699 and D2700. MON determination is tested at the engine speed of 900 rpm, which is higher than that of 600 rpm for RON determination. However, they were tested under the same unit by using 2 paraffinic hydrocarbons as reference, i.e., iso-octane with 100 octane and heptane with 0 octane. If two substances are mixed, the mixture is called "Primary Reference Fuel (PRF)". For example, if 95 percent of iso-octane is mixed with 5 percent of heptane, the octane numbers will be 95 (both RON and MON). The sensitivity is 0 (Sensitivity = RON-MON). However, if the test fuel has RON 95 and MON 85, it sensitivity is 10. Kalghatgi [3] explained that PRF did not indicate the real antiknock quality as the engine requires. However, this is due the fact that RON test was discovered in 1930. At that time the compression pressure of the engine was 0.5 bars and the engine efficiency could not be comparable with nowadays. [9] After that MON test was discovered and it could better represent the engine knock condition than RON. As a result, antiknock index of fuel is defined as (RON + MON)/2 or K = 0.5 until now.

The K factor depends on the engine speed and load, but is independent of fuel. This means that under different operating conditions, a certain fuel with given RON and MON will exhibit different knocking behavior. US Coordinating Research Council (CRC) has limited the K factor of the engine

during 1947-1996 to 1. After that Mittal and Heywood showed that the K factor was reduced to 0 for the engine technology in 2008. However, the current engine technology is more advance developed than the past resulting in the K factor is further reduced lower than 0 downward the negative value. Current natural aspirated Japanese and European engines show the similar trend. In addition, the engine with turbocharger exhibits more negative K factor. [4], [5], [10], [11] This is the reason why the modern engine requires fuel with high sensitivity or high octane index for engine knock prevention.

According to the PTT in-house project R&T024 GDI Combustion Research, the important of fuel sensitivity in term of knock prevention. The experiment was conducted by comparing the antiknock quality of primary reference fuel (PRF) and commercial unleaded gasoline (ULG95) using single cylinder Ricardo GDI research engine. The octane numbers (RON and MON) as measured by CRF engine and their sensitivity are shown in Table 2.1. It shows that both ULG95 and PRF have the same RON number (RON 95.4), but ULG 95 has MON number of 86.7, which is lower than PRF number of 95.4. As a result, ULG95 has higher sensitivity than PRF. Fig. 2.1 shows that experimental result on antiknock property of both ULG95 and PRF in research engine. The antiknock property can be demonstrated by comparing the ignition time at crank angle degree before TDC (CAD BTDC) at a certain knock intensity or at knock-limited spark advance (KSLA). It shows that at KLSA of 0.5 bar, PRF can be ignited at 11.75 CAD BTC before knocking happened, whereas ULG 95 can be ignited at more advanced timing at 13.58 CAD BTC before knocking. This means ULG95 has better antiknock property than PRF at the same knock limit. This result shows clearly that octane sensitivity of fuel directly impacts to the antiknock property rather than either RON or MON only.

Table 5.1 Octane numbers of PTT ULG95 and PRF95.4

Fuel	RON	MON	Sensitivity
PTT ULG 95	95.4	86.7	8.7
PRF 95.4	95.4	95.4	0

Note: *Test was conducted using single cylinder CFR engine. PRF95.4 contents; 95.4% iso-octane and 4.6% n-heptane.*

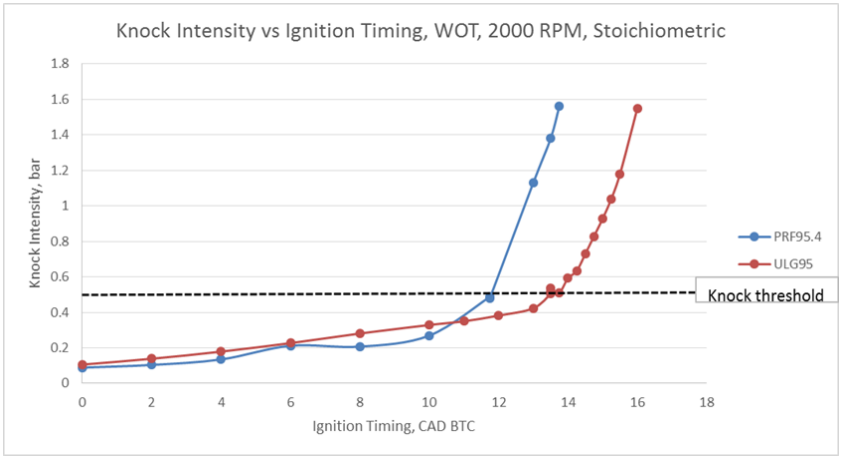

Figure 5.6 Relationship between knock intensity and ignition timing of PTT ULG95 and PRF95.4, respectively

5.3) Combustion Characteristics in Ricardo GDI Research Engine

Knocking behavior of a certain fuel was studied using Ricardo GDI research engine. Fuels used in this study were ethanol-blended gasolines at different ethanol contents. Both ethanol and 2 grades of base gasolines (G-base 1 and G-base 2) were obtained from the PTT depots, which is for commercially distribution.

5.3.1 Engine Test Bench

The engine used in this work is Ricardo Hydra GDI research engine with single cylinder and direct injection as shown in Fig. 5.7, whereas its specifications are listed in Table 5.2. The engine is also equipped with many instruments as follow;

a) *Kistler pressure transducer for cylinder pressure measurement,*

b) *AVL IndiCom for receiving and recording data,*

c) *ETAS Lambda meter LA4 for measuring Air/Fuel ratio,*

d) *ECU from Cosworth programmed by PiCalTools*

e) *Fuel injection control unit programmed by Drivven*

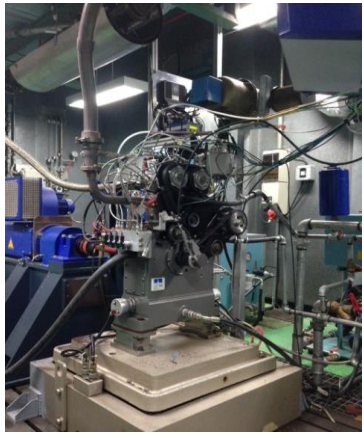

Figure 5.7 Ricardo Hydra GDI research engine

Table 5.2 Ricardo Hydra GDI research engine specifications

Bore (mm)	86
Stroke (mm)	86
Displacement (cc.)	500
Length of connecting rod (mm)	143.5
Compression ratio	11.5
Cam configuration	DOHC
Numbers of valve	4 valve per cylinder
Valve system	Dual VVT
Fuel delivery	Direct injection at the middle of cylinder
Fuel pump pressure (bar)	5-200
Max. engine speed (rpm)	6500
Min. engine speed (rpm)	1000
Max. torque (N.m)	40
Max. power (kW)	22
Fuel type	Gasoline, ethanol blended gasoline (E0-E85)

5.3.2 Knock Intensity (KI) Measurement

Generally, engine operating at low engine speed with high load has more chance to knock [8] Therefore, this work designs the test by referring to such situation by setting the engine parameters as listed in Table 5.3.

Table 5.3 Engine conditions for knock determination

Engine speed (rpm)	2000 and 2500
Throttle degree (%throttle)	30 and 100
Air/Fuel ratio (λ)	1 (Stoichiometric), 0.8 (Rich) and 1.2 (Lean)
Avg. Knock Intensity Limit (bar)	0.5
Engine oil temperature (°C)	80
Coolant temperature (°C)	80

Knock signal analysis from the engine was collected by AVL IndiCom. It collected the cylinder pressure signal and filtered at 5-10 kHz by electronic filter inside the program as shown in Fig. 5.8. Knock intensity formula was then generated by numerical support program CalGraf. All filtered signal will be absolute value and the maximum value of intensity of each cycle was counted only. After collecting for 400 cycles, the average knock intensity can be obtained and set as KI value. The experiment was carried out by advancing the ignition timing at different crank angle degree before TDC and record the KI value. As the ignition timing became earlier, the KI intensity became raising as well as engine torque. Finally, when the KI increased until reaching the limited KI value (In this work KI at limited at 0.5 bar) or knock-limited spark advance (KLSA), how much the ignition timing is advanced will indicate the antiknock property of the test fuels.

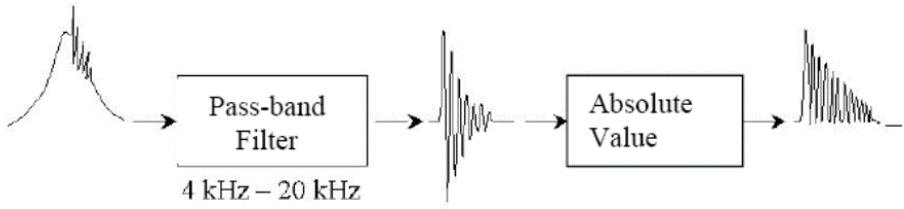

Figure 5.8 Cylinder pressure signal processing for knock intensity determination

5.3.3 Test Fuels

The ethanol-blended gasolines used in this work were prepared from two grades of base gasolines (E0), named as G-base 1 and G-base 2. Each grade of base gasoline will be mixed with 20 (E20), 30 (E30), 50 (E50) and 85 (E85) percent by volume of ethanol, respectively. RON and MON of all fuels were evaluated by single cylinder CFR engine according to ASTM D2699

and D2700 and their results are shown in Table 5.4 and Fig. 5.9. It was found that each fuel reflected its own sensitivity, in which E85 shows the highest sensitivity. The physical and chemical properties of each fuel blend are also shown in Table 5.5 and Table 5.6.

***Table 5.4** Types of test fuels as well as their octane numbers (RON and MON) and sensitivity*

Fuel / Octane no.	G-base 1				
	E0	E20	E30	E50	E85
RON	87.1	96.1	98.7	102.4	105.2
MON	79.9	84.5	85.5	87.5	88.6
Sensitivity	7.2	11.6	13.2	15.0	16.6

Fuel / Octane no.	G-base 2				
	E0	E20	E30	E50	E85
RON	92.1	98.5	100.8	103.2	105.6
MON	83.5	86.2	87.2	88.2	89.1
Sensitivity	8.6	12.3	13.6	15.0	16.5

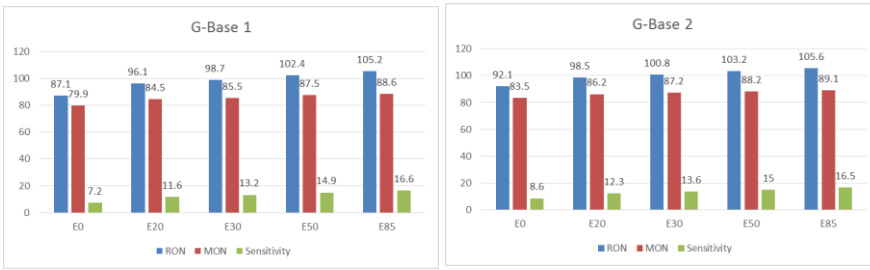

***Figure 5.9** Octane numbers (RON and MON) comparison between each fuel blend*

***Table 5.5** Physical and chemical properties of each test fuel*

Properties	G-base 1				
	E0	E20	E30	E50	E85
1. Density (g/cm3) at 15.6°C	0.7399	0.7492	0.7554	0.7659	0.7808
2. Sulfur (%wt.)	0.0019	0.0015	0.0010	0.0007	0.0004
3. Silver strip corrosion	No. 1	No. 1	No. 1	No. 1	No. 1
4. Oxidation stability (mins)	>360	>360	>360	>360	>360
5. Washed gum (mg/100ml)	1.0	0.6	<0.5	<0.5	<0.5
6. Distillation					
10%vol. (°C)	55.6	53.9	55.2	59.0	69.4
50%vol. (°C)	95.7	71.1	73.0	75.8	77.6
90%vol. (°C)	157.1	150.0	148.8	126.7	78.9
End point (°C)	190.1	187.0	183.7	176.5	161.3
Residue (%vol.)	0.9	0.9	1.0	0.9	1.0
7. Vapour pressure at 37.8°C (kPa)	51.5	58.6	56.4	52.6	39.4
8. Benzene (%vol.)	0.89	0.69	0.59	0.43	0.20
9. Aromatic (%vol.)	27	22	19	14	25
10. Olefins (%vol.)	14.3	11.4	9.4	6.7	4.5
11. Water contents (%wt.)	0.010	0.062	0.079	0.107	0.146
12. Ethanol contents (%vol.)	-	19	30	49.3	76.40
13. C,H,O contents (%mass)					
C:	86.34	79.40	75.40	66.84	69.64
H:	13.64	13.51	13.45	13.16	12.33
O:	0.01	7.09	11.15	19.95	18.03
14. Heating value (MJ/kg)	46.290	42.683	41.068	37.623	33.316

***Table 5.6** Physical and chemical properties of each test fuel*

Properties	G-base 2				
	E0	E20	E30	E50	E85
1. Density (g/cm3) at 15.6°C	0.7420	0.7503	0.7561	0.7662	0.7804
2. Sulfur (%wt.)	0.0014	0.0011	0.0008	0.0005	0.0003
3. Silver strip corrosion	No. 1	No. 1	No. 1	No. 1	No. 1
4. Oxidation stability (mins)	>360	>360	>360	>360	>360
5. Washed gum (mg/100ml)	1.0	0.6	<0.5	<0.5	<0.5
6. Distillation					
10%vol. (°C)	56.6	54.3	55.8	59.4	69.6
50%vol. (°C)	96.9	71.2	73.1	75.7	77.7
90%vol. (°C)	159.3	155.2	151.8	129.5	79.0
End point (°C)	194.4	190.5	188.0	179.7	164.8
Residue (%vol.)	0.9	1.0	1.1	1.1	1.1
7. Vapour pressure at 37.8°C (kPa)	51.4	58.4	56.2	52.0	39.0
8. Benzene (%vol.)	0.73	0.57	0.50	0.36	0.17
9. Aromatic (%vol.)	28	23	20	14	25
10. Olefins (%vol.)	13.2	10.5	8.7	6.0	4.0
11. Water contents (%wt.)	0.013	0.064	0.081	0.102	0.140
12. Ethanol contents (%vol.)	-	19	31	49.24	76.51
13. C,H,O contents (%mass)					
C:	86.30	79.20	75.50	67.04	69.46
H:	13.62	13.51	13.42	13.21	12.32
O:	0.09	7.29	11.08	19.75	18.22
14. Heating value (MJ/kg)	46.361	42.606	40.690	36.486	33.290

5.4) Result Discussion

5.4.1 Antiknock Property Evaluation

Some test results on antiknock property of each fuel blend evaluated by Ricardo Hydra GDI research engine at engine speed of 2,000 rpm are shown in Fig. 5.10 - 5.15..

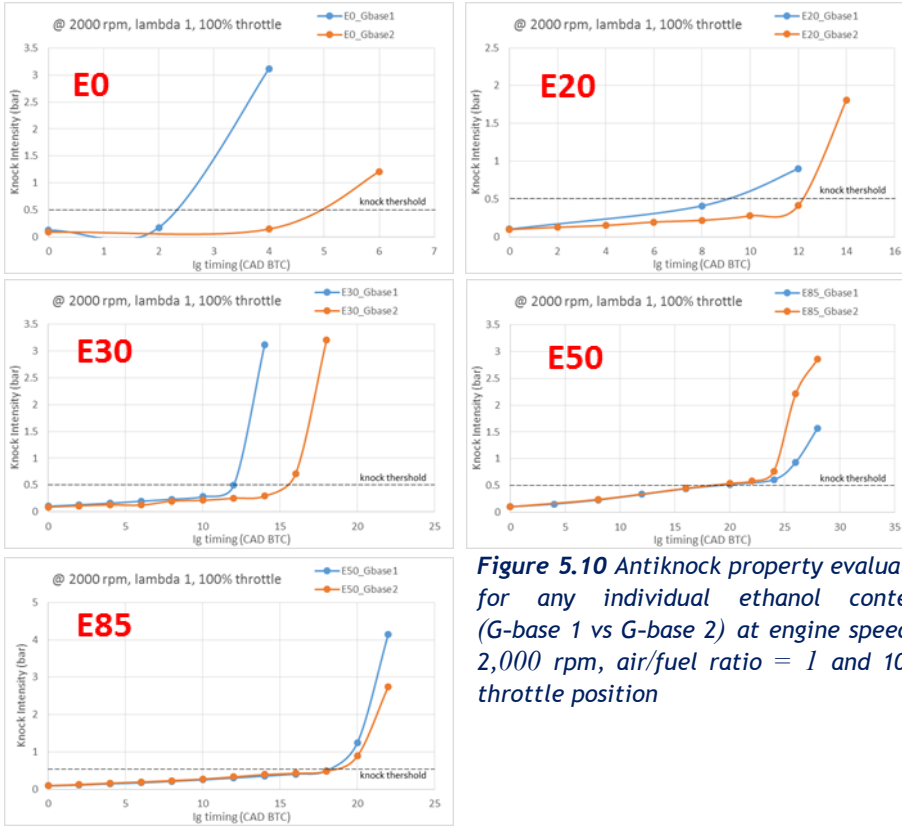

Figure 5.10 *Antiknock property evaluation for any individual ethanol contents (G-base 1 vs G-base 2) at engine speed of 2,000 rpm, air/fuel ratio = 1 and 100% throttle position*

Fig. 5.10 shows the knock intensity in relationship with the ignition timing of E0, E20, E30, E50 and E85 comparing between G-base 1 and G-base 2. The air/fuel ratio was kept at 1 with full throttle position. (100%) It was found that in case of E0, E20 and E85 comparing between G-base 1 and G-base 2, G-base 2 gasoline can allow the ignition timing to be more advance than that of G-base 1 at the same KLSA at 0.5 bar. However, for E50 and E85, the advance ignition timings of both fuel blends with G-base 1 and G-base 2 were not different significantly.

If the amount of ethanol content in each G-base fuel was considered, both G-base gasolines showed the similar trend, in which the more ethanol content in G-base, the better antiknock property was obtained as shown in Fig. 5.11.

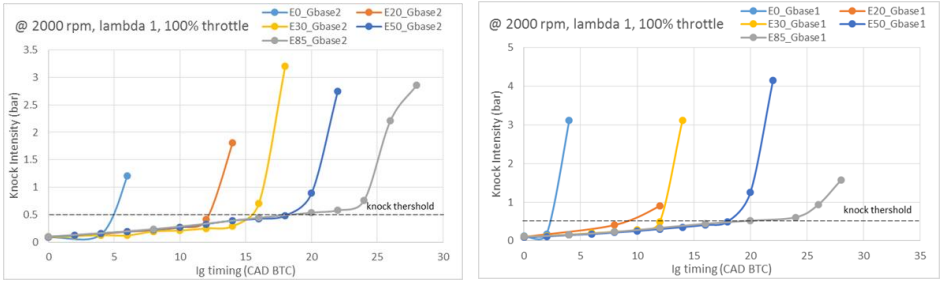

***Figure 5.11** Antiknock property evaluation for each group of G-base gasolines at engine speed of 2000 rpm, air/fuel ratio = 1 and 100% throttle position*

As the engine operated at full throttle condition under the controlling air/fuel ratio at 0.8 with same engine speed at 2,000 rpm, it was found that only E0 fuel from G-base 2 showed better antiknock property than those blends from G-base 1. However, there was no significantly different on other fuels as can be illustrated in Fig. 5.12.

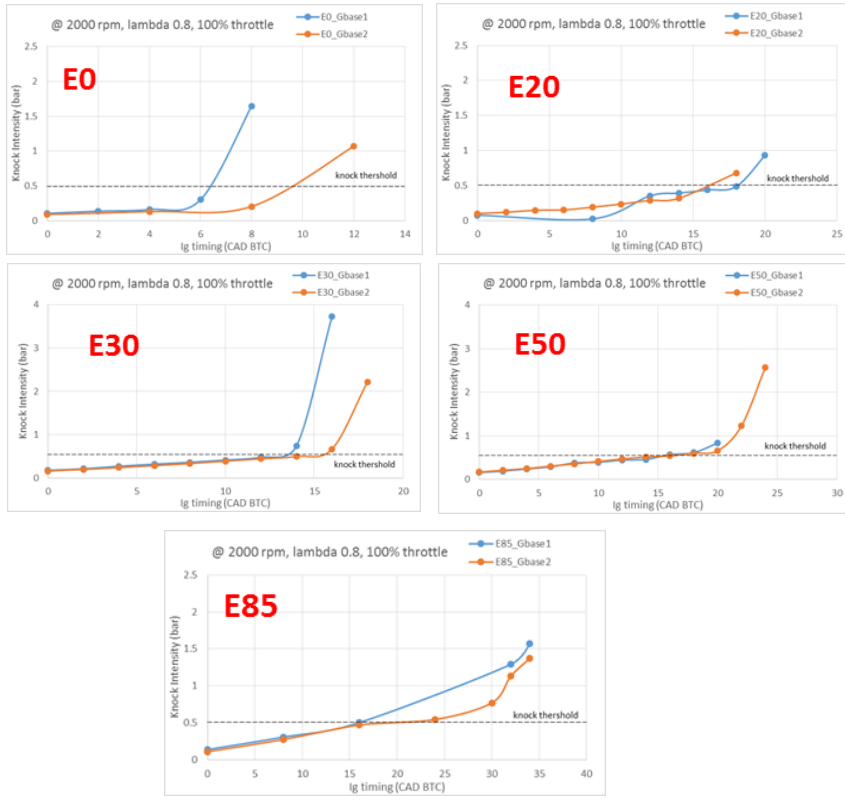

Fig. 5.12 *Antiknock property evaluation for any individual ethanol contents (G-base 1 vs G-base 2) at engine speed of 2,000 rpm, air/fuel ratio = 0.8 and 100% throttle position*

If the content of ethanol is the parameter for consideration, it was found that it was found the fuels prepared from both G-bases gave a similar trend as shown in Fig.5.13. E0 from both G-bases had worse antiknock properties compared to ethanol blends. In addition, there were no significantly different in ignition timing among each ethanol blended fuels.

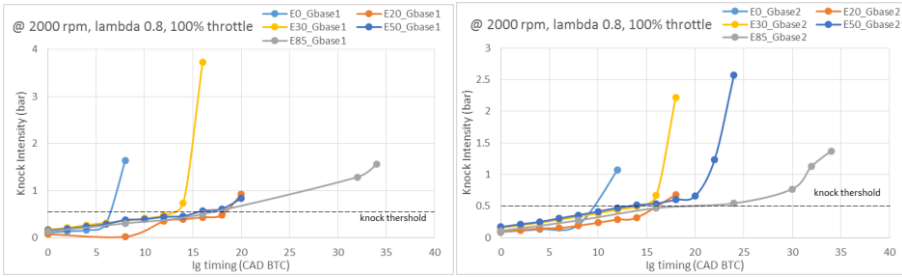

***5.13** Antiknock property evaluation for each group of G-base gasolines at engine speed of 2,000 rpm, air/fuel ratio = 0.8 and 100% throttle position*

The results were obtained by changing the air/fuel ratio to 1.2, but other parameters, such as engine speed (at 2,000 rpm) and full throttle position, were kept the same. It was found that fuel G-base 2 fuels could be ignited at more advance timing than the fuel G-base 1 in case of E0, E20, E30 and E50. However, for E85, there were no significantly different in ignition timing between the fuels prepared from G-base 1 and G-base 2 as shown in Fig. 5.14.

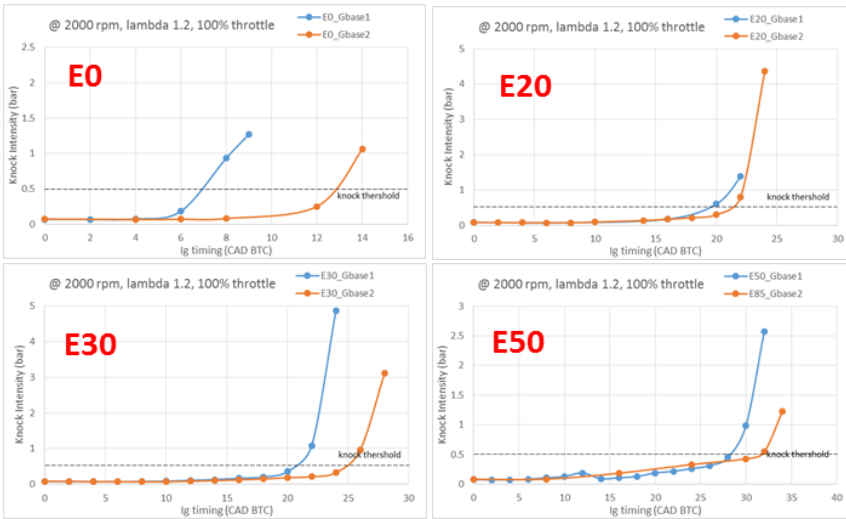

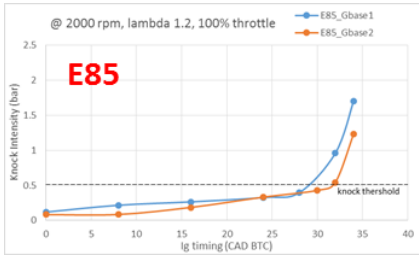

Figure 5.14 *Antiknock property evaluation for any individual ethanol contents, (G-base 1 vs G-base 2) at engine speed of 2,000 rpm, air/fuel ratio = 1.2 and 100% throttle position*

When comparing between each fuels prepared from each G-base as shown in Fig. 5.15, the results found the fuels prepared from both G-bases showed different trend. In case of G-base 1, E20 and E30 could be ignited at more advance timing than that without ethanol (E0) but the ignition timing of E20 and E30 fuels did not show any different at this knock limit value and still lower than E50 and E85. For G-base 2, E20 could be ignited at more advance timing compared to E0. Antiknock property of E30 and E50 were not significant difference and had a better antiknock property compared to E20. However, E85 presented the best antiknock property in G-base 2 group.

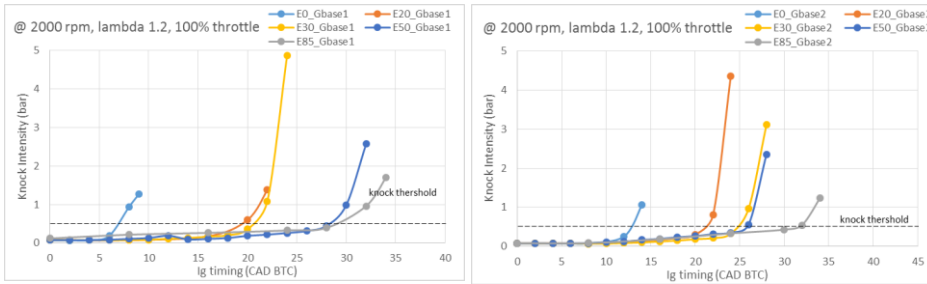

Figure 5.15 *Antiknock property evaluation for each group of G-base gasolines at engine speed of 2,000 rpm, air/fuel ratio = 1.2 and 100% throttle position*

All of the test in conditions presented in Table 5.3 were completed and summarized in 2 group. The first group is considered by comparing between G-base gasoline and another group is compared by ethanol content. The summary of ignition timing between the fuel blends with different ethanol contents prepared from G-base 1 and G-base 2 at 2000

rpm engine operation are shown in Table 4.1. In case of rich combustion, E0 prepared from G-base 2 could be ignited at more advanced timing compared to G-base 1 in both throttle positions. However, there was no significantly different advanced timing for ethanol blends. (E20, E30, E50 and E85) At stoichiometric air/fuel ratio, E0, E20 and E30 prepared from G-base 2 had a better antiknock property. Besides, advanced ignition timing of E50 and E85 prepared from both G-bases did not show significant difference. E0, E20, E30 and E50 prepared from G-base 2 presented a better advanced ignition timing compared to G-base 1 for lean combustion but there were no significant difference in case of E85 test.

***Table 5.7** Summary of ignition timing between the fuel blends prepared from G-base 1 and G-base 2 at 2000 rpm.*

λ	0.8 (Rich)		1 (Stoichiometric)		1.2 (Lean)	
%throttle	30	100	30	100	30	100
E0	Gb1 < Gb2	Gb1 < Gb2	Gb1 < Gb2	Gb1 < Gb2	Gb1 < Gb2	Gb1 < Gb2
E20	Gb1 ≅ Gb2	Gb1 ≅ Gb2	Gb1 < Gb2	Gb1 < Gb2	Gb1 < Gb2	Gb1 < Gb2
E30	Gb1 ≅ Gb2	Gb1 ≅ Gb2	Gb1 < Gb2	Gb1 < Gb2	Gb1 < Gb2	Gb1 < Gb2
E50	Gb1 ≅ Gb2	Gb1 ≅ Gb2	Gb1 ≅ Gb2	Gb1 ≅ Gb2	Gb1 < Gb2	Gb1 < Gb2
E85	Gb1 ≅ Gb2	Gb1 ≅ Gb2	Gb1 ≅ Gb2	Gb1 ≅ Gb2	Gb1 ≅ Gb2	Gb1 ≅ Gb2

***Note**: Gb1: G-base1 Gb2: G-base2*
<: less advance ignition timing
≅: same ignition timing

Table 5.8 presents the summary of ignition timing between the fuel blends with different ethanol contents prepared from G-base 1 and G-base 2 at 2500 rpm engine operation. For rich combustion study, the results were similar to 2000 rpm engine operation which was E0 prepared from G-base 2 had a better advanced timing compared to G-base 1 in both throttle positions and there were no significant difference for other ethanol blended fuels between both G-bases. In case of stoichiometric combustion with 30% and 100% throttle position, E0 from G-base 2 offered a better advanced ignition timing. About E20 test in stoichiometric combustion with controlled throttle position at 30%, there was no difference between G-base 1 and 2 but at 100% throttle position E20 from G-base 2 showed *a better advanced ignition timing*

compared to G-base 1. In addition, E30, E50 and 85 prepared from both G-base also showed no significant difference. Lean burn condition presented a similar result in both controlled throttle positions. E0 and E20 prepared from G-base 2 could be ignited earlier than G-base 1. However, there were no significant difference among E30, E50 and E85 in both G-bases.

***Table 5.8** Summary of ignition timing between the fuel blends prepared from G-base 1 and G-base 2 at 2500 rpm.*

λ	0.8 (Rich)		1 (Stoichiometric)		1.2 (Lean)	
%throttle	30	100	30	100	30	100
E0	Gb1 < Gb2	Gb1 < Gb2	Gb1 < Gb2	Gb1 < Gb2	Gb1 < Gb2	Gb1 < Gb2
E20	Gb1 ≅ Gb2	Gb1 ≅ Gb2	Gb1 ≅ Gb2	Gb1 < Gb2	Gb1 < Gb2	Gb1 < Gb2
E30	Gb1 ≅ Gb2	Gb1 ≅ Gb2	Gb1 ≅ Gb2	Gb1 ≅ Gb2	Gb1 ≅ Gb2	Gb1 ≅ Gb2
E50	Gb1 ≅ Gb2	Gb1 ≅ Gb2	Gb1 ≅ Gb2	Gb1 ≅ Gb2	Gb1 ≅ Gb2	Gb1 ≅ Gb2
E85	Gb1 ≅ Gb2	Gb1 ≅ Gb2	Gb1 ≅ Gb2	Gb1 ≅ Gb2	Gb1 ≅ Gb2	Gb1 ≅ Gb2

Note: *Gb1: G-base1 Gb2: G-base2*
<: less advance ignition timing
≅: same ignition timing

If the content of ethanol is the parameter for consideration, Table 5.9 demonstrates the summary of ignition timing between the fuels with different ethanol content at 2000 rpm engine operation. There were a similar results for rich combustion in both throttle positions. E0 had a worse advanced ignition timing compared to ethanol blended fuels (E20, E30, E50 and E85) in both G-bases. At stoichiometric combustion with 30% throttle position, ethanol blended fuels (E20, E30, E50 and E85) offered better advanced ignition timing in case of G-base 1. For G-base 2, E20 had a better advanced ignition timing compared to E0 but still worse compared to E30, E50 and E85. Stoichiometric combustion with full throttle position results showed a similar trend in both G-bases. More ethanol content could improve antiknock property. However, at 50% and 85% of ethanol content, there were no significantly different test results in both G-bases. Lean burn of G-base 1 at 30% throttle position results presented E20 and E30 had better advanced ignition timing compared to

E0 but still worse compared to E50 and E85. At full throttle position, E50 and E85 could be ignited earlier than E20 and E30. Besides, E20 and E30 gave better advanced ignition timing compared to E0. In case of G-base 2 lean burn study at 30% throttle position, E85 had the best advanced ignition timing followed with E20, E30 and E50. E0 had the worst advanced ignition timing in this group. For full throttle controlled, E30 and E50 had better advanced ignition timing compared to E20 and E20 also offered better advanced ignition timing compared to E0. However, the best fuel presented best advanced ignition timing was E85.

***Table 5.9** Summary of ignition timing between the fuel blends with different ethanol contents at 2000 rpm engine operation.*

λ	0.8 (Rich)		1 (Stoichiometric)		1.2 (Lean)	
%throttle	30	100	30	100	30	100
G-base 1	E0<E20≅E30≅E50≅E85	E0<E20≅E30≅E50≅E85	E0<E20≅E30≅E50≅E85	E0<E20<E30<E50≅E85	E0<E20≅E30<E50≅E85	E0<E20≅E30<E50≅E85
G-base 2	E0<E20≅E30≅E50≅E85	E0<E20≅E30≅E50≅E85	E0<E20<E30≅E50≅E85	E0<E20<E30<E50≅E85	E0<E20≅E30≅E50<E85	E0<E20<E30≅E50<E85

Note: *Gb1: G-base1 Gb2: G-base2*
<: less advance ignition timing
≅: same ignition timing

Results from 2500 rpm engine operations are shown in Table 5.10 which is the summary of ignition timing between the fuels with different ethanol content. There were a similar results for rich combustion at 30% throttle position in both G-bases. E0 had a worse advanced ignition timing compared to ethanol blended fuels (E20, E30, E50 and E85). For rich combustion of fuels prepared from G-base 1 with 30% throttle position, E50 and E85 could be ignited earlier than E30 and E30 gave a better advanced ignition timing E20 and E0. In case of G-base 2, E50 and E85 had better advanced ignition timing compared to E20 and E30. Also, E20 and E30 were still better than E0. At stoichiometric combustion with 30% throttle position, ethanol blended fuels (E20, E30, E50 and E85) offered better advanced ignition timing in both G-bases. When controlling throttle at 100% position, E50 and E85 showed better advanced ignition timing compared to E30 and E30 gave a better advanced ignition timing

E20 and E0 as well in both G-bases. About lean burn study, the results from both G-bases were similar trend in case of controlled throttle position at 30%. E50 and E85 presented better advanced ignition timing compared to E30 and E30 was still than E20 and E0. At full throttle position, fuels prepared from G-base 1 had a results that E0 had a worse advanced ignition timing compared to ethanol blended fuels (E20, E30, E50 and E85) and there were no significant difference between E50 and E85. In case of G-base 2 test, E85 had the best advanced ignition timing followed with E20, E30 and E50. E0 had the worst advanced ignition timing in this group.

***Table 5.10** Summary of ignition timing between the fuel blends with different ethanol contents at 2500 rpm engine operation.*

λ	0.8 (Rich)		1 (Stoichiometric)		1.2 (Lean)	
%throttle	30	100	30	100	30	100
G-base 1	E0<E20≅E30≅E50≅E85	E0<E20<E30<E50≅E85	E0<E20≅E30≅E50≅E85	E0<E20<E30<E50≅E85	E0<E20<E30<E50≅E85	E0<E20<E30<E50≅E85
G-base 2	E0<E20≅E30≅E50≅E85	E0<E20≅E30<E50≅E85	E0<E20≅E30≅E50≅E85	E0<E20<E30<E50≅E85	E0<E20<E30<E50≅E85	E0<E20≅E30≅E50<E85

Note: *Gb1: G-base1 Gb2: G-base2*
<: less advance ignition timing
≅: same ignition timing

5.4.2 Thermal Efficiency

According to the results of antiknock property evaluation in previous section, the advanced ignition timing at KLSA (0.5 bar) were considered for thermal efficiency determination. Thermal efficiency results of controlling throttle position at 30% for each fuel are presented in Fig. 5.16- 5.17 and Table 5.11- 5.12 Fig. 5.16 shows thermal efficiency of Ricardo Hydra GDI research engine at 2000 rpm operation. Fuels prepared from both G-bases presented a similar trend of thermal efficiency. Ethanol blended fuels offered better thermal efficiency compared to E0 for all air/fuel ratios. Engine thermal efficiency from E0 in rich, stoichiometric and lean combustion were 22%, 26% and 30%, respectively. Ethanol blended fuels presented 3-6% higher efficiency

compared to gasoline. In case of 2500 rpm engine operation at 30% throttle position, Ethanol blended fuels showed better efficiency compared to gasoline around 2-5% for all combustion conditions as presented in Fig. 5.17 and Table 5.12.

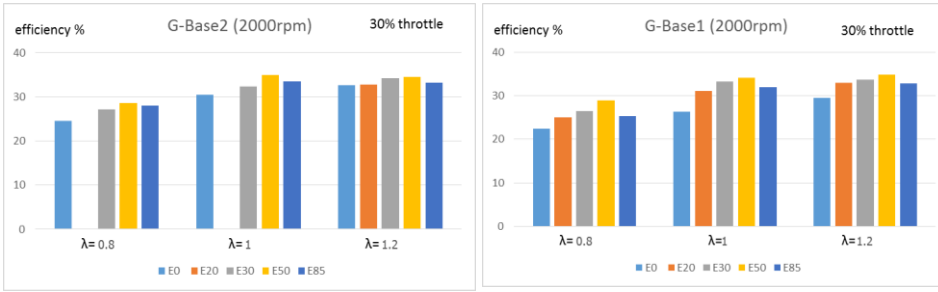

***Figure 5.16** Thermal efficiency of Ricardo Hydra GDI research engine at 2000 rpm operation with 30% throttle position*

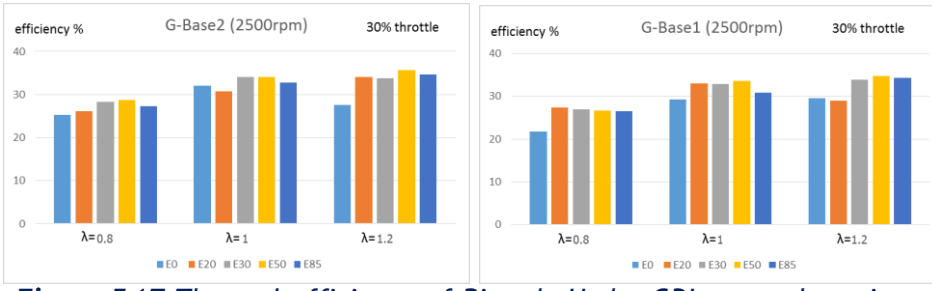

***Figure 5.17** Thermal efficiency of Ricardo Hydra GDI research engine at 2500 rpm operation with 30% throttle position*

***Table 5.11** Thermal efficiency (%) of Ricardo Hydra GDI research engine at 2000 rpm operation with 30% throttle position*

Fuel	G-base 1			G-base 2		
	rich	stoich	lean	Rich	stoich	Lean
E0	22.47	26.28	29.54	24.56	30.43	32.59
E20	25.03	31.04	32.95	N/A	N/A	32.79
E30	26.53	33.30	33.76	27.11	32.34	34.25
E50	28.95	34.10	34.87	28.52	34.89	34.49
E85	25.30	31.95	32.80	28.04	33.52	33.24

Table 5.12 *Thermal efficiency (%) of Ricardo Hydra GDI research engine at 2500 rpm operation with 30% throttle position*

Fuel	G-base 1			G-base 2		
	rich	stoich	lean	Rich	stoich	Lean
E0	21.77	29.28	29.54	25.28	32.01	27.62
E20	27.41	32.95	28.99	26.20	30.71	34.07
E30	26.93	32.87	33.88	28.28	34.10	33.78
E50	26.67	33.57	34.69	28.73	34.09	35.71
E85	26.52	30.92	34.35	27.35	32.81	34.72

Fig. 5.18 and 5.19 present the thermal efficiency results obtained from engine running at full throttle position for both G-bases. Furthermore, Table 5.13 and 5.14 also shows the figures related to Fig. 5.18 and 5.19, respectively. All results presented a similar trend with controlling throttle position at 30%. Fig. 5.18 demonstrates thermal efficiency of Ricardo Hydra GDI research engine at 2000 rpm operation. Ethanol blended fuels from G-bases 1 gave better thermal efficiency compared to E0, 5-6% approximately for all air/fuel ratios. When considering G-base 2, ethanol blended fuels had 1-4% better efficiency compared to gasoline for all combustion conditions. According to Fig.5.19, there were thermal efficiency obtained from 2500 rpm engine operations. Ethanol blended fuels gave better thermal efficiency compared to gasoline. For G-base 1, thermal efficiency from E0 in rich, stoichiometric and lean combustion were 22%, 27% and 31%, respectively. In addition, ethanol blended had an efficiency in range of 24-27%, 30-34% and 32-34% for rich, stoichiometric and lean burn, respectively. Besides, ethanol blended fuels prepared from G-base 2 had higher thermal efficiency compared to E0 approximately 1-4%.

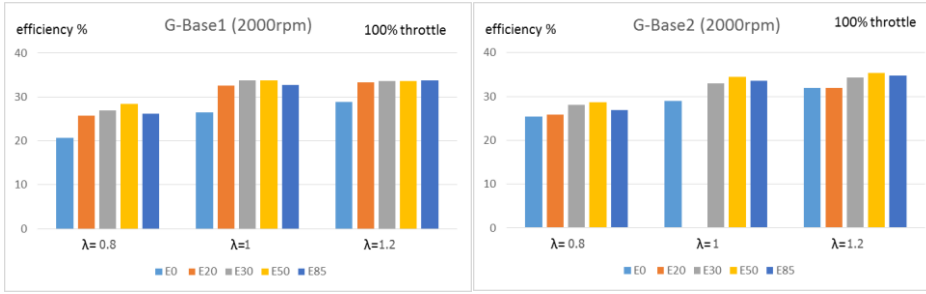

Figure 5.18 *Thermal efficiency of Ricardo Hydra GDI research engine at 2000 rpm operation with full throttle position*

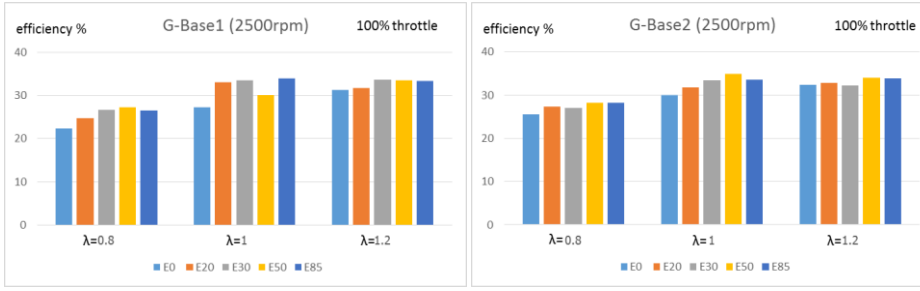

Fig. 5.19 *Thermal efficiency of Ricardo Hydra GDI research engine at 2500 rpm operation with full throttle position*

Table 5.13 *Thermal efficiency (%) of Ricardo Hydra GDI research engine at 2000 rpm operation with full throttle position*

Fuel	G-base 1			G-base 2		
	Rich	stoich	lean	rich	stoich	Lean
E0	20.73	26.43	28.91	25.34	29.02	31.87
E20	25.73	32.50	33.38	25.92	N/A	31.89
E30	26.90	33.69	33.55	28.11	32.93	34.25
E50	28.45	33.73	33.62	28.60	34.48	35.37
E85	26.16	32.66	33.71	26.93	33.52	34.72

Table 5.14 *Thermal efficiency (%) of Ricardo Hydra GDI research engine at 2500 rpm operation with full throttle position*

Fuel	G-base 1			G-base 2		
	Rich	stoich	lean	rich	stoich	Lean
E0	22.34	27.29	31.30	25.51	29.98	32.38
E20	24.73	33.09	31.73	27.30	31.78	32.87
E30	26.61	33.46	33.60	27.08	33.46	32.28
E50	27.34	30.02	33.49	28.27	34.87	34.05
E85	26.48	34.02	33.41	28.24	33.63	33.88

5.4.3 Octane Number vs Thermal Efficiency

One interested benefit of ethanol blended is octane booster. The relationships between octane number (RON, MON and sensitivity) and obtained thermal efficiency was studied. Fig. 5.20 presents the relationships between RON, MON and thermal efficiency. According to Fig.5.20, ethanol blended fuels have higher efficiency compared to gasoline in both graphs. The relationships shows that increasing RON and MON could improve thermal efficiency. Furthermore, the relationships is quite linear for both RON and MON. As mentioned in Chapter 2, octane sensitivity of fuel directly impacts to the antiknock property rather than either RON or MON. Thus, the sensitivity of fuels were plotted against thermal efficiency as shown in Fig.5.21. The relationships presents increasing sensitivity of fuel can improve thermal efficiency as well. From Fig 5.21, ethanol blended fuels such as E20, E30, E50 and E85 which have higher sensitivity could offer better thermal efficiency compared to gasoline.

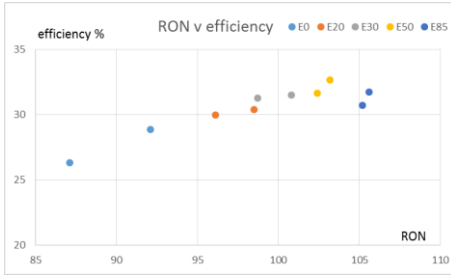

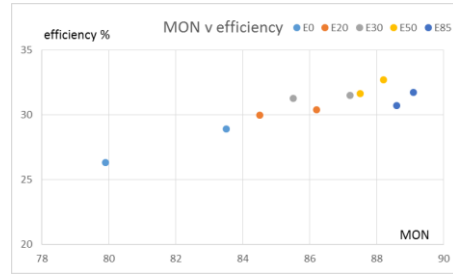

Figure 5.20 *Relationships between RON, MON and thermal efficiency from Ricardo Hydra GDI research engine*

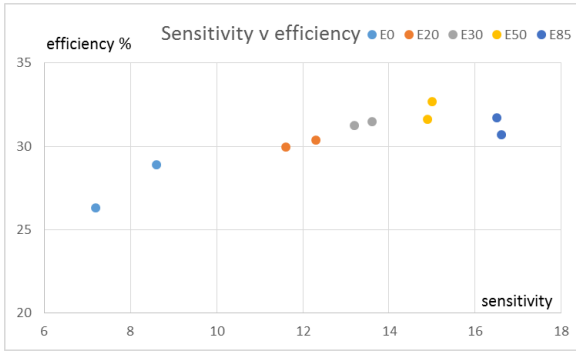

Figure 5.21 *Relationships between sensitivity and thermal efficiency from Ricardo Hydra GDI research engine*

5.5) Conclusion

The antiknock property of fuels was investigated by adjusting the ignition timing and measuring the knock intensity. At a certain knock threshold limit, the fuel which can be ignited more advance ignition timing, will be better in antiknock property. The study was carried out using single cylinder Ricardo Hydra research engine at several conditions by varying engine speed, air/fuel ratio and throttle position. Tested fuel used in this study were neat gasoline and ethanol blended gasolines at different ethanol contents i.e., E0, E20, E30, E50 and E85. In addition,

each fuel blends were also prepared from two grades of base gasolines. (G-base 1 and G-base 2) The results of antiknock property of the test fuels are summarized in topic 5.4.1. According to Table 5.7- 5.8, gasoline prepared from G-base 2 which has higher octane number could be ignited at more advanced ignition timing than the G-Base 1 in all air/fuel ratios and all throttle positions. For ethanol blended fuels (E20, E30, E50 and E85), there was no significantly different advanced timing among each G-base in rich combustion study. In case of stoichiometric combustion, there were difference advanced ignition timing between fuels prepared from G-base 1 and 2 in range of 0-30% blended. However, E50 and E85 showed no significant difference between each G-base for stoichiometric combustion study. About lean burn study at 2000 rpm engine speed, more ethanol content could improve antiknock property. However, E50 and E85% showed no significantly different test results in both G-bases. For engine speed at 2500 rpm with learn burn, E0 and E20 prepared from G-base 2 gave a higher advanced ignition timing and other fuels from G-base 2 were not significantly different compared to G-base1. When ethanol content is the parameter for consideration as in Table 5.9 - 5.10, E0 had a worse advanced ignition timing compared to ethanol blended fuels in both G-bases in rich combustion study. In case of stoichiometric and lean combustion, increasing ethanol content could improve antiknock property. However, at the 50% and 85% of ethanol content, there was no significant difference of advanced ignition timing between both fuels. The advanced ignition timing at KLSA (0.5 bar) were considered for thermal efficiency determination. Gasoline fuels gave 20-29% thermal efficiency and ethanol blended fuels offers 7-17% (rel.) better thermal efficiency. The range of thermal efficiency from using ethanol blended fuels was 25-35% approximately and there was no significant difference among ethanol fuels. In addition, the relationships between octane number (RON, MON and sensitivity) and obtained thermal efficiency was studied and found that increasing RON and MON could improve thermal efficiency. Octane sensitivity is one of fuel property which directly impacts to the antiknock behavior. The sensitivity of fuels were plotted

against thermal efficiency to investigate the relation between both parameters. Increasing sensitivity of ethanol blended fuels could improve thermal efficiency. The obtained thermal efficiency from ethanol blended fuels were in range of 30-34%.

The antiknock property of gasoline and ethanol blended gasolines were studied and showed the relationship between the octane number (RON and MON) as well as sensitivity and antiknock property of fuels. As the octane index (OI) increased by adding a certain amount of ethanol, the fuels performed better antiknock property because of sensitivity increasing according to the equation OI = RON – KS. Thus, increasing ethanol content in fuels offered better antiknock property and allowed more advanced ignition timing. Ethanol blended fuels had a better efficiency compared to gasoline fuel. Although gasolines have higher energy density but ethanol blended fuels offered better In this study, E20, E30, E50 and E85 presented the efficiency improvement at λ =0.8 around 14%, λ =1 around 17% and λ =1.2 around 7% compared to E0. However, all of test results in this study were tested under the fixed compression ratio. Varying compression ratio and some other parameters might improve the obtained thermal efficiency and the suitable conditions will be found for each fuel to meet the best efficiency.

5.6) References

[1] Celik M. and Ozalyan B., Gasoline Direct Injection, website: www.intechopen.com.

[2] National Ethanol Conference Grapevine, TX February 20, 2015 Higher Ethanol Blends for Improved Efficiency

[3] Heywood, J.B. 1998, "Internal combustion engine fundamentals", Ch.9, McGraw Hill Book Co.,

[4] Kalghatgi, G.T. 2001. "Fuel anti- knock—Part II. Vehicle Studies—How

Relevant Is Motor Octane Number (MON) for Modern Engines?" SAE Paper No. 2001-01-3585. SAE International.

[5] Bell, A. 2010. "Modern SI Engine Control Parameter Responses and Altitude Effects with Fuels of Varying Octane Sensitivity." SAE Paper No. 2010-01-1454. SAE International.

[6] Coordinating Research Council. 1995. "Vehicle Performance Effect of Octane on Knock Sensor Equipped Vehicles." CRC Report No. 597.

[7] Whelan, D.E., Schmidt, G.K., and Hischier, M.E. 1998. "An Acceleration Based Method to Determine the Octane Number Requirement of Knock Sensor Vehicles." SAE Paper No. 982721. SAE International.

[8] Kalghatgi, G.T. 2001. "Fuel Anti-knock Quality—Part I. Engine studies." SAE Paper No. 2001-01-3 584. SAE International.

[9] Mittal, V., and Heywood, J.B. 2009. "The Shift in Relevance of Fuel RON and MON to Knock Onset in Modern SI Engines over the Last 70 Years." SAE Paper No. 2009-01-2622. SAE International.

[10] Kalghatgi, G.T., Nakata, K., and Mogi, K. 2005. "Octane Appetite Studies in Direct Injection Spark Ignition (DISI) Engines." SAE Paper No. 2005-01-0244. SAE International.

[11] Kalghatgi, G.T. 2005. "Auto-Ignition Quality of Practical Fuels and Implications for Fuel Requirements of Future SI and HCCI Engines." SAE Paper No. 2005-01-0239. SAE International.